



engineers | scientists | innovators

---

# **GROUNDWATER FLOW AND FATE AND TRANSPORT MODEL CALIBRATION REPORT**

## **LOWER ISSAQUAH VALLEY ISSAQUAH, WASHINGTON**

*Prepared for*

The City of Issaquah  
1775 – 12th Ave NW  
Issaquah, WA 98027

*Prepared by*

Geosyntec Consultants, Inc.  
520 Pike Street, Suite 2600  
Seattle, Washington 98101

Project Number: PNG0989

August 2023

# Groundwater Flow and Fate and Transport Model Calibration Report

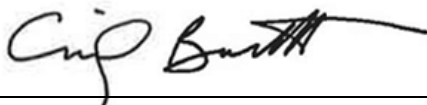
## Lower Issaquah Valley Issaquah, Washington

*Prepared for*

City of Issaquah, Washington  
1775- 12<sup>th</sup> Ave NW  
Issaquah, WA 98027

*Prepared by*

Geosyntec Consultants, Inc.  
520 Pike Street, Suite 2600  
Seattle, Washington 98101



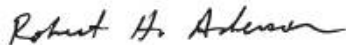
---

Cindy Bartlett, LG  
Principal Geologist and Project Manager



---

Julie Chambon, PhD, PE (CA)  
Principal Engineer and Lead Modeler



---

Bob Anderson, LHG  
Senior Principal Hydrogeologist

Project Number: PNG0989

August 2023

## TABLE OF CONTENTS

TABLE OF CONTENTS.....	I
LIST OF FIGURES .....	II
LIST OF TABLES .....	III
ACRONYMS AND ABBREVIATIONS .....	IV
1. INTRODUCTION .....	1
1.1 Background .....	1
1.2 Objectives .....	2
2. GROUNDWATER FLOW MODEL DEVELOPMENT .....	2
2.1 Numerical Model Domain, Grid, and Layers .....	2
2.2 Simulation Period .....	3
2.3 Model Boundaries and Stresses .....	3
2.3.1 Specified Head Boundary .....	4
2.3.2 Specified Flux Boundary .....	4
2.3.3 Rivers .....	4
2.3.4 Areal Recharge .....	4
2.3.5 Production Wells .....	4
2.3.6 Initial Conditions .....	5
2.4 Material Properties .....	5
3. GROUNDWATER FLOW MODEL CALIBRATION .....	6
3.1 Calibration Data .....	6
3.1.1 Calibration to Steady-State Conditions .....	6
3.1.2 Calibration to Transient Conditions .....	6
3.2 Calibration Process .....	8
3.3 Calibration Results .....	8
3.3.1 Steady-State Water Levels .....	8
3.3.2 Historical Transient Water Levels .....	9
3.3.3 Transducer Data .....	10
3.4 Summary of Flow Model Calibration Results .....	10
4. SIMULATED GROUNDWATER FLOW BALANCE .....	10
5. CONTAMINANT FATE AND TRANSPORT MODEL .....	11
5.1 Grid Refinements .....	12

5.2	Simulation Period and Stress Periods.....	12
5.3	Transport Properties .....	13
5.4	PFAS Sources in Model .....	14
6.	CONTAMINANT FATE AND TRANSPORT MODEL CALIBRATION .....	16
6.1	PFAS Calibration Data.....	16
6.2	Calibration Results .....	16
7.	CALIBRATION SENSITIVITY ANALYSIS .....	17
7.1	Groundwater Flow Model Calibration Sensitivity .....	17
7.1.1	Parameters .....	17
7.1.2	Sensitivity Assessment.....	18
7.2	Fate and Transport Model Calibration Sensitivity .....	18
7.2.1	Parameters .....	18
7.2.2	Sensitivity Assessment.....	19
8.	SUMMARY AND NEXT STEPS.....	19
9.	REFERENCES .....	21

## LIST OF FIGURES

Figure 2-1	Model Domain, Grid and Boundary Conditions
Figure 2-2	Model Cross-Sections
Figure 2-3	Elevation of Model Layers
Figure 2-4	Thickness of Model Aquitards
Figure 2-5	Lake Sammamish Stage
Figure 2-6	Specified Flow at Western and Eastern Margins
Figure 2-7	Riverbed Conductance
Figure 2-8	Recharge Rate
Figure 2-9	Pumping Rates at Production Wells
Figure 2-10	Hydraulic Properties
Figure 3-1	Observation Locations
Figure 3-2	Pumping Rates at Production Wells During Selected SPWD Transducer Data Period
Figure 3-3	Simulated vs. Observed Groundwater Levels for Steady State Simulation



Figure 3-4	Simulated Groundwater Elevation Contours (Steady-State)
Figure 3-5	Hydrographs of Simulated and Simulated Water Levels
Figure 3-6	Hydrographs of Observed and Simulated Water Levels at Cluster Wells
Figure 3-7	Hydrographs of Observed and Simulated Water Levels – May 2016 through April 2017
Figure 3-8	Hydrographs of Observed and Simulated Water Levels – September through November 2021
Figure 3-9	Hydrographs of Observed and Simulated Water Levels – October 2022 through March 2023
Figure 4-1	Water Balance for Historical Simulation
Figure 6-1	Measured and Simulated PFOS Simulated Concentrations in Shallow Aquifer
Figure 6-2	Measured and Simulated PFOS Simulated Concentrations in A Zone Aquifer
Figure 6-3	Measured and Simulated PFOS Simulated Concentrations in B Zone Aquifer
Figure 7-1	Sensitivity Assessment for Fate and Transport Model

## **LIST OF TABLES**

Table 2-1	Summary of Hydrostratigraphic Units Identified in Boring Logs
Table 2-2	Production Well Summary
Table 2-3	Summary of Calibrated Hydraulic Properties
Table 3-1	Observation Locations and Average Groundwater Elevations
Table 4-1	Simulated Steady-State Water Balance
Table 5-1	Fate and Transport Model Parameters
Table 6-1	Simulated PFAS Concentrations
Table 7-1	Summary of Sensitivity Runs and Calibration Sensitivity Results

## ACRONYMS AND ABBREVIATIONS

3D	three-dimensional
µg/L	micrograms per liter
AFFF	aqueous film-forming foam
AFY	acre-feet per year
City	City of Issaquah
Ecology	Washington State Department of Ecology
EFR	Eastside Fire and Rescue
Geosyntec	Geosyntec Consultants, Inc.
HG Model	Regional Conceptual Hydrogeological Model
IAA	interagency agreement
LIV	Lower Issaquah Valley
ME	mean error
MTCA	Washington State Model Toxics Control Act
ng/L	Nanograms per liter
NSC	normalized sensitivity coefficient
Partnership	Issaquah Valley Per- and Poly-Fluoroalkyl Substances Partnership
PFAS	per- and polyfluoroalkyl substances
PFBS	perfluorobutanesulfonic acid
PFOA	perfluorooctanoic acid
PFOS	perfluorooctanesulfonic acid
PFHxS	perfluorohexanesulfonic acid
RMSE	root mean square error
SAL	state action level
SPWD	Sammamish Plateau Water District
USGS	United State Geological Survey

## 1. INTRODUCTION

This report transmits the final deliverable for the interagency agreement (IAA<sup>1</sup>) between the Washington State Department of Ecology (Ecology) and the City of Issaquah (City) and has been prepared by Geosyntec Consultants, Inc. (Geosyntec) on behalf of the City. The purpose of this report is to document the development and calibration of a three-dimensional (3D) groundwater flow and fate and transport model for the Lower Issaquah Valley (LIV).

### 1.1 Background

Previous studies conducted by the Issaquah Valley Per- and Poly-Fluoroalkyl Substances (PFAS) Partnership (Partnership), which includes the City, Eastside Fire and Rescue (EFR), and Ecology, have focused along the central portion of the LIV and former fire training source areas where aqueous film forming foams (AFFFs) have been used. The Study Area for the 3D model extends from the Issaquah-Hobart Gap to Lake Sammamish and from the eastern portion of the City to Tibbetts Creek.

A 3D numerical groundwater model was developed in 2017 (CDM Smith, 2017) by Sammamish Plateau Water District (SPWD) using a proprietary finite element code (DYNFLOW) to evaluate PFAS transport in the LIV. The City converted the DYNFLOW model to a public domain numerical model (MODFLOW, the CARA MODFLOW model) as part of the City's CARA update (Geosyntec, 2022a). In addition, the City conducted two-dimensional (2D) numerical modeling along the main groundwater flow paths from two mid-valley source areas towards City production wells COI-PW04 and COI-PW05 to improve our understanding of migration pathways and vertical transport within the LIV aquifer system (Geosyntec, 2021).

This 3D groundwater flow and PFAS fate and transport model incorporates aquifer data and hydrogeological information collected since the City's CARA groundwater modeling was completed and data from PFAS investigations completed since 2017. The CARA MODFLOW model formed the basis for the development of the numerical groundwater and fate and transport model for this work.

As part of this IAA, the City developed a Regional Conceptual Hydrogeological Model (HG Model) for the LIV, including identification of data gaps (Geosyntec, 2022b). Geosyntec prepared a Data Gaps Investigation Work Plan Addendum for additional investigations of the deeper aquifer, and a deep monitoring well (COI-MW08) was installed along the dominant groundwater flow path (Geosyntec, 2022c). The deep monitoring well was installed in November-December 2022 and documented in a Well Installation Completion Report (Geosyntec, 2023).

Prior to the data gaps investigation, Geosyntec documented the preliminary development and calibration of the updated 3D groundwater flow model based on the HG Model for the LIV (Geosyntec, 2022d).

---

<sup>1</sup> IAA No. C2200183

This report documents the refinements and completion of the 3D groundwater flow model based on the results of fieldwork conducted by the City and EFR, including refinement of model setup and flow model calibration, and set up and calibration of the fate and transport model to simulate PFAS migration in the LIV aquifer system (i.e., 2023 LIV Model).

## 1.2 Objectives

The objectives of this modeling work were to:

- Refine the CARA MODFLOW model, including layering, boundary conditions, and hydraulic properties based on the HG Model and additional investigations performed by EFR and the City as part of the IAA work;
- Calibrate the groundwater flow model based on historical and recently collected water levels under steady-state and transient conditions;
- Setup and calibrate the PFAS fate and transport model based on historical and recently collected PFAS groundwater concentrations; and
- Perform sensitivity analysis of the groundwater flow and fate and transport model calibration to assess model limitations.

## 2. GROUNDWATER FLOW MODEL DEVELOPMENT

The 3D model for groundwater flow was developed using MODFLOW-NWT, an industry-standard finite-difference code for groundwater flow simulations.

### 2.1 Numerical Model Domain, Grid, and Layers

The model domain is illustrated in Figure 2-1, where the scale is 1 inch = 5,250 feet. The model domain is approximately five square miles. The model domain was developed based on the geology to represent the extent of the LIV. The model extends from the Issaquah-Hobart Gap in the south to Lake Sammamish in the north.

The hydrostratigraphy is represented with nine layers, consistent with the CARA MODFLOW model and the HG Model, and summarized in the table below. The layering is based on the CARA MODFLOW model that was adjusted to better represent the hydrostratigraphic units based on historical boring logs, new wells installed as part of the investigations performed under the IAA, and regional geology. Table 2-1 includes a summary of the Hydrostratigraphic Units identified at each boring. The model layering is illustrated along two cross-sections in Figures 2-2a and 2-2b and the top elevations of Layers 2 through 7 and Layer 9<sup>2</sup> are shown in Figures 2-3a–g. The thicknesses of the three aquitards (represented by Layers 2, 4, and 6) are shown in Figures 2-4a–c.

---

<sup>2</sup> Layer 8 is not included as a separate figure since it has similar hydraulic properties to Layer 7 (refer to Figure 2-2b cross section and summary table on next page).

MODFLOW Layers	Hydrostratigraphic Unit	Material
1	Shallow Aquifer (including Aquitard 1*)	Fine sand
2		Silt (variable thickness/discontinuous)
3		Sand
4	Shallow Aquitard (Aquitard 2*)	Silt
5	A Zone Aquifer	Fine to medium, poorly graded sand with gravel
6	Deep Aquitard	Grey silt and clay
7 and 8**	B Zone Aquifer and B/C Zone Aquifer	Coarse sand and gravel grading to a silty medium coarse sand Glaciofluvial channels
9	Lower Deep Aquitard	Silt

\*Discontinuous lenses of silt/fine sand

\*\* Layers 7 and 8 both represent the B and B/C Zone Aquifers. Two layers are used to provide better vertical discretization.

## 2.2 Simulation Period

Flow model calibration was performed so that predicted groundwater elevations matched observed groundwater elevations for both steady-state and transient conditions. The steady-state conditions represent average annual groundwater elevations, recharge, and flow conditions between October 2017 and April 2023, which were selected based on data availability and because operation of production wells remained fairly consistent throughout this period (i.e., SPWD production wells SP-PW07 and SP-PW08 are not operating, SPWD production well SP-PW09 is operating, and the four City production wells COI-PW01, COI-PW02, COI-PW04 and COI-PW05 are operating). Currently, well COI-PW05 is not operating.

Calibration to transient conditions was performed using a historical transient simulation and multiple short-term transient simulations.

The historical transient simulation is based on water level data between October 2017 and April 2023, and boundary conditions (i.e., recharge, pumping rates, specified head) were varied monthly to match seasonal water level fluctuations. The historical transient simulation period was divided into 66 stress periods of one month to represent the variations in boundary conditions. One time-step was defined for each stress period.

The short-term transient simulations are based on water level data collected with pressure transducers over week-long periods and stress periods were defined to correspond to weekly fluctuations in boundary conditions (i.e., recharge) and to production well start/stop times.

## 2.3 Model Boundaries and Stresses

The boundary conditions are shown in Figure 2-1.

### 2.3.1 Specified Head Boundary

Groundwater flow in the model domain is from south to north. Specified head boundaries are applied to the south of the model at Issaquah-Hobart Gap and the north of the model at Lake Sammamish. The head value assigned at Issaquah-Hobart Gap is set to a constant head value of 190 feet NAVD88 based on groundwater elevation. For the northern boundary, the head values vary quarterly for the historical transient simulation based on the lake stage recorded by the United State Geological Survey (USGS)<sup>3</sup> (Figure 2-5). The average value (30.3 feet NAVD88) is used for the steady-state simulation.

### 2.3.2 Specified Flux Boundary

The eastern and western margins of the model are specified flow boundaries (also known as specified flux boundaries) representing mountain-front recharge into the LIV along the foothills. The transient flux boundary conditions are shown on Figure 2-6. Total steady-state flux from this boundary is 115,000 and 195,000 cubic feet per day (1,000 and 1,600 acre feet per year [AFY]) along the eastern and western margins, respectively. This corresponds to an average of 2 inches of discharge from the watershed areas outside of the model domain. For the historical transient simulation, the flux varies consistently with precipitation fluctuations (Figure 2-6) and ranges from 0 to 800,000 cubic feet per day, which corresponds to a maximum of 0.01 inch per day of discharge from watershed areas outside of the model domain.

### 2.3.3 Rivers

River boundary conditions are defined along Issaquah and Tibbett Creeks (Figure 2-1). River stages are defined based on monitored elevations at the five stream gauging stations installed and monitored by Farallon and on the digital elevation model along each river and are assumed constant, consistent with the CARA MODFLOW model. The riverbed conductance values were adjusted as part of model calibration, and vary between 1 and 8 square feet per day per foot of river length (Figure 2-7).

### 2.3.4 Areal Recharge

Areal recharge is defined uniformly throughout the model domain and at each location, and recharge flux is assigned to the highest active cell (i.e., if the cell in Layer 1 is dry at a specific location because the simulated water level is below the bottom of the cell, the recharge flux defined at that location is applied to Layer 2). Total steady-state recharge from precipitation is 5,100 AFY, corresponding to an average recharge rate of 20 inches per year over the entire model domain. The transient recharge rate ranges from 0 to 4.5 inches per month and is consistent with precipitation patterns (Figure 2-8).

### 2.3.5 Production Wells

The production wells were defined in the model based on the screen intervals (shown in Table 2-2) and the pumping rates provided in Figure 2-9. For the period selected for the historical transient simulation, SPWD production wells SP-PW07 and SP-PW08 were not operating. The

---

<sup>3</sup> <https://waterdata.usgs.gov/monitoring-location/12122000/#parameterCode=62614&startDT=2017-01-01&endDT=2022-11-14>

pumping rates for SPWD and City wells are based on records provided by the City and SPWD. The pumping rate for Lakeside wells (simulated as a single well in MODFLOW) is based on the CDM Smith Model Report (2017) and documentation in the Well 9 [SP-PW09] Aquifer Performance Test Report (Carr, 1993). The pumping rate for the Darigold well is based on information provided by Darigold in February 2023.<sup>4</sup> Steady-state pumping rates are also provided in Table 2-2.

### 2.3.6 Initial Conditions

The simulated steady-state conditions (heads) were used as initial conditions (starting heads) for the historical transient simulation.

## 2.4 Material Properties

Material properties assigned to each cell of the model include horizontal conductivity, vertical anisotropy, specific storage, and specific yield. There are nine hydrostratigraphic units in the model representing the layered system of aquifers and intervening aquitards. Sand and gravel units (aquifers) have higher hydraulic conductivity, while silt and silt clay units (aquitards) have lower hydraulic conductivity. As described in Section 3, the calibration process included adjusting input parameters until the model simulation closely matched observations. The distribution of material properties (hydraulic conductivity and storage coefficient) was the end product of the calibration process. The hydraulic conductivity values were adjusted as part of the calibration process taking into account previous estimates from aquifer tests and modeling studies. In addition, hydraulic conductivity estimated based on grain size analysis from samples collected during installation of monitoring well COI-MW08 (Geosyntec, 2023) was also considered:

- Two of the grain size samples were collected from silt layers within the Deep Aquitard, and the estimated hydraulic conductivity for this unit was approximately 0.5 feet per day.
- One grain size sample was collected from a silty sand within the B Zone Aquifer, and the estimated hydraulic conductivity for this unit was between 10 and 25 feet per day.
- One grain size sample was collected within a poorly-graded sand within the B Zone Aquifer, and the estimated hydraulic conductivity for this unit was between 80 and 200 feet per day.

Figure 2-10 shows the post-calibration distribution of hydraulic conductivity assignments. The calibrated hydraulic conductivities are summarized in Table 2-3 and the range of material properties is consistent with previous estimates from aquifer tests and modeling studies, and with grain size analysis from samples collected during installation of monitoring well COI-MW08 (Geosyntec, 2023).

---

<sup>4</sup> Email from Darigold Senior Environmental Manager on February 10, 2023.



As shown in Figure 2-10, aquifers extend over the entire model domain, while Aquitards 1 and 2 are not present in the southern portion of the LIV. In addition, material with high hydraulic conductivity (300 – 450 feet per day) is present on the eastern side of the LIV which is consistent with the conceptual model of the high-permeability delta deposits concentrated along the eastern valley area (Geosyntec, 2022b and Golder Associates, 1993). Generally hydraulic conductivity in aquifers is lower in the northern portion of the model, consistent with the conceptual model of lower permeability material in the vicinity of Lake Sammamish.

All horizontal hydraulic conductivity assignments are isotropic, i.e., the same in all horizontal directions. Calibration was achieved with a vertical anisotropy (ratio of horizontal to vertical hydraulic conductivity) of 10 over the entire model domain (horizontal conductivity is 10 times higher than vertical conductivity). A vertical anisotropy of 10 is typical for groundwater modeling applications and is consistent with previous observations that the long-term water-level fluctuations and pumping test responses limited vertical anisotropy (i.e., 10 or lower) within the aquifers (Golder Associates, 1993). The calibrated specific yield and specific storage are also uniform at 0.20 and  $1 \times 10^{-5}$  feet<sup>-1</sup>, respectively. There are limited data available for specific yield and storage, and acceptable calibration was achieved without adding complexity.

### 3. GROUNDWATER FLOW MODEL CALIBRATION

#### 3.1 Calibration Data

The primary output from a model consists of hydraulic head (water level) and groundwater flux at every active cell for every model time-step. The model was calibrated both to long-term flow conditions and to short-term water level fluctuations observed during multiple pumping rate fluctuations at production wells. The model was calibrated to five calibration datasets, as described below.

##### 3.1.1 Calibration to Steady-State Conditions

###### Calibration Data Set 1: Average Steady-State Water Levels

Average water level data measured at 78 monitoring wells were used in the steady-state model calibration. The average water levels were calculated based on available measured water levels between October 2017 and April 2023. Water level data were also categorized by aquifer unit. These steady-state observation data are summarized in Table 3-1, and locations are shown on Figure 3-1. As illustrated in Table 3-1 and Figure 3-1, there are limited data (four locations) for the B and B/C aquifers.

##### 3.1.2 Calibration to Transient Conditions

###### Calibration Data Set 2: Historical Water Levels

Water level data between October 2017 and April 2023 were used for calibration to historical transient conditions. A total of 1,214 head observations from 78 monitoring wells were used in



the transient calibration process. For calibration of the historical transient simulation, the model was run from October 2017 to July 2023<sup>5</sup> with monthly stress periods.

In addition, the following transducer data were used to calibrate the groundwater flow model using multiple short-term (i.e., multi-weeks) transient simulations:

- Data from transducers deployed in multiple SPWD monitoring wells between 2016 and 2021;
- Data from transducers deployed in multiple COI monitoring wells between May 2016 and August 2017; and
- Data from transducers deployed in multiple monitoring wells in October 2022 as part of the work performed under the IAA (Geosyntec, 2022c).

Three specific periods were selected for calibration of the short-term transient simulations. The periods are illustrated in Figure 3-2 and summarized below:

- Calibration Data Set 3: May 7, 2016, through April 29, 2017 (Figure 3-2A):
  - For SPWD production wells, only one of the three production wells is operating at a time in this period, and SP-PW07 and SP-PW08 are not operating after mid-October 2016.
  - For City production wells, pumping rates decrease significantly at COI-PW01 and COI-PW02 in September 2016, COI-PW05 starts pumping in August 2016, and COI-PW04 is off for a few days in July 2016.
- Calibration Data Set 4: September 10, 2021, through November 3, 2021 (Figure 3-2B):
  - Production well SP-PW09 stops pumping on October 6, 2021, through November 5, 2021, and SP-PW07 and SP-PW08 were not pumping during this period.
  - Production well COI-PW05 stops pumping in October 2021. The other City's production wells are pumping continuously.
- Calibration Data Set 5: October 1, 2022, through April 8, 2023 (Figure 3-2C):
  - Production well COI-PW04 is pumping continuously except for an inactive period of 13 days starting on March 8, 2023.
  - Production well SP-PW09 starts pumping in November 2022.

For calibration to the transducer data, the model was run for the three simulation periods listed above. The stress periods were set to correspond to well start/stop times, and the time steps were

---

<sup>5</sup> The simulation period for the historical transient simulation was from October 2017 to July 2023. Water level data was only available through April 2023. Simulated water levels between May and July 2023 were not compared to observed data, as those were not available.

set to 1 to 4 days. The initial head was set using the simulated heads from the steady-state model for May 2016 and from the historical simulation run for September 2021 and October 2022.

## 3.2 Calibration Process

Calibration was performed iteratively between the steady-state and historical (multi-years)/short-term (multi-weeks) transient simulations, including using automatic calibration with PEST. The hydraulic properties of horizontal hydraulic conductivity, storativity, and riverbed conductance were systematically adjusted to improve the fit between observed and simulated calibration data (steady-state water levels, historical water levels, and transducer data). In addition, boundary conditions such as mountain-front recharge and areal recharge were adjusted as part of the calibration.

The calibration results presented below are based on the final version of the LIV Model, which includes the refinements on the material properties and boundary conditions.

## 3.3 Calibration Results

### 3.3.1 Steady-State Water Levels

Figure 3-3 presents a scatter diagram for the 78 steady-state calibration observations. Each point on the graph represents an observed water level (x-axis) plotted against its corresponding simulated water level (y-axis). The centerline represents perfect agreement (calibration) between observed and simulated, and the distance away from the centerline represents the magnitude of the error for each point. The scatter diagram provides a visual illustration of the goodness of fit achieved during this preliminary calibration process.

In addition to the visual illustration provided by the scatter diagram, a number of quantitative metrics were used to assess model error. The following statistics were generated to quantify the calibration set:

- Mean error (ME) – The mean difference between the observed head and the corresponding simulated head;
- Root mean square error (RMSE) – The square root of the average of the squared differences between the simulated head and the corresponding observed head;
- RMSE % – The RMSE divided by the range of observed heads across the model domain, consistent with Section 6.4 of ASTM D5981 (ASTM, 1998e1). The RMSE normalized by the range of observed data can be a useful metric because it puts the RMSE in context with the range of water levels that the model simulates. However, the RMSE as % of the range of the observed data is sensitive to the data set and can be a misleading indicator of the quality of the model calibration. For example, in the case of the B and B/C Zone Aquifers, where available observed groundwater levels varied only 5.4 feet in elevations from four monitoring locations, the % RMSE of 34% for this zone was relatively larger than the % RMSEs in other zones despite having a comparable residual of 1.8 feet; and

- Coefficient of determination ( $R^2$ ) - statistical measure of how close data points are to a fitted regression line, or how well a line fits the data. A set of X, Y (observed, simulated) points could closely fit a line and thus the line fitted to the points would have a high  $R^2$  value, but the set of points could be a poor match to the line defined by  $X=Y$ , which is the target for a model calibration. The  $R^2$  value relevant to a model calibration must be for an  $X=Y$  line.

$$R^2 = 1 - \frac{\sum_{n=1}^m (obs_n - sim_n)^2}{\sum_{n=1}^m (obs_n - \text{mean obs})^2}$$

where:

$obs_n$  = nth observed value

$sim_n$  = nth simulated value

mean obs = mean of the observed values.

The calibration metrics are summarized for all observed data per aquifer zones and for the entire model domain in the table in Figure 3-3. The calibration metrics outlined in this section are summarized for each aquifer zone and for the entire model domain in Figure 3-3. Table 3-1 presents the ME for each of the 78 observation locations.

The simulated water level contours for the steady-state model for the three main aquifer zones are shown in Figures 3-4a-c with residuals at the individual observation locations.

### 3.3.2 Historical Transient Water Levels

The model was calibrated to fit the observed head at the monitoring wells between 2017 and 2023. Hydrographs of the simulated and observed heads between 2017 and 2023 at 78 monitoring wells are shown in Figure 3-5a-d. Only three of the 78 individual calibration wells showed a poor fit to the model, as follows:

- B-7 screened in the Shallow Zone Aquifer (Figure 3-5a): the simulated water levels are higher than the observed water levels, but the fluctuations are consistent. The observed water levels at this well are uncertain as the elevation of the top of casing is not based on surveyed data. Therefore, the lack of fit is likely due to an error in the estimated top of casing. As there are several observation locations in the western portion of the model, this data gap is not significant and other locations can be used to evaluate the consistency of the simulated water levels with observed data.
- B-2 and B-4 screened in the Shallow Zone Aquifer (Figure 3-5b): the simulated water levels present larger fluctuations than the observed water levels. Those wells are located along the western edge of the valley (Figure 3-4a). The smaller observed fluctuations may be due to a more uniform mountain front recharge along the western edge in this area than in the area in the vicinity of the monitoring wells NWN monitoring wells. The steady-state residuals for these wells are ~1 foot, indicating that the steady-state recharge is consistent with observed water levels.

In general, simulated water levels are slightly overestimated in the southern portion of the LIV in the vicinity of Memorial Field and Rainier Trail potential source areas (see Section 5.4), as illustrated by the hydrographs for RT-MW01, RT-MW03, MF-MW02, MF-MW03, MF-MW04.

In addition to the visual illustration provided by the hydrographs, statistics were generated to quantify the calibration data set. The ME is -0.35 feet, and the RMSE is 3 feet. The RMSE corresponds to 8% of the observed head range (36.5 feet).

Hydrographs of the simulated and observed water levels at selected monitoring wells located in a well cluster are shown in Figures 3-6a-b to illustrate the observed and simulated vertical head difference between monitoring wells screened at different depths. Generally, the observed water levels do not indicate significant vertical head difference, consistent with the simulated water levels.

The historical transient simulation results indicate that the model can reproduce the major recharge mechanisms impacting water levels and the observed water level differences between the main aquifer zones.

### 3.3.3 Transducer Data

Hydrographs of the simulated and observed water levels are shown in Figures 3-7 through 3-9 for the three simulation periods. The fit between the simulated and observed heads is generally good and indicates that the model can reproduce short-term water level fluctuations in addition to the long-term fluctuations noted in the previous section.

## 3.4 Summary of Flow Model Calibration Results

The calibration of the groundwater flow model (steady-state and long-term/short-term transient) is summarized as follows:

- Simulated heads mimic the important aspects of the flow system, such as magnitude and direction of the head contour.
- Calibrated material properties are consistent with the conceptual model and within the range of measured or previously estimated values.
- Comparison of simulated and observed hydrographs at monitoring wells is satisfactory, and the model can reproduce the major recharge mechanisms impacting water levels.
- Comparison of Simulated and observed hydrographs at monitoring wells during short-term changes of production well operations and/or recharge is satisfactory.

## 4. SIMULATED GROUNDWATER FLOW BALANCE

The groundwater flow model provides a tool for assessing and predicting the groundwater flow field under varying conditions. In particular, the groundwater flow model can be used to generate potentiometric surfaces and flow vectors at various times and at multiple depths within the flow system. The potentiometric surfaces provide a means to assess the variation in the flow field with depth and to evaluate the timing and distribution of historical shifts in the flow regime.

The groundwater flow model can also be used to evaluate the water balance. The water balance provides an accounting of the various components of water inflow to, and outflow from, the model domain. The steady-state values of these components are indicative of the primary drivers of the flow field.

The simulated steady-state water balance is provided in Table 4-1.

The total groundwater flow through the model is approximately 11,000 AFY or 15 cfs. This is similar to and in the same order of magnitude as the estimated flow in previous studies (Golder Associates, 1993; 2000), which estimated a total inflow/outflow of 18 to 25 cfs through the LIV. The majority of the inflow is through areal recharge (almost 50%) and mountain-front recharge (25%). The rest of the inflow consists of river leakage (20%) and southern inflow (10%). The highest simulated river leakage is from Tibbetts Creek, however this value is not well constrained as there are no data available in the vicinity of Tibbetts Creek. The river leakage from Tibbetts Creek has limited impact on the groundwater flow field in the central LIV, which is the focus of this study. The simulated inflow/outflow from the North Fork, East Fork, and main stem of Issaquah Creek (~10% of total inflow) are better constrained with monitoring wells located in the vicinity of these rivers. Issaquah Creek is simulated as a losing stream south of the East Fork confluence, with a hinge point in the area around the East Fork confluence where the stream transitions from gaining to losing, which is consistent with previous evaluations (Golder, 2002), and with data collected at stream gauging stations and nearby monitoring wells by Farallon, which indicates a losing stream at stream gauging station 4 south of the East Fork confluence and a gaining stream at stream gauging station 2 north of the confluence (Geosyntec, 2022; Farallon, 2023), as shown in Figure 4-1. The East Fork Issaquah Creek is simulated as a losing stream (Figure 4-1), which is consistent with data collected at stream gauging station 3 and nearby monitoring well by Farallon (Geosyntec, 2022; Farallon, 2023).

The simulated water balance for the transient historical simulation is shown in Figure 4-2. The change in storage illustrates the significant water level fluctuations observed in the LIV in response to recharge and dry periods.

Under transient conditions, the location of the hinge point where Issaquah Creek transitions from gaining to losing varies slightly (~1,000 feet) between south of the East Fork confluence in wet conditions (January through April) and north of the East Fork confluence in dry conditions (July through October).

## 5. CONTAMINANT FATE AND TRANSPORT MODEL

Based on Washington State Department of Health State Action Levels (SALs) for drinking water, and the prevalent PFAS compounds detected in the LIV, three PFAS compounds were selected for fate and transport simulation, consistent with the IAA:

- Perfluorooctanesulfonic acid [PFOS]
- Perfluorohexanesulfonic acid [PFHxS]
- Perfluorobutanesulfonic acid [PFBS]

AFFFs released to the soil surface typically consist of a complex mixture of PFAS compounds. The PFAS compounds listed above are assumed to be present at different concentrations in AFFFs. In addition, transport properties, e.g., partitioning in unsaturated zone and sorption to aquifer sediments in the saturated zone of each PFAS vary significantly. Those transport properties determine the fate and transport, such as the downgradient migration rate for each compound. For example, compounds with higher sorption will tend to migrate at a slower rate in the subsurface. The source concentrations for the three PFAS compounds used in the model are based on measured concentrations in shallow groundwater, as described in Section 5.3.

The three PFAS are simulated with the fate and transport model, but fate and transport calibration focused on PFOS (see Section 6.1).

## 5.1 Grid Refinements

The model layers 2 through 8 used in the calibrated flow model were sub-divided into three layers each for the fate and transport simulations to provide better vertical discretization and better represent transport pathways and concentration gradients. Layers were sub-divided uniformly and hydraulic properties from the parent layer was kept unchanged. The table below summarizes the original flow model layers and subdivided transport model layers.

Flow Model Layers	Transport Model Layers
1	1
2	2-4
3	5-7
4	8-10
5	11-13
6	14-16
7	17-19
8	20-22
9	23

## 5.2 Simulation Period and Stress Periods

Based on historical usage of AFFF at potential sources, which started in 1970s, a 53-year (1970 to 2023) simulation period is used. The flow model for the fate and transport simulation was setup using the steady-state model inputs for all boundary conditions (areal and mountain front recharge, northern and southern specific heads, and rivers) except for the production wells, which operations have changed since 1970s. Based on well installation dates and historical information on well operation, six stress periods were defined with the following constant pumping rates assigned at each production well.

		Pumping Rates in gallons per minute								
Stress Period Start	Stress Period End	COI-PW01	COI-PW02	COI-PW04	COI-PW05	SP - PW07	SP-PW08	SP-PW09	Darigold	Lakeside
1/1/1970	1/1/1980	400	400	0	0	0	0	0	0	0
1/1/1980	1/1/1985	400	400	0	0	0	0	0	0	0
1/1/1985	1/1/1995	400	400	150	130	500	500	0	0	220
1/1/1995	1/1/2005	400	400	150	130	500	350	0	220	220
1/1/2005	1/1/2017	220	450	66	195	500	500	260	220	220
1/1/2017	7/1/2023	220	450	160	230	0	0	900	400	600

### 5.3 Transport Properties

Transport properties were defined uniformly in the model domain based on literature values and model scale and were adjusted as part of model calibration. The transport properties are summarized in Table 5-1.

The effective porosity for the entire model is defined at 15%, based on typical effective porosity of alluvial sands and gravel between 10% and 25% (McWhorter and Sunada, 1977). The use of uniform effective porosity for the entire model is reasonable in the absence of site-specific data and is consistent with previous simulations (CDM Smith, 2017; Geosyntec, 2021). Future refinements of transport properties may be appropriate based on additional data.

Longitudinal dispersivity was calculated using an empirical relationship between longitudinal dispersivity and scale of flow proposed by Schulze-Makuch (2005):

$$\alpha = c(L)^m$$

Where:

$\alpha$  = longitudinal dispersivity in meters

$c$  = a parameter characteristic for a geologic medium

$L$  = the flow distance in meters

$m$  = a scaling exponent

Based on the values for the parameters  $c$  and  $m$  in unconsolidated sediments (0.085 and 0.81 using considered studies, 0.112 and 0.70 for studies with high and intermediate reliabilities, and 0.20 and 0.44 for studies with high reliability only), and a scale of interest of approximately 3,000 feet, the resultant longitudinal dispersivity varies between 10 and 70 feet. The longitudinal dispersivity value was adjusted through calibration to a value of 20 feet. The horizontal and vertical transverse dispersivities were adjusted through calibration to values of 10% and 0.5% of the longitudinal dispersivity, respectively, which is consistent with literature values reporting transverse horizontal and vertical dispersivities one to two orders of magnitude and between 100 and 1,000 times lower than horizontal dispersivity, respectively (Gelhar et al., 1992).



Sorption is a process that slows the movement and mass of contaminants through attachment of contaminants to the matrix of the aquifer. It is defined by the partitioning (or distribution) coefficient ( $K_d$ ).  $K_d$  is often correlated with the organic carbon content of the aquifer matrix and can be calculated as the product of fraction of organic carbon ( $f_{oc}$ ) multiplied by the organic carbon distribution coefficient ( $K_{oc}$ ) for the contaminant.  $K_{oc}$  varies depending on the specific contaminant compound being evaluated, while  $f_{oc}$  is a soil property. Sorption is assumed to vary linearly with concentration (linear isotherm), and  $f_{oc}$  is assumed equal to 0.1%. Site-specific  $f_{oc}$  values are not available and a  $f_{oc}$  value of 0.1% is consistent with sand and gravel materials in the Puget Sound. The  $K_{oc}$  coefficients are based on literature values for PFAS (Table 5-1) (Interstate Technology Regulatory Council, 2020, which includes estimated  $K_{oc}$  coefficients for PFOS sorption to soil from six studies published between 2010 and 2019). The retardation factor ( $R$ ) is calculated based on  $K_d$ , bulk density ( $\rho_b$ ), and porosity, and corresponds to the factor between groundwater velocity and solute transport velocity. Site-specific total porosity values are not available and for this work, the total porosity is estimated to 30% based on typical total porosity of alluvial sands and gravel between 20% and 45% (McWhorter and Sunada, 1977), and the bulk density is calculated based on quartz density and total porosity.

## 5.4 PFAS Sources in Model

The five PFAS sources in the LIV identified under Washington State Model Toxics Control Act (MTCA) were considered for the fate and transport model.

- 175 Newport Way (EFR Headquarters)
  - Historical AFFF training occurring from the early 1980s to the late 1990s at the 175 Newport Way is believed to be the primary source of PFAS detected in COI-PW04. Typically, one to three 5-gallon buckets of AFFF were expended at the site up to 12 times per year (Farallon, 2019). Other activities at the site, such as washdown and equipment maintenance procedures, may also have contributed to PFAS detections in groundwater (Farallon, 2019). PFOA, PFOS, PFHxS, PFHxA, and PFBS were detected at average concentrations of 310, 5,000, 1,200, 640, 200 nanograms per liter (ng/L), respectively, in shallow groundwater samples at the 175 Newport Way site. For the purposes of the model simulations, these concentrations were used as source concentrations in groundwater at 175 Newport Way and assumed to have increased linearly from 0 in 1980 to the values listed above in 1985 and remain constant afterwards, based on the high recharge and downward vertical gradient observed at the site.
- 555 Northwest Holly Street, which includes Dodd Fields Park and Issaquah Valley Elementary School West Playfield (the School), was also identified as a former AFFF training area.
  - Historical AFFF training occurred here from the early 1970s to the early 1980s approximately once or twice a year. The quantity of AFFF used per training event is assumed to have been similar to 175 Newport Way (one to three 5-gallon buckets per event) (Farallon, 2019). PFOA, PFOS, PFHxS, PFHxA, and PFBS in shallow groundwater samples were detected at



average concentrations of 8, 550, 200, 10, 20 ng/L, respectively, at the Dodd site and at average concentrations of 15, 250, 160, 55, 45 ng/L, respectively at the School site. Two source areas are defined in the model, and for the purposes of the model simulations, these concentrations were used as source concentrations in groundwater beneath the two source areas and assumed to have increased linearly from 1970 to 1980 and remain constant afterwards.

- Southern portion of King County Parcel No. 5279100070 north of 190 East Sunset Way (Memorial Field) was also identified as a former AFFF training area.
  - Historical AFFF training occurred here from the early 1980s to the mid-1990s approximately once or twice a year. Training exercises were similar to those performed at the School. Typically, one to three 5-gallon buckets of AFFF concentrate was expended during each training event (Farallon, 2019). PFOA, PFOS, PFHxS, PFHxA, and PFBS were detected at average concentrations of 4, 100, 30, 2, 10 ng/L, respectively, in shallow groundwater samples at the site. For the purposes of the model simulations, these concentrations were used as source concentrations in groundwater at Memorial Field and assumed to have increased linearly from 1980 to 1990 and remain constant afterwards.
- Central portion of King County Parcel No. 3424069043 west of 135 East Sunset Way (Rainier Trail) was also identified as a former AFFF training area.
  - Historical AFFF training occurred here from the early 1970s to the early 1980s approximately once a year. Training exercises were similar to those performed at Memorial Field. Typically, one to three 5-gallon buckets of AFFF concentrate was expended during each training event (Farallon, 2019). PFOA, PFOS, PFHxS, PFHxA, and PFBS were detected at average concentrations of 15, 50, 30, 8, 10 ng/L, respectively, in shallow groundwater samples at the site. For the purposes of the model simulations, these concentrations were used as source concentrations in groundwater at Rainier Trail and assumed to have increased linearly from 1970 to 1980 and remain constant afterwards.

In the model, the PFAS sources are simulated with specified concentrations defined at the water table (i.e., in Layer 1), simulating the transport of PFAS originating at the water table, which becomes a “continuous” (i.e., until the end of the simulation in July 2023) source of PFAS that can move to downgradient areas long after the release of AFFF at the ground surface. This model does not simulate AFFF releases to the unsaturated soil surface, AFFF partitioning in the soil following release, or the transport of PFAS in the unsaturated zone. Soil can be a significant reservoir for PFAS that then leaches to the water table and begins to flow with groundwater. Because of complex retention processes in the unsaturated zone, PFAS concentrations in unsaturated soil are generally order of magnitude higher than concentrations in groundwater, and significant retention of PFAS in the vadose zone over long timeframes is expected (Brusseau et al., 2020). Applying a specified source concentration for PFAS at the water table beneath the source area that is lower than the soil concentration is an appropriate approach to defining the groundwater transport pathway in this evaluation. This approach is consistent with the previous

two-dimensional (2D) numerical modeling of PFAS migration (Geosyntec, 2021). Alternative approaches include simulating PFAS transport through the vadose zone using unsaturated zone models and using the simulated PFAS flux at the water table as an input to the groundwater fate and transport model. Because of the complex retention processes occurring in the vadose zone and the uncertainty about AFFF releases, this approach is uncertain. Instead, measured concentrations in groundwater were used for this modeling work to define PFAS sources.

The model simulates time-varying sources of PFAS at the water table beneath those source areas since the estimated start of the potential PFAS releases at each location (1980 to 2023 for 175 Newport Way, Rainier Trail and Memorial Field and 1970 to 2023 for Dodd Fields Park, Issaquah Valley Elementary School West Playfield), i.e., linearly increasing concentrations followed by constant concentrations at the average measured groundwater concentrations (as detailed above). The historical groundwater concentrations beneath the sources are unknown and likely fluctuated over time. The model does not simulate the vadose zone processes that determine the volume and concentration of PFAS at the water table. However, this simplified approach is reasonable and common practice in groundwater modeling for groundwater fate and transport simulation and to better understand contaminant migration in the subsurface.

## 6. CONTAMINANT FATE AND TRANSPORT MODEL CALIBRATION

Consistent with the IAA, the fate and transport calibration was mostly qualitative and focused on matching the observed regional PFOS plumes in the Shallow and A Zone Aquifers.

### 6.1 PFAS Calibration Data

The three PFAS are simulated with the fate and transport model, but fate and transport calibration focused on PFOS as described below.

Monitoring data were used to generate PFOS plumes in the Shallow and A Zone Aquifers as part of the development of the hydrogeological regional model (Geosyntec, 2022b). In addition, average monitoring data for PFOS, PFHxS, and PFBS were used to compare simulated concentrations. Most PFAS monitoring data are available after 2020, with a few data points between 2016 and 2020; therefore, the ability to calibrate to historical concentrations is limited.

### 6.2 Calibration Results

The simulated PFOS concentrations are compared with the interpolated PFOS plumes and concentrations in the Shallow, A and B Zone Aquifers in Figures 6-1, 6-2, and 6-3, respectively. The comparison indicates the following:

- Shallow Aquifer: The shape of the simulated plume in the Shallow Aquifer (Figure 6-1b) generally mimics the interpolated contours (Figure 6-1a). The simulated plume is narrower and slightly longer, especially along the western margin. The simulated core of the plume is slightly longer but generally provides a good fit for 0.5 to 1 micrograms per liter ( $\mu\text{g/L}$ ) contours.
- A Zone Aquifer: The simulated concentrations (Figure 6-2b) are generally consistent with measured concentrations, but the model does not reproduce the high

concentrations detected on the western side at IES-MW10, as the core of the plume is simulated slightly more east than the interpolated plume contours (Figure 6-2a).

- In the B Zone Aquifer, the simulated contours are consistent with the concentrations detected at COI-MW08 and COI-PW05, but comparison of observed and simulated concentrations is limited to these two data points. In general, the simulated PFOS plume in the B Zone Aquifer is similar with a slightly smaller overall footprint compared to the A Zone Aquifer. The simulated core of the plume in the B-zone is similar to the A-zone, but the margins of the plume are narrower. Additional data is needed to confirm the extent of the plume simulated for the B Zone Aquifer.

In addition, the simulated PFAS concentrations in 2023 are compared to average measured concentrations at 68 wells in Table 6-1. The simulated PFOS, PFHxS, and PFBS concentrations are generally consistent (i.e., order of magnitude consistency) with the observed concentrations. However, some of the observed discrepancies include the following:

- PFAS concentrations close to the 175 Newport Way Site, as the model does not represent the heterogeneous concentrations detected in close vicinity;
- PFAS concentrations in the A Zone Aquifer at the Issaquah Valley Elementary School and Dodd Fields Park Site, as the model overestimates concentrations on the eastern side and underestimates concentrations on the western side at IES-MW10. This may be due to different historical groundwater flow fields from historical pumping patterns that are not taken into account in the fate and transport model; and
- PFAS concentrations at SPWD production wells, which are underestimated with the model. This may be due to different historical groundwater flow fields from historical pumping patterns that are not taken into account in the fate and transport model.

## 7. CALIBRATION SENSITIVITY ANALYSIS

### 7.1 Groundwater Flow Model Calibration Sensitivity

A sensitivity analysis was performed to evaluate how the calibrated flow model responds to changes in the model inputs. The sensitivity analysis consisted of independently varying selected model parameters to quantitatively assess how the changes in parameters affect the calibration metrics.

Sensitivity analysis is often used in modeling to evaluate how robust the results of a model are relative to the uncertainty of its inputs. By understanding relationships between input and output variables in a model, future analysis can be focused on variables or in areas where that will most improve the robustness of a model. Unexpected relationships between inputs and outputs can also be evaluated through sensitivity analysis to identify potential errors in the model.

#### 7.1.1 Parameters

The sensitivity analysis evaluated four input parameters (Table 7-1):

- Horizontal hydraulic conductivity;

- Vertical anisotropy ratio;
- Riverbed conductance; and
- Areal and mountain front recharge.

Model sensitivity is expressed in terms of predicted hydraulic head versus observed hydraulic head.

### 7.1.2 Sensitivity Assessment

For each sensitivity run, the steady-state calibration period was simulated with all input parameters equal to the baseline calibrated model except for the specified sensitivity parameter (P). The outputs from the sensitivity runs were used to calculate new calibration error statistics. The normalized sensitivity coefficient (NSC; in percent) for hydraulic head was calculated based on the change in RMSE for each sensitivity run ( $\Delta\text{RMSE}$ , in feet) and compared to the baseline RMSE ( $\text{RMSE}_0$ , in feet) as follows:

$$\text{NSC (head)} = (\Delta\text{RMSE}/\text{RMSE}_0)/(\Delta P/P_0)$$

Where  $\Delta P$  is the change in parameter value (in units consistent with the parameter units) and  $P_0$  is the calibrated parameter value (in units consistent with the parameter units).

Table 7-1 presents the NSC for each sensitivity run. An absolute NSC above 20% is considered to be associated with a sensitive parameter.

Overall, the calibrated steady-state model is sensitive to all parameters with absolute NSC above 30%, except for the vertical anisotropy ratio. In particular, the calibrated steady-state model is very sensitive to the parameters defining recharge (areal and mountain front), as well as to a reduction in hydraulic conductivity, indicated by the very large NSC values (100% – 600%) for those parameters. In contrast, the model is not very sensitive to the vertical anisotropy, indicating the model would be equally well calibrated with a lower vertical anisotropy ratio. This suggests that, in general, adding further fine-scale complexity to individual layers (discontinuous silt lenses, for example) is not likely to improve the calibration of heads in the model.

The sensitivity analysis indicates that the hydraulic parameters used in the model are overall well constrained by observed water-level data and further adjustment of hydraulic properties is unlikely to result in a better hydraulic calibration to existing water levels. Therefore, the model provides a robust tool that is aligned with existing water level data and can be confidently used for further predictive simulations of groundwater flow.

## 7.2 Fate and Transport Model Calibration Sensitivity

Four model simulations were run to illustrate model sensitivity compared to the calibrated fate and transport model results.

### 7.2.1 Parameters

The sensitivity analysis evaluated input parameters as follows:

- Enhanced transport with sorption coefficient and effective porosity varied by a factor 0.5 and dispersion varied by a factor of 1.5;
- Reduced transport with sorption coefficient and effective porosity varied by a factor 1.5 and dispersion varied by a factor of 0.5;
- Decreased sorption with sorption coefficient varied by a factor of 0.5; and
- Hydraulic conductivity varied by a factor of 1.2.

Model sensitivity is evaluated by visually comparing the simulated PFOS plumes.

### 7.2.2 Sensitivity Assessment

For each sensitivity run, the fate and transport calibration period was simulated with all input parameters equal to the baseline calibrated model except for the specified sensitivity parameters. The simulated PFOS plumes in the Shallow and A Zone Aquifers are compared to the calibrated model results in Figures 7-1a-d.

As shown in Figures 7-1a-c, varying transport parameters does not change the simulated PFOS plumes significantly, and the results are similar to the calibrated model results. This indicates that, while the transport parameters are not well constrained by calibration to independent measurements, further refinement of those parameters through independent measurements will have a lesser effect on model accuracy than hydraulic properties, which are well constrained by calibration as discussed in Section 7.1.2. Therefore, even though there are some uncertainties in the exact values for these transport properties, this uncertainty is not expected to change the model results. The sensitivity of simulated PFOS concentrations to a change in hydraulic properties is illustrated in Figure 7-1d. This shows that hydraulic properties are more sensitive than the transport parameters, as the simulated PFOS plumes are different than for the calibrated model results. However, the difference is not significant, and the model predicts observed PFOS concentrations fairly well.

The combined sensitivity analysis of both hydraulic parameters and contaminant transport properties indicates that the parameters used in the model are overall well constrained by observed data and further adjustment of model properties is unlikely to result in a better calibration to existing data. Therefore, the model provides a robust tool that is aligned with existing water level and PFAS data and can be confidently used for further predictive simulations of future PFAS concentrations, potential remedial actions or the effects of future water supply pumping patterns on the geometry and extent of the PFAS plume.

## 8. SUMMARY AND NEXT STEPS

This report documents the development and calibration of the numerical groundwater flow and fate and transport model for the LIV (2023 LIV Model). The 2023 LIV Model was developed based on previous modeling studies and further refined following additional data collection as part of the IAAs.<sup>6</sup> The flow model calibration included calibration to five calibration datasets

---

<sup>6</sup> Multiple IAAs between Ecology and either the City of Issaquah or Eastside Fire & Rescue.

under both steady-state and transient conditions, including long-term (5 years) and short-term transient data. PFAS fate and transport simulations were performed for three PFAS compounds, PFOS, PFHxS, and PFBS. Fate and transport calibration was performed by varying transport parameters and historical source terms to match current observations of PFOS plumes. Flow and fate and transport calibrations matched observed data/measurements and are within standard specifications for calibration. The model provides a robust tool that is aligned with existing water level and PFAS data and can be confidently used for further predictive simulations of future PFAS concentrations, potential remedial actions or the effects of future water supply pumping patterns on the geometry and extent of the PFAS plume.

Next steps: The 2023 LIV Model provides a tool that can be used to evaluate pumping strategies, remedial objectives, potential future well locations, and compliance strategies for PFAS in the LIV aquifer system, including evaluation of PFAS on the east side of the LIV.

Model limitations and data gaps: The model presented in this report is a well-calibrated groundwater flow and fate and transport model that is suitable for use as a screening tool for a range of applications as outlined above. However, there are still limitations with respect to the overall distribution of measured water-levels and PFAS concentrations in some areas. For example, data in the B Zone Aquifer is limited to only a few locations and time frames and understanding of migration pathways of PFAS to the east side of the LIV is limited. The model was designed with the expectation of continuous refinement as additional data is collected, particularly in conjunction with the assessment of remedial actions. This modeling effort has identified several data gaps that will provide valuable data for further refinement of the flow and fate and transport model. These data gaps do not, however, prevent the model from being used now as a tool to support future analyses. Specific data gaps include the following:

- Further delineation B-Zone Aquifer, including its hydraulic properties and the extent of PFAS in the aquifer;
- Further characterization of stream/aquifer interactions along the Issaquah Creek in the vicinity of COI-PW04 and COI-PW05;
- Further characterization of PFAS transport processes in the subsurface, including sorption parameters (i.e.,  $f_{oc}$  values or  $K_d$  values) and aquifer parameters controlling advective transport (i.e., total and effective porosity);
- Aquifer distribution and hydraulic characteristics north of COI-PW04 and COI-PW05 (towards Lake Sammamish); and
- Continued monitoring of water levels and PFAS concentrations throughout the aquifer system, include consideration for performing pumping tests at multiple locations, to provide additional data for model verification and refinements.

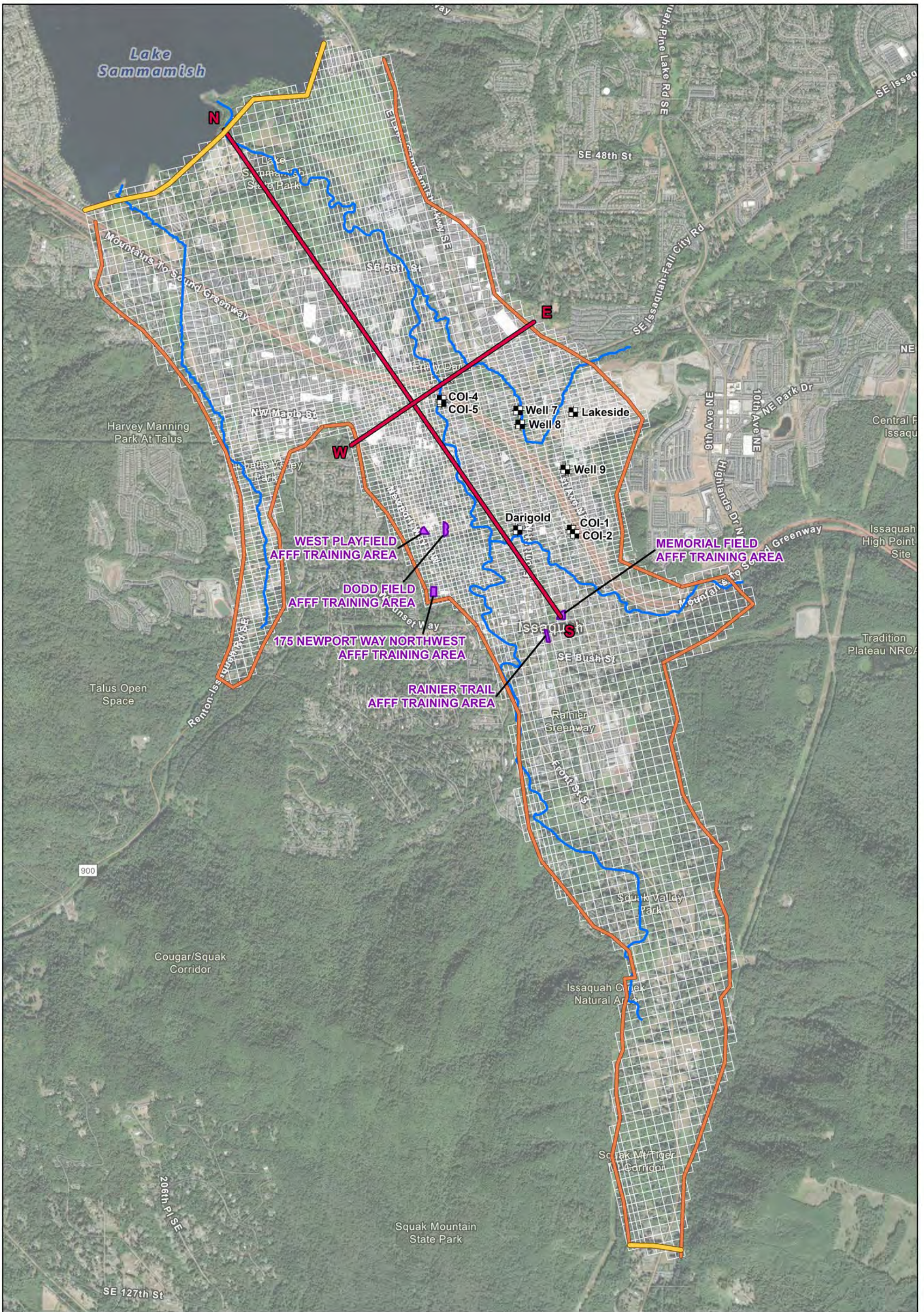


## 9. REFERENCES

- Brusseau, Anderson, Guo, 2020. PFAS concentrations in soils: Background levels versus contaminated sites. *Science of the Total Environment*, 740 (140017).  
<https://doi.org/10.1016/j.scitotenv.2020.140017>
- CDM Smith, 2017. Groundwater Model Development and Applications for PFC Risk Mitigation. April.
- Farallon, 2023. Draft Tables and Figures. June 22.
- Gelhar, Welty, and Rehfeldt, 1992. A critical review of data on field-scale dispersion in aquifers, *Water Resources Research*, 28 (7), pages 1955–1974.
- Geosyntec Consultants (Geosyntec), 2021. Groundwater Flow and PFAS Transport Modeling Report, Issaquah, Washington. September 2021.
- Geosyntec, 2022a. Critical Aquifer Recharge Area (CARA) Mapping and Assessment Report, Issaquah, Washington. November (*revision publication date pending*).
- Geosyntec, 2022b. Regional Conceptual Hydrogeological Model. December 30.
- Geosyntec, 2022c. Data Gaps Investigation Work Plan Addendum 1 – Hydrogeological Characterization Well Installation. October 7.
- Geosyntec, 2022d. Preliminary Groundwater Flow Model Calibration. December.
- Geosyntec, 2023. Well Installation Completion Report. January.
- Golder Associates, 1993. Lower Issaquah Valley Wellhead Protection Plan. November.
- Golder Associates, 2000. Groundwater Modeling of Pumping at Well COI-6. November.
- Interstate Technology Regulatory Council, 2020. Table 4-1 (<https://pfas-1.itrcweb.org/>). Accessed December 2020.
- McWhorter, D. B., & Sunada, D.K., 1977. Ground-water hydrology and hydraulics. Fort Collins, Colo: Water Resources Publications
- Schulze-Makuch, D., 2005. Longitudinal dispersivity data and implications for scaling behavior. *Ground Water*, 43: 443–456.

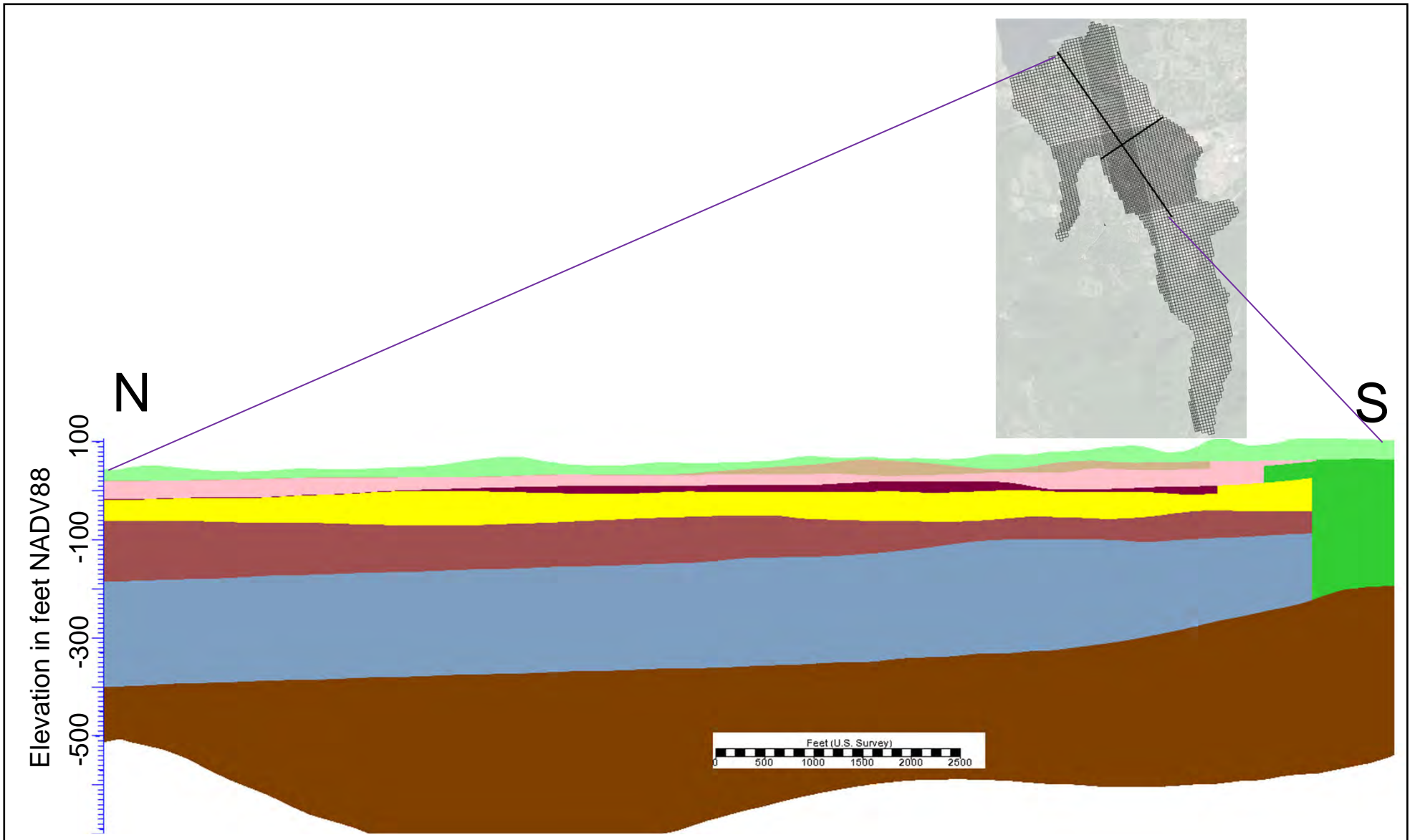
# FIGURES





<b>Legend</b> Specific Head Mountain Front Recharge Model Grid Pumping Well Location Cross-Section Transect AFFF Training Area River		<b>Notes:</b> Aerial imagery source: Esri, July 2022.	<b>Model Domain, Grid and Boundary Conditions</b>  Lower Issaquah Valley Issaquah, Washington   PNG0989      August 2023	<b>Figure</b>  <b>2-1</b>





- Shallow Aquifer (fine sand)
- Shallow Aquifer (silt)
- Shallow Aquifer (sand)
- Aquitard (silt)
- A Zone Aquifer (fine to medium sand, poorly graded sand with gravel)
- Deep Aquitard (grey silt and clay)
- B Zone Aquifer (Coarse sand and gravel grading to a silty medium coarse sand)
- BC Zone Aquifer (Glaciofluvial channels)
- Lower Deep Aquitard (silt)

Vertical exaggeration is x5

### North-South Cross Section

City of Issaquah, WA

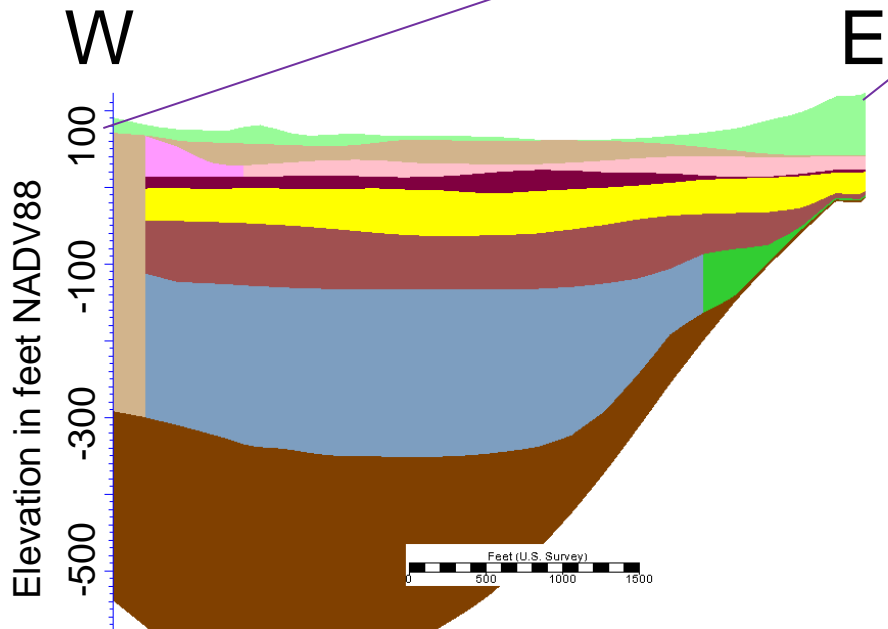
**Geosyntec**   
 consultants

PNG0989

August 2023

**Figure**

**2-2a**



- Shallow Aquifer (fine sand)
- Shallow Aquifer (silt)
- Shallow Aquifer (sand)
- Aquitard (silt)
- A Zone Aquifer (fine to medium sand, poorly graded sand with gravel)
- Deep Aquitard (grey silt and clay)
- B Zone Aquifer (Coarse sand and gravel grading to a silty medium coarse sand)
- BC Zone Aquifer (Glaciofluvial channels)
- Lower Deep Aquitard (silt)

Vertical exaggeration is x5

**West-East Cross-Section**

City of Issaquah, WA

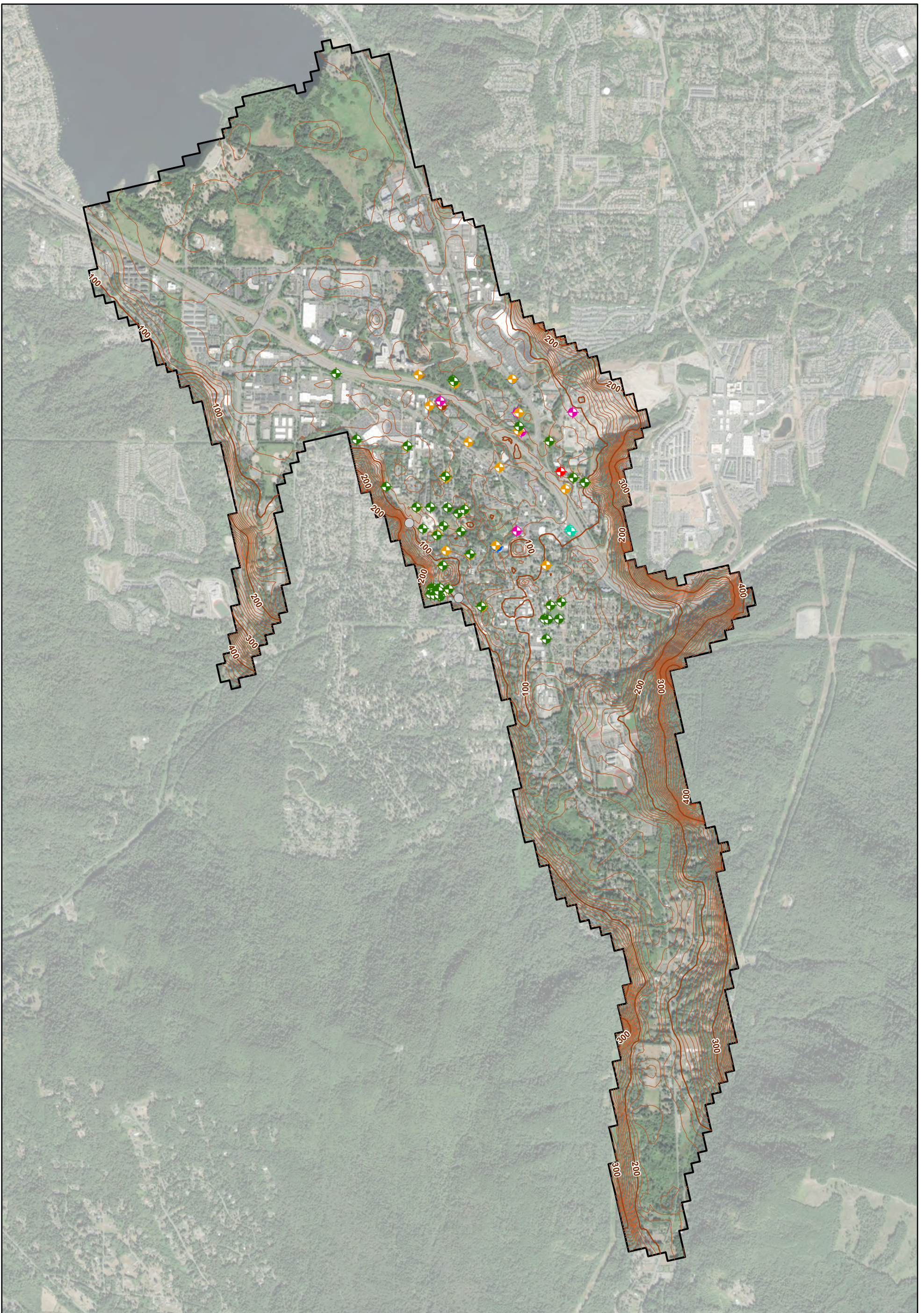





**Figure  
2-2b**

PNG0989

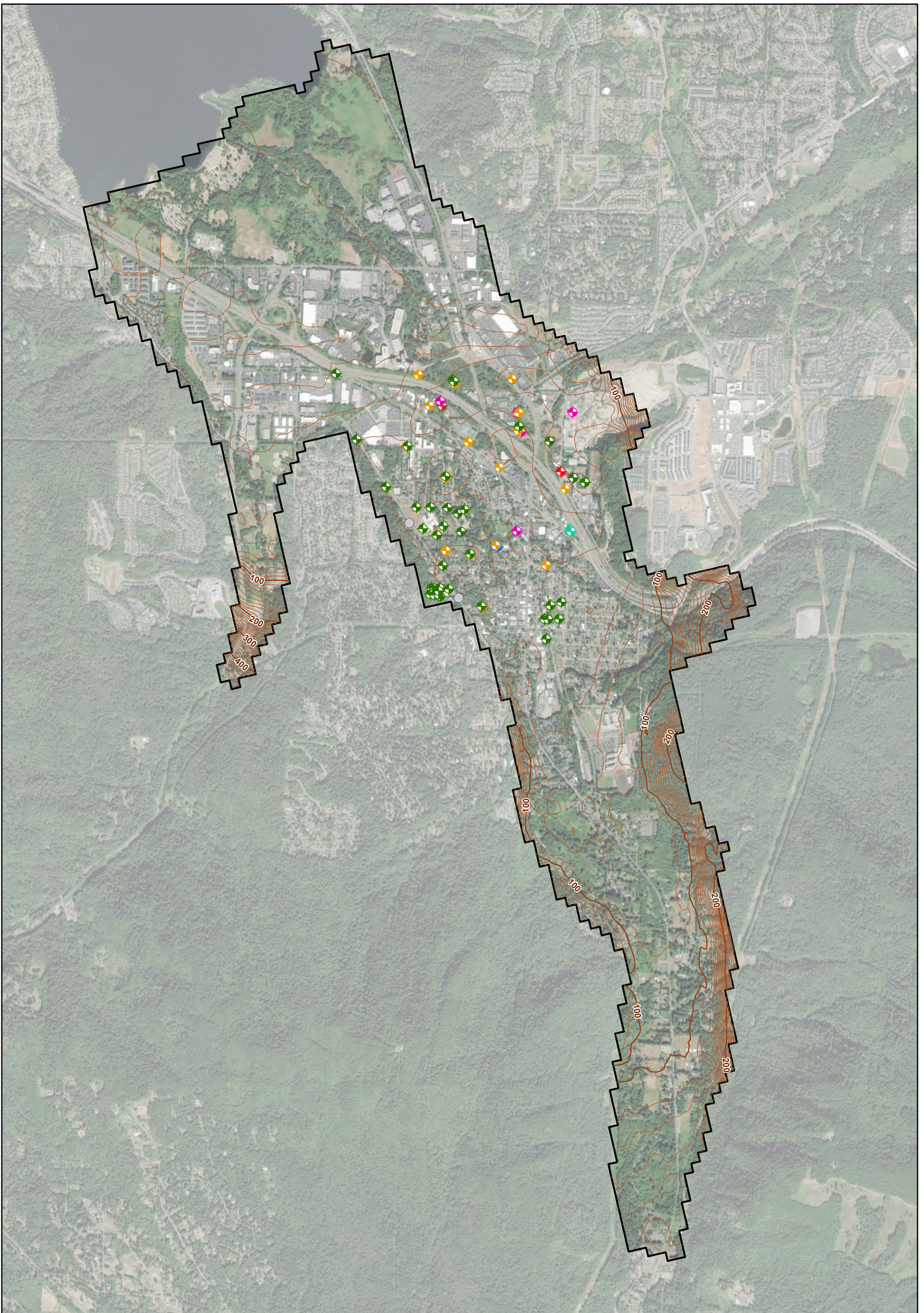
August 2023





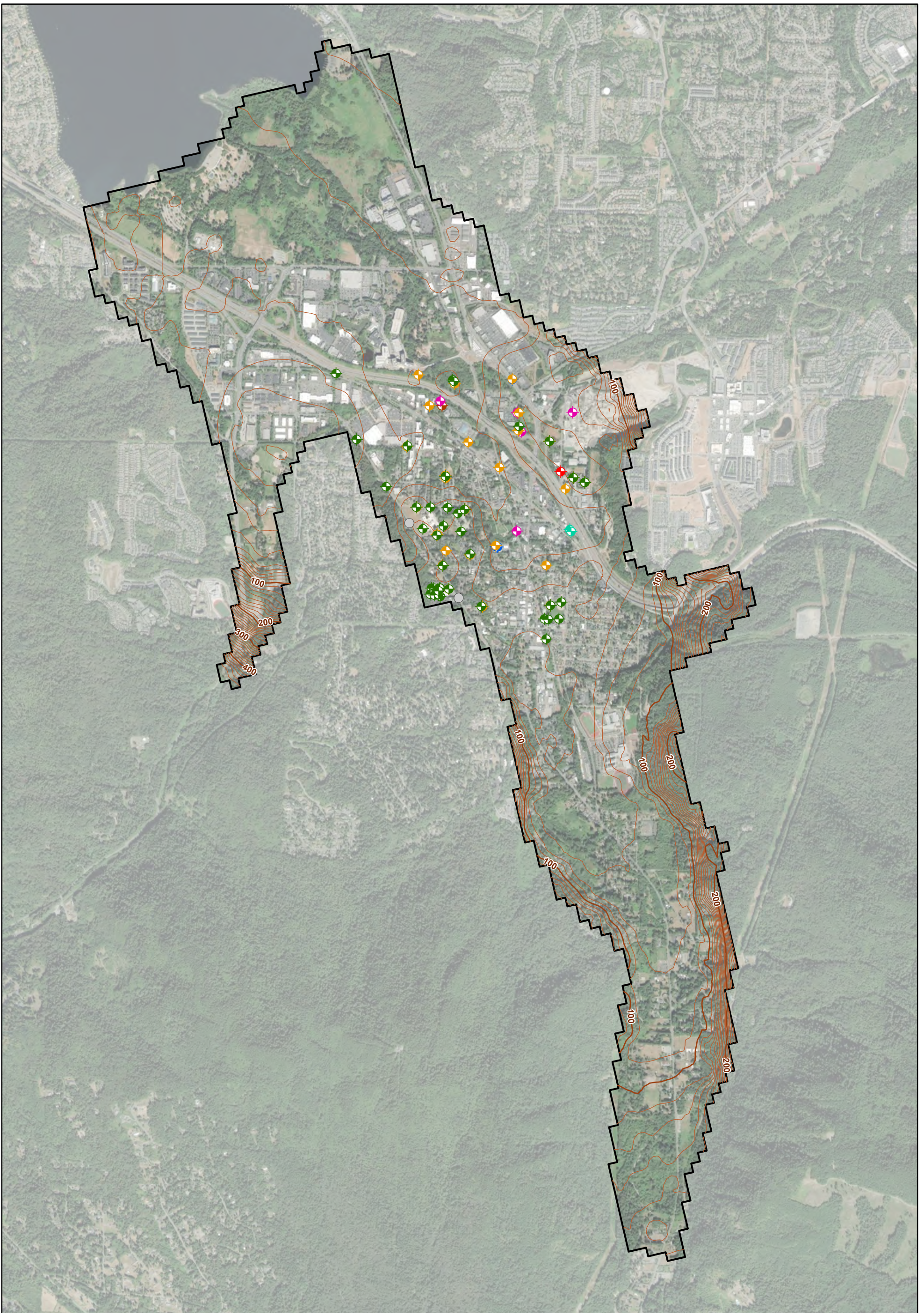
<b>Legend</b> <ul style="list-style-type: none"> <li><span style="color: brown;">—</span> Model Layer 1 Elevation - 100 ft Interval</li> <li><span style="color: brown;">—</span> Model Layer 1 Elevation - 10 ft Interval</li> <li><span style="border: 1px solid black; display: inline-block; width: 10px; height: 10px;"></span> Model Domain</li> <li><span style="color: green;">◆</span> Shallow Zone Monitoring Well</li> <li><span style="color: yellow;">◆</span> A Zone Monitoring Well</li> <li><span style="color: blue;">◆</span> B Zone Monitoring Well</li> <li><span style="color: grey;">●</span> Temporary Well</li> <li><span style="color: orange;">●</span> Piezometer</li> <li><span style="color: cyan;">◆</span> Shallow Zone Production Well</li> <li><span style="color: pink;">◆</span> A Zone Production Well</li> <li><span style="color: brown;">◆</span> B Zone Production Well</li> <li><span style="color: red;">◆</span> C Zone Production Well</li> </ul>		 	<b>Elevation of Model Layers</b> <b>Top of Model Layer 1 (Ground Surface)</b> Lower Issaquah Valley Issaquah, Washington	
<b>Notes:</b> Aerial imagery source: Esri, July 2022.			<b>Figure</b> <b>2-3a</b>	
		PNG0989	August 2023	





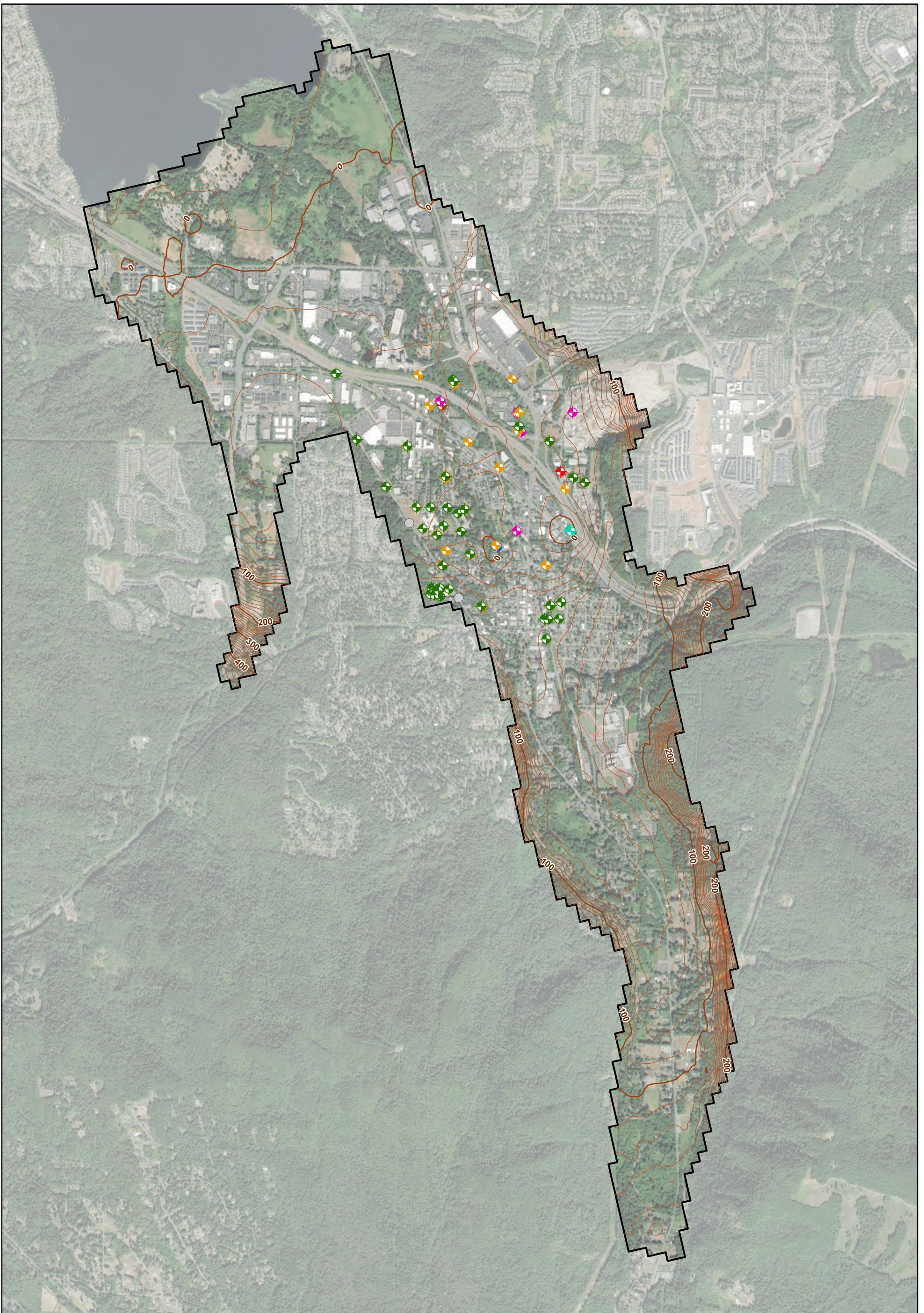
<b>Legend</b> 			<b>Elevation of Model Layers</b> <b>Top of Model Layer 2 (Aquitard 1)</b> Lower Issaquah Valley Issaquah, Washington	
<b>Notes:</b> Aerial imagery source: Esri, July 2022.				<b>Figure</b> <b>2-3b</b>
		0 2,000 Feet	PNG0989	August 2023





<b>Legend</b> 			<b>Elevation of Model Layers Top of Model Layer 3 (Shallow Aquifer)</b> Lower Issaquah Valley Issaquah, Washington	
<b>Notes:</b> Aerial imagery source: Esri, July 2022.				<b>Figure 2-3c</b>
		PNG0989	August 2023	





**Legend**

Model Layer 4 Elevation - 100 ft Interval	Shallow Zone Monitoring Well	Shallow Zone Production Well
Model Layer 4 Elevation - 10 ft Interval	A Zone Monitoring Well	A Zone Production Well
Model Domain	B Zone Monitoring Well	B Zone Production Well
	Temporary Well	C Zone Production Well
	Piezometer	

**Notes:**  
Aerial imagery source: Esri, July 2022.

**Elevation of Model Layers**  
**Top of Model Layer 4 (Aquitard 2)**

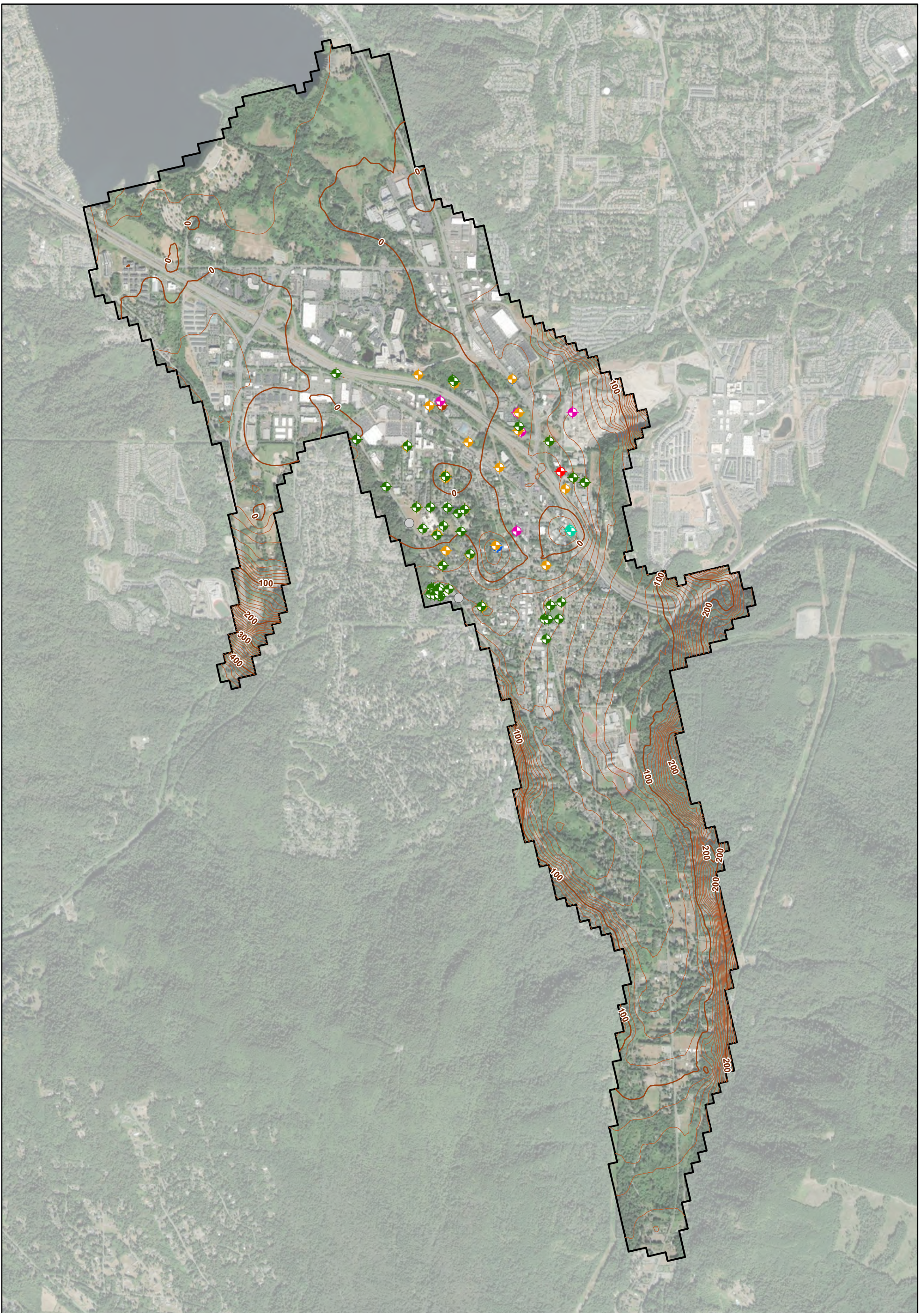
Lower Issaquah Valley  
Issaquah, Washington

**Geosyntec**  
consultants

**Figure**  
**2-3d**

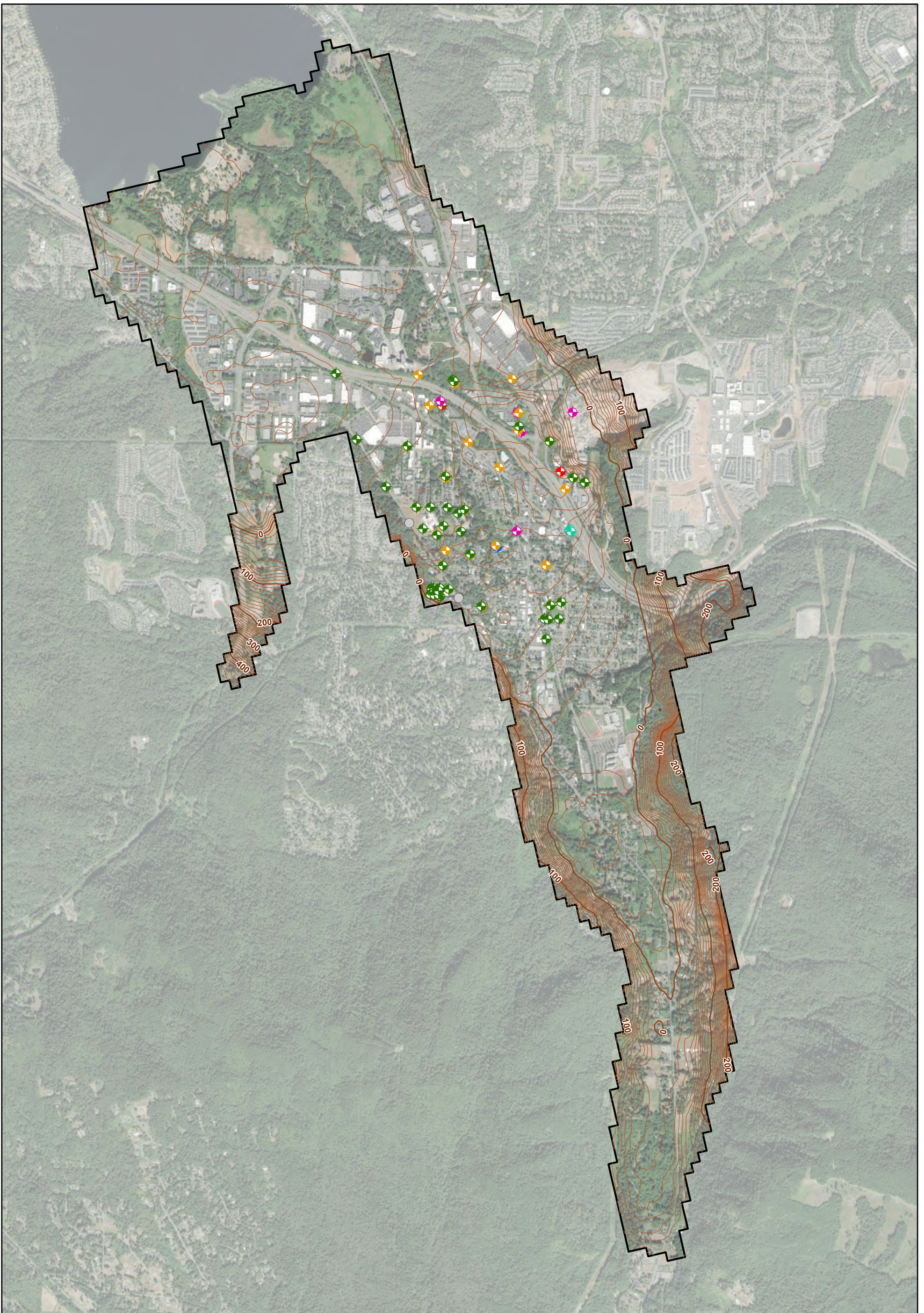
PNG0989	August 2023
---------	-------------





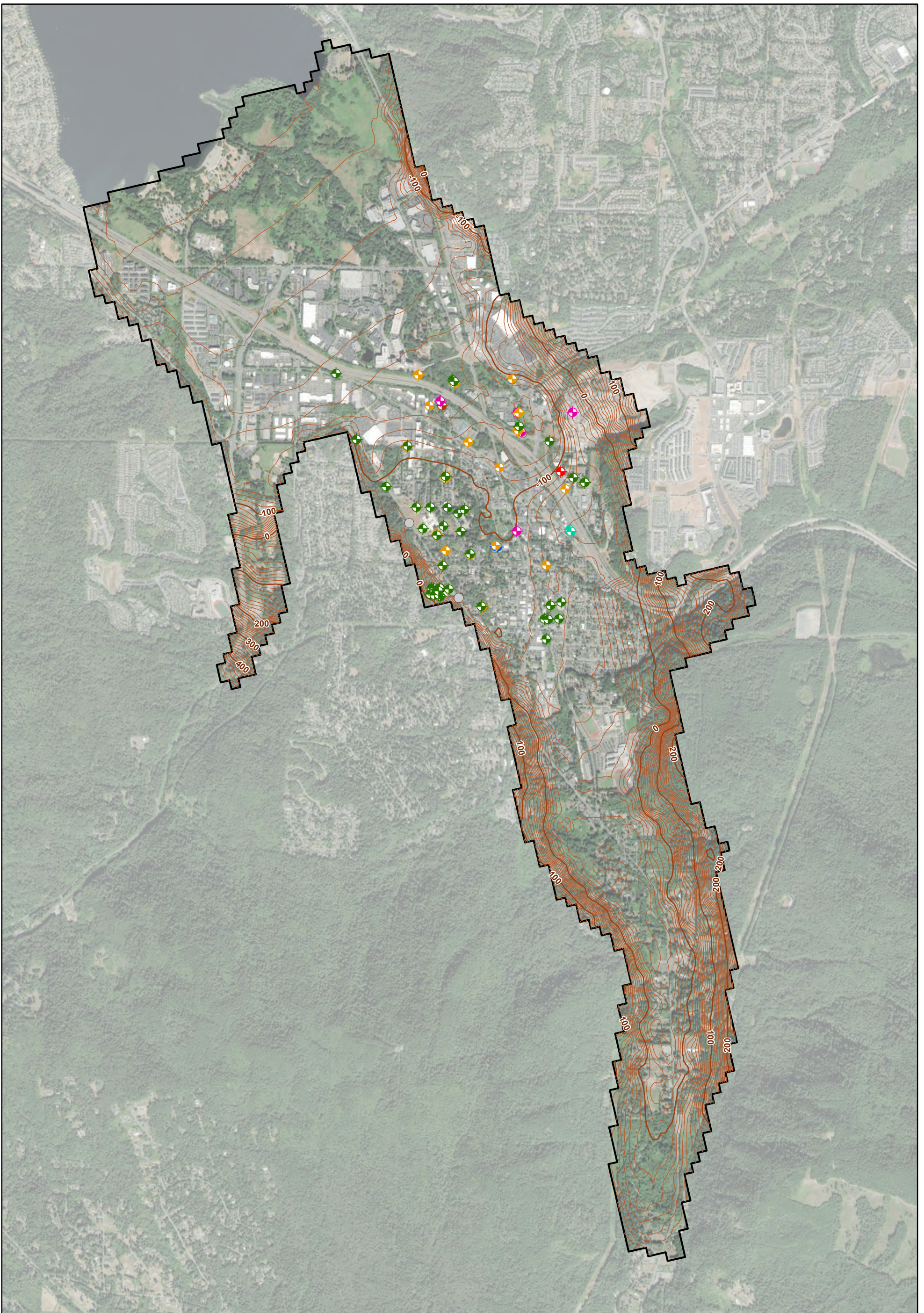
<b>Legend</b> 			<b>Elevation of Model Layers Top of Model Layer 5 (A Aquifer)</b> Lower Issaquah Valley Issaquah, Washington	
<b>Notes:</b> Aerial imagery source: Esri, July 2022.				<b>Figure 2-3e</b>
		PNG0989	August 2023	





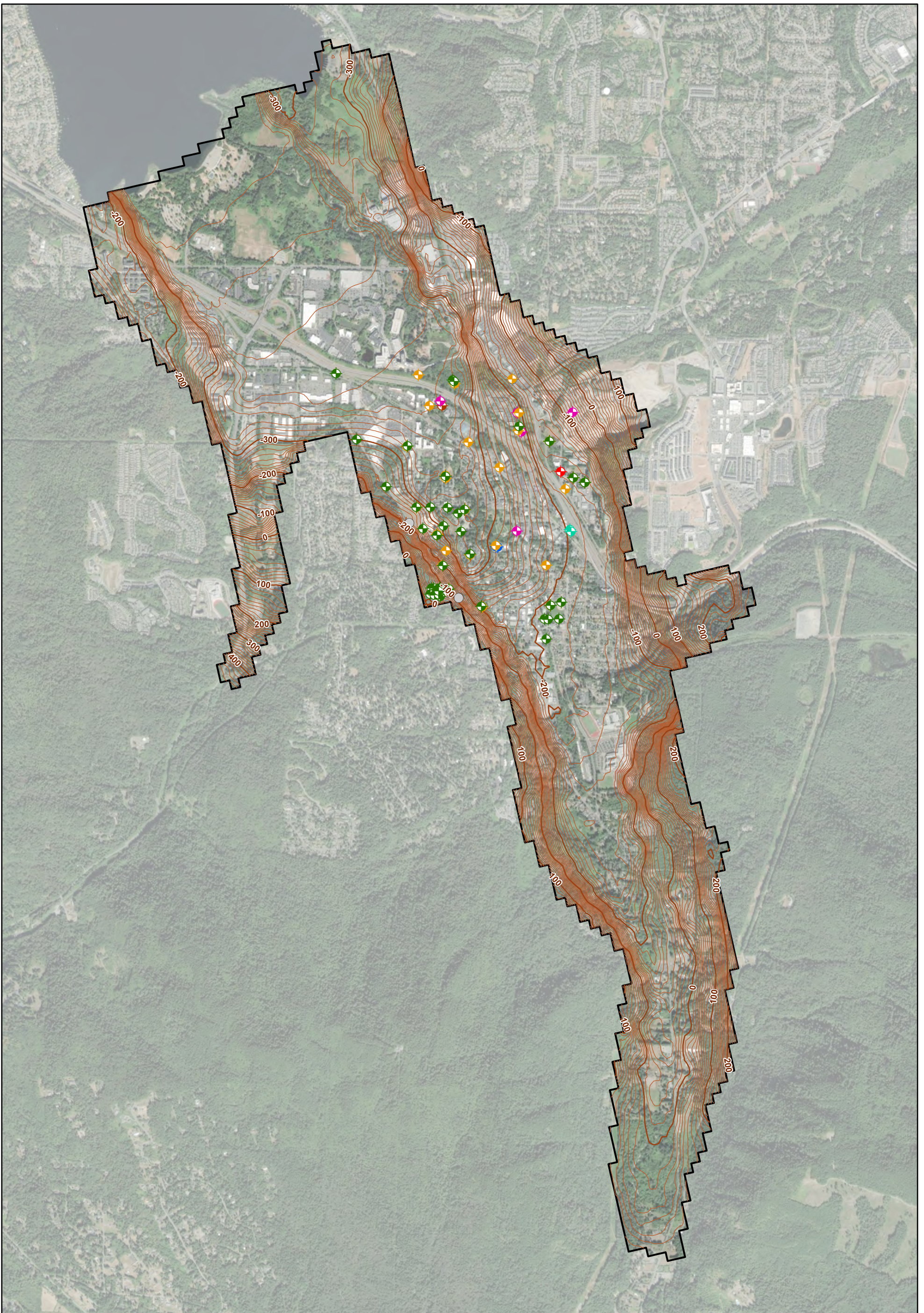
<b>Legend</b> — Model Layer 6 Elevation - 100 ft Interval — Model Layer 6 Elevation - 10 ft Interval □ Model Domain ◆ Shallow Zone Monitoring Well ◆ A Zone Monitoring Well ◆ B Zone Monitoring Well ● Temporary Well ● Piezometer ◆ Shallow Zone Production Well ◆ A Zone Production Well ◆ B Zone Production Well ◆ C Zone Production Well		N  0 2,000 Feet 	<b>Elevation of Model Layers</b> <b>Top of Model Layer 6 (Deep Aquitard)</b> Lower Issaquah Valley Issaquah, Washington	
<b>Notes:</b> Aerial imagery source: Esri, July 2022.			 Geosyntec consultants	<b>Figure</b> <b>2-3f</b>
			PNG0989	August 2023





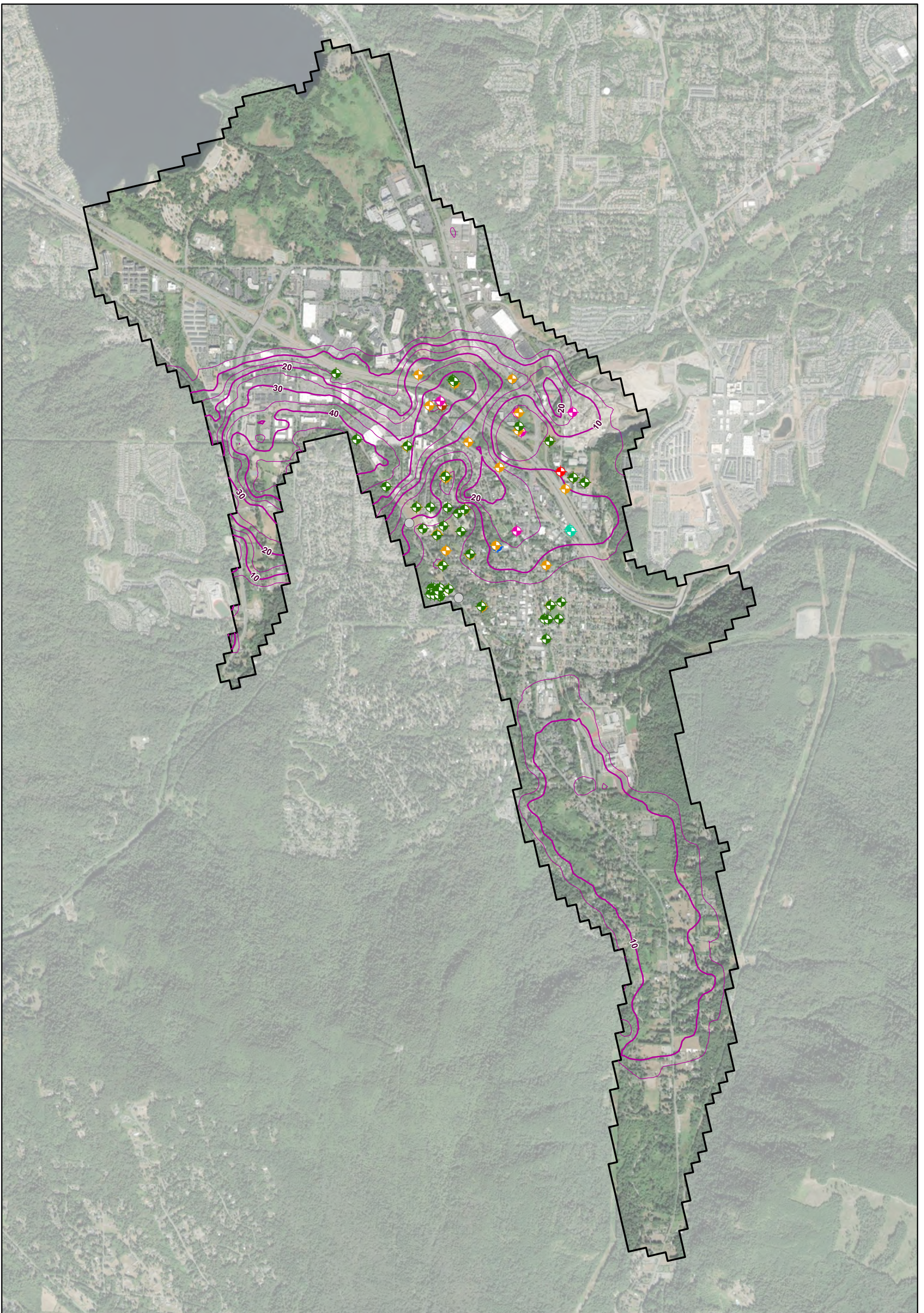
<b>Legend</b> — Model Layer 7 Elevation - 100 ft Interval — Model Layer 7 Elevation - 10 ft Interval □ Model Domain ● Shallow Zone Monitoring Well ● A Zone Monitoring Well ● B Zone Monitoring Well ● Temporary Well ● Piezometer ● Shallow Zone Production Well ● A Zone Production Well ● B Zone Production Well ● C Zone Production Well		N  0 2,000 Feet 	<b>Elevation of Model Layers</b> <b>Top of Model Layer 7 (B and B/C Aquifers)</b> Lower Issaquah Valley Issaquah, Washington	
<b>Notes:</b> Aerial imagery source: Esri, July 2022.			<b>Figure</b> <b>2-3g</b>	PNG0989      August 2023





<b>Legend</b> — Model Layer 9 Elevation - 100 ft Interval — Model Layer 9 Elevation - 10 ft Interval □ Model Domain ◆ Shallow Zone Monitoring Well ◆ A Zone Monitoring Well ◆ B Zone Monitoring Well ● Temporary Well ● Piezometer ◆ Shallow Zone Production Well ◆ A Zone Production Well ◆ B Zone Production Well ◆ C Zone Production Well		N  0 2,000 Feet 	<b>Elevation of Model Layers</b> <b>Top of Model Layer 9 (Lower Deep Aquitard)</b> Lower Issaquah Valley Issaquah, Washington	
<b>Notes:</b> Aerial imagery source: Esri, July 2022.			<b>Figure</b> <b>2-3h</b>	PNG0989      August 2023






**Legend**

- Model Layer 2 Thickness - 10 ft Interval
- Model Layer 2 Thickness - 5 ft Interval
- Model Domain
- ◆ Shallow Zone Monitoring Well
- ◆ A Zone Monitoring Well
- ◆ B Zone Monitoring Well
- Temporary Well
- Piezometer
- ◆ Shallow Zone Production Well
- ◆ A Zone Production Well
- ◆ B Zone Production Well
- ◆ C Zone Production Well


**Notes:**  
Aerial imagery source: Esri, July 2022.

**Thickness of Model Aquitards**  
**Thickness of Layer 2 (Aquitard 1)**


Lower Issaquah Valley  
Issaquah, Washington



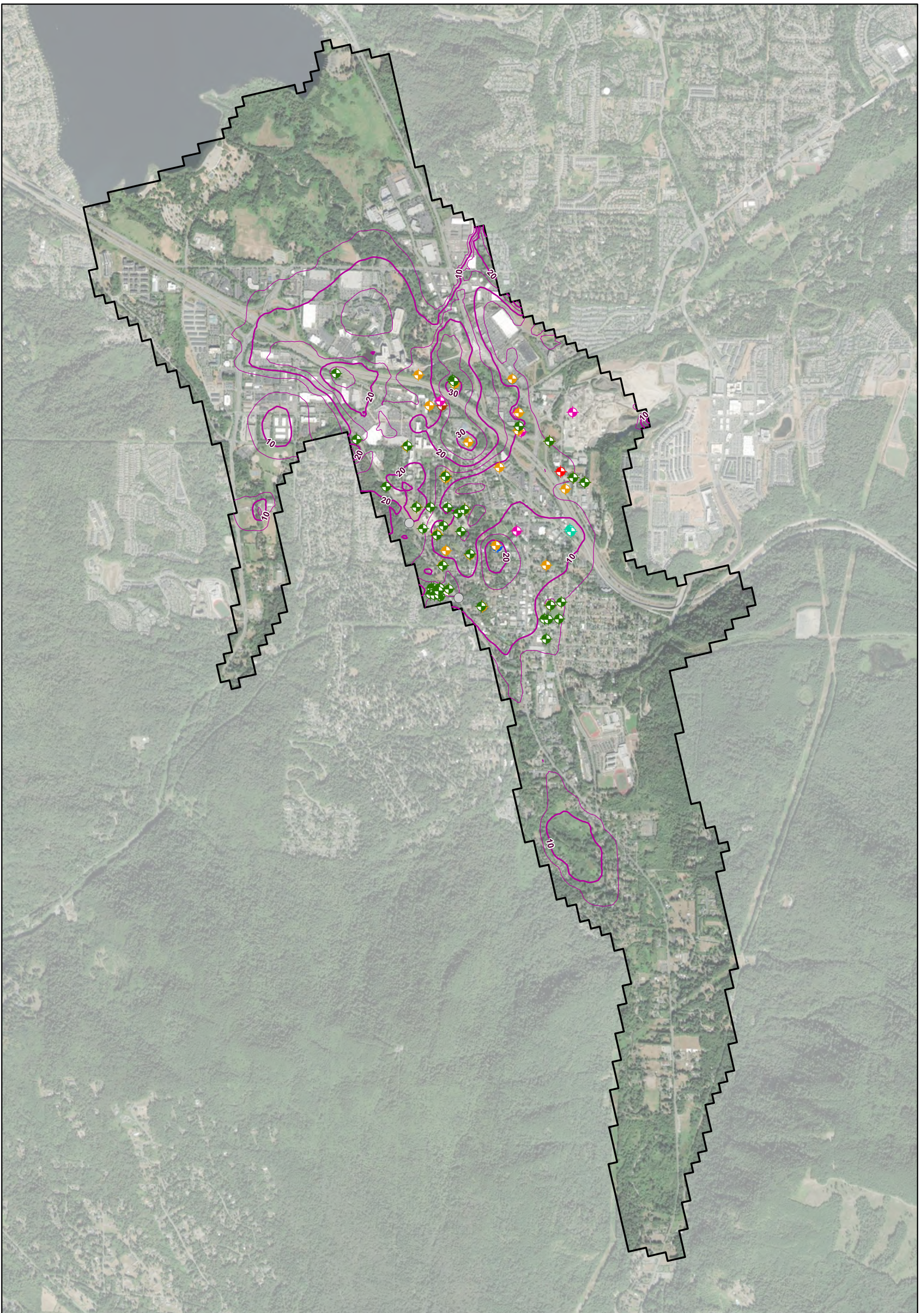
N



0 2,000  
Feet

	<b>Figure</b>
PNG0989	August 2023
<b>2-4a</b>	






**Legend**

- Model Layer 4 Thickness - 10 ft Interval
- Model Layer 4 Thickness - 5 ft Interval
- Model Domain
- ◆ Shallow Zone Monitoring Well
- ◆ A Zone Monitoring Well
- ◆ B Zone Monitoring Well
- Temporary Well
- Piezometer
- ◆ Shallow Zone Production Well
- ◆ A Zone Production Well
- ◆ B Zone Production Well
- ◆ C Zone Production Well


**Notes:**  
Aerial imagery source: Esri, July 2022.

**Thickness of Model Aquitards**  
**Thickness of Layer 4 (Aquitard 2)**


Lower Issaquah Valley  
Issaquah, Washington



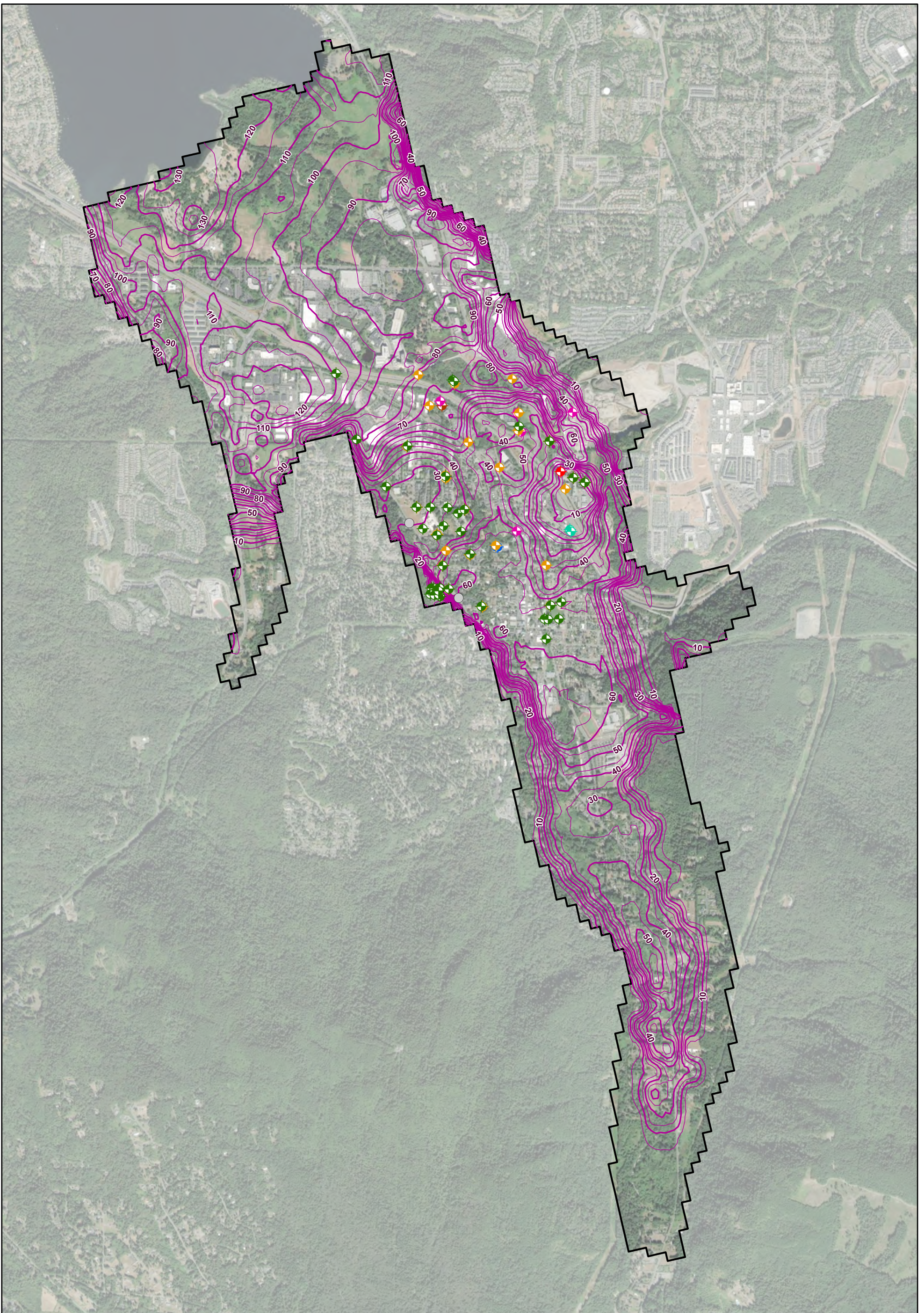
N



0 2,000  
Feet

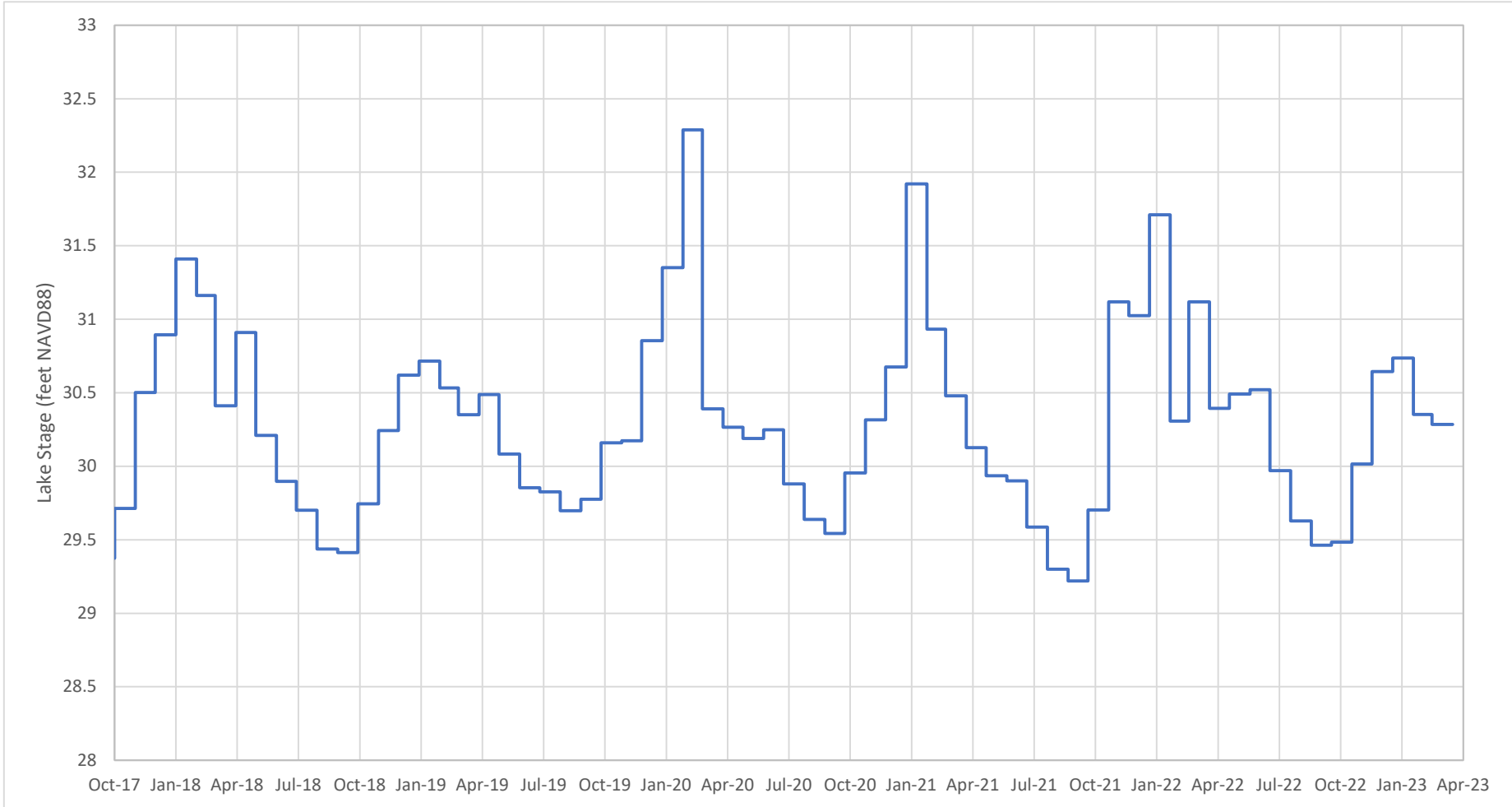
	<b>Figure</b>
PNG0989	August 2023
<b>2-4b</b>	





<b>Legend</b> <ul style="list-style-type: none"> <li><span style="color: purple;">—</span> Model Layer 6 Thickness - 10 ft Interval</li> <li><span style="color: purple;">—</span> Model Layer 6 Thickness - 5 ft Interval</li> <li><span style="border: 1px solid black; display: inline-block; width: 10px; height: 10px;"></span> Model Domain</li> <li><span style="color: green;">◆</span> Shallow Zone Monitoring Well</li> <li><span style="color: yellow;">◆</span> A Zone Monitoring Well</li> <li><span style="color: blue;">◆</span> B Zone Monitoring Well</li> <li><span style="color: grey;">●</span> Temporary Well</li> <li><span style="color: orange;">●</span> Piezometer</li> <li><span style="color: green;">◆</span> Shallow Zone Production Well</li> <li><span style="color: pink;">◆</span> A Zone Production Well</li> <li><span style="color: orange;">◆</span> B Zone Production Well</li> <li><span style="color: red;">◆</span> C Zone Production Well</li> </ul>		<b>Thickness of Model Aquitards</b> <b>Thickness of Layer 6 (Deep Aquitard)</b> Lower Issaquah Valley Issaquah, Washington	
<b>Notes:</b> Aerial imagery source: Esri, July 2022.			
			<b>Figure</b> <b>2-4c</b>
		PNG0989	August 2023





Lake stage from United State Geological Survey (USGS)  
<https://waterdata.usgs.gov/monitoring-location/12122000/#parameterCode=62614&startDT=2017-01-01&endDT=2023-04-01>

**Lake Sammamish Stage**

Lower Issaquah Valley  
 Issaquah, Washington



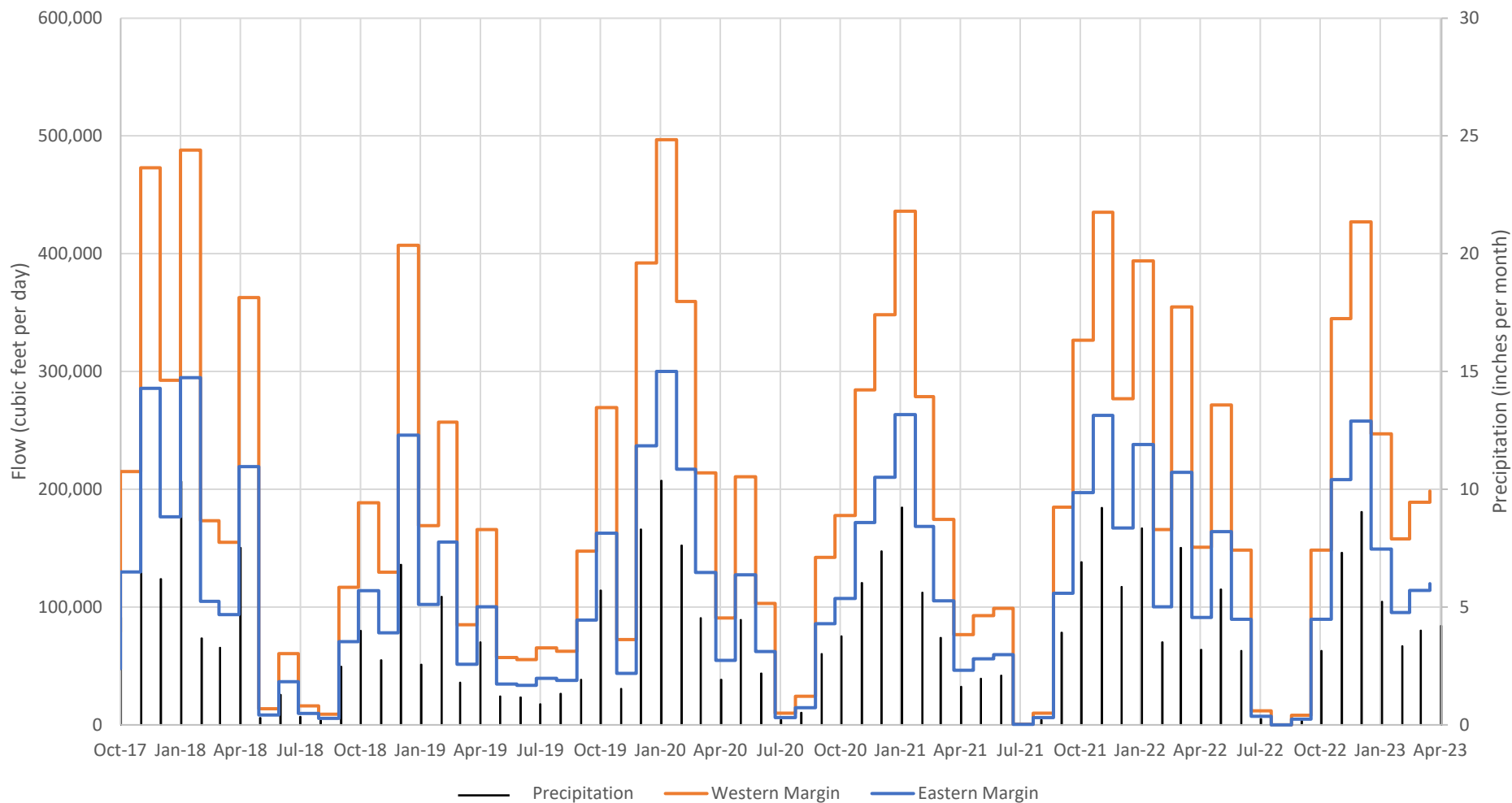
**Figure**

**2-5**

PNG0989

May 2023





Precipitation from National Oceanic and Atmospheric Administration (NOAA)

[Daily Summaries Station Details: ISSAQUAH 3.6 NW, WA US, GHCND:US1WAKG0059 | Climate Data Online \(CDO\) | National Climatic Data Center \(NCDC\) \(noaa.gov\)](#)

[Daily Summaries Station Details: ISSAQUAH 0.5 SSW, WA US, GHCND:US1WAKG0284 | Climate Data Online \(CDO\) | National Climatic Data Center \(NCDC\) \(noaa.gov\)](#)

**Specified Flow at Western and Eastern Margins**

Lower Issaquah Valley  
Issaquah, Washington



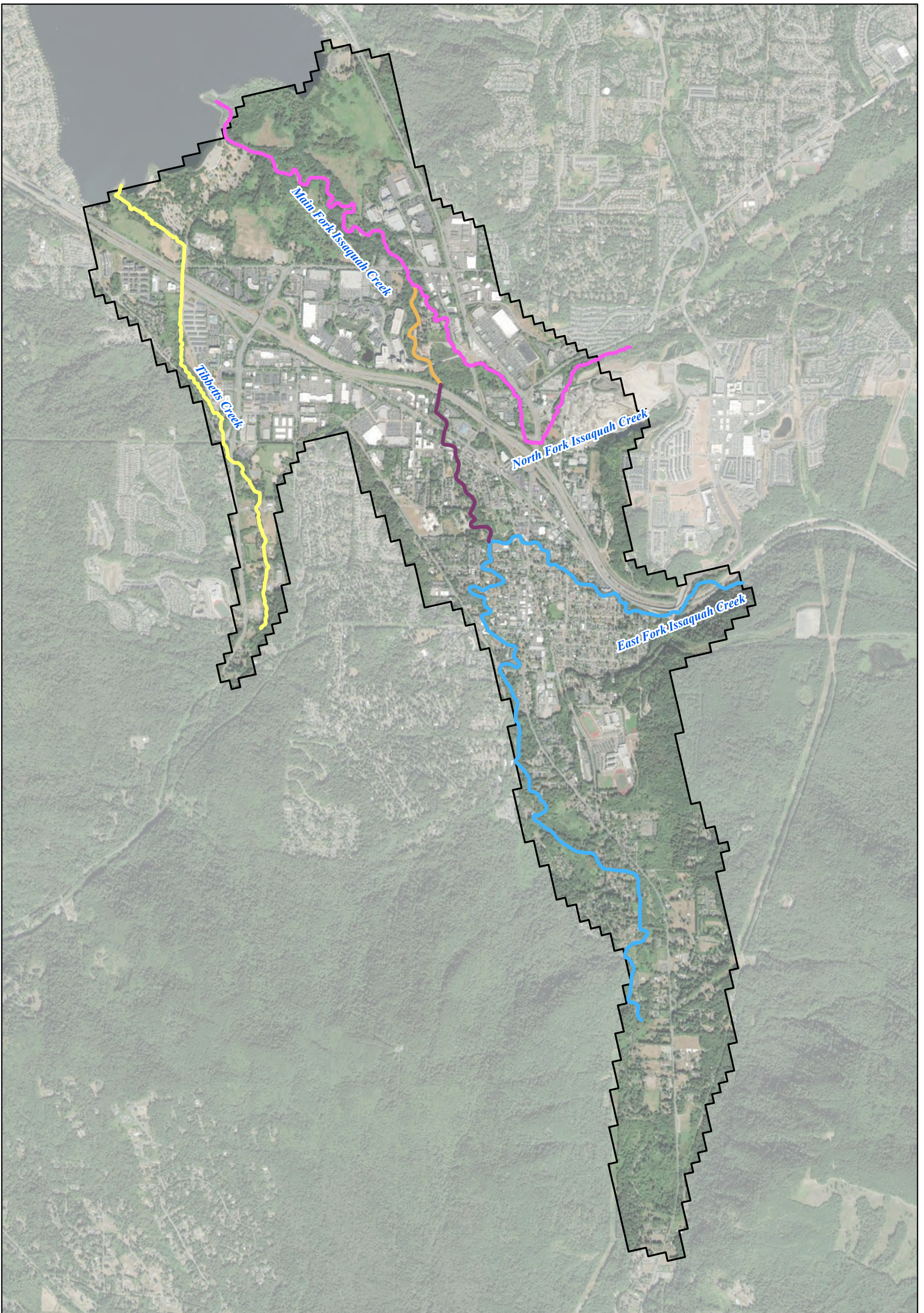
**Figure**

PNG0989

August 2023

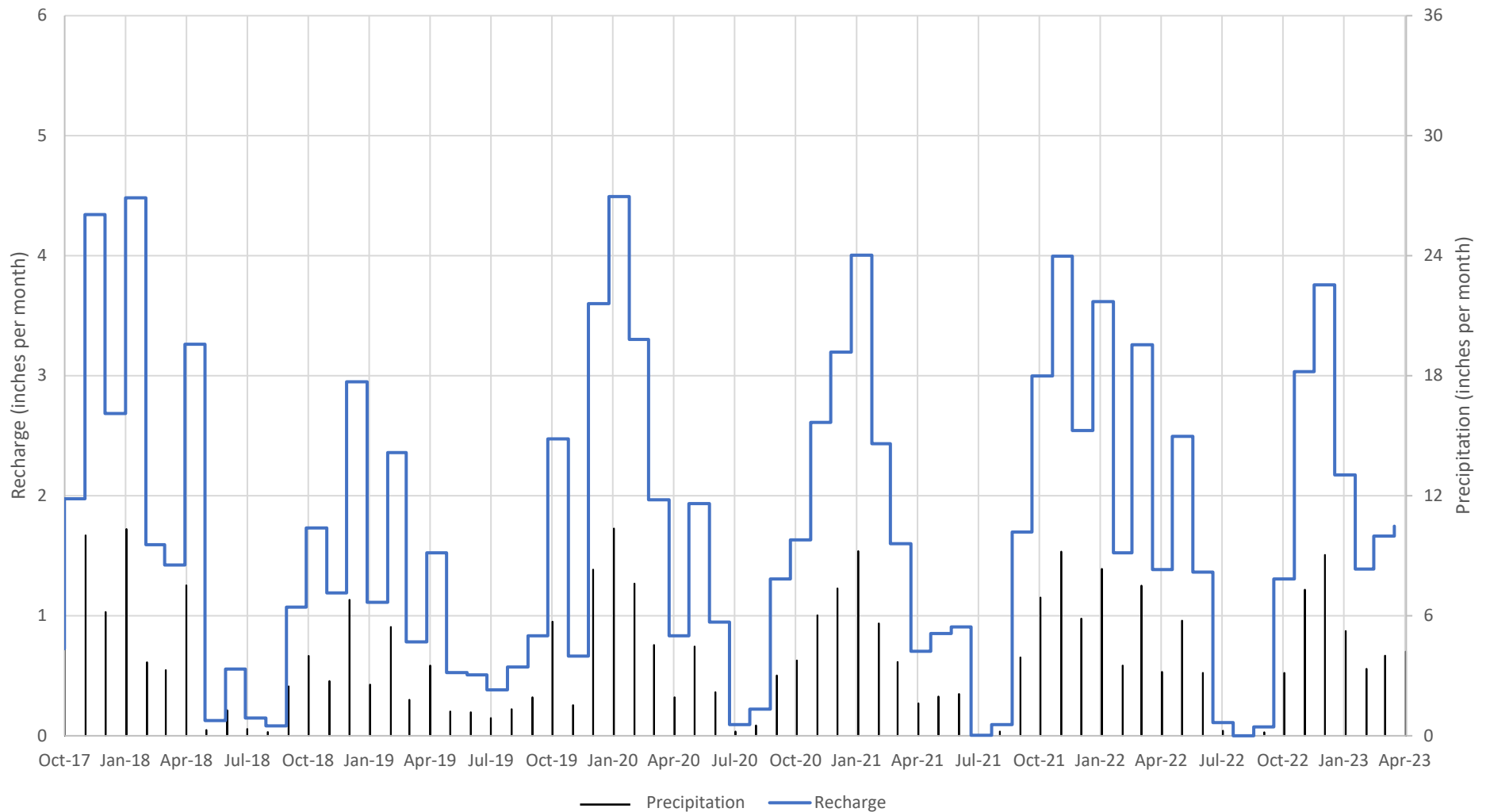
**2-6**





<p><b>Legend</b></p> <p><b>Riverbed Conductance*</b></p> <ul style="list-style-type: none"> <li><span style="color: blue;">—</span> 1</li> <li><span style="color: orange;">—</span> 1.2</li> <li><span style="color: purple;">—</span> 3</li> <li><span style="color: yellow;">—</span> 6</li> <li><span style="color: pink;">—</span> 8.2</li> </ul>	<p> Model Domain</p>	<p><b>Notes:</b></p> <ul style="list-style-type: none"> <li>* Conductance is in square feet per day per foot of river length.</li> <li>- Aerial imagery source: Esri, July 2022.</li> </ul> <div style="text-align: right;">  N   0 2,000 Feet         </div>	<p><b>Riverbed Conductance</b></p> <p>Lower Issaquah Valley Issaquah, Washington</p> <p><b>Geosyntec</b> consultants</p>	
			<p>PNG0989</p> <p>August 2023</p>	<p><b>Figure</b></p> <p><b>2-7</b></p>





Precipitation from National Oceanic and Atmospheric Administration (NOAA)

[Daily Summaries Station Details: ISSAQUAH 3.6 NW, WA US, GHCND:US1WAKG0059 | Climate Data Online \(CDO\) | National Climatic Data Center \(NCDC\) \(noaa.gov\)](#)

[Daily Summaries Station Details: ISSAQUAH 0.5 SSW, WA US, GHCND:US1WAKG0284 | Climate Data Online \(CDO\) | National Climatic Data Center \(NCDC\) \(noaa.gov\)](#)

**Areal Recharge**

Lower Issaquah Valley  
Issaquah, Washington

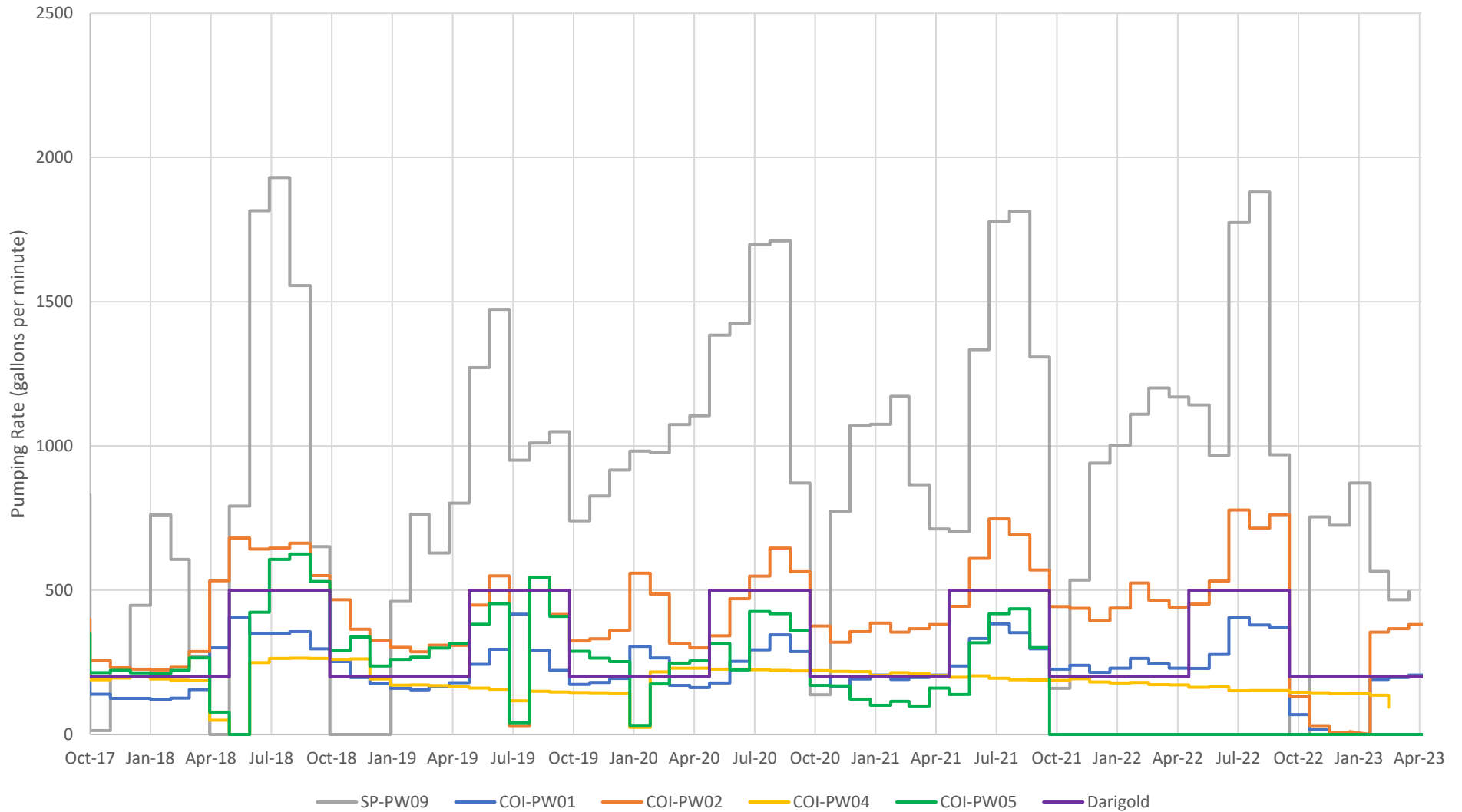


**Figure**

**2-8**

PNG0989

May 2023



Pumping rate at Lakeside well is constant at 600 gallons per min (not shown on graph)

**Pumping Rates at Production Wells**

Lower Issaquah Valley  
Issaquah, Washington

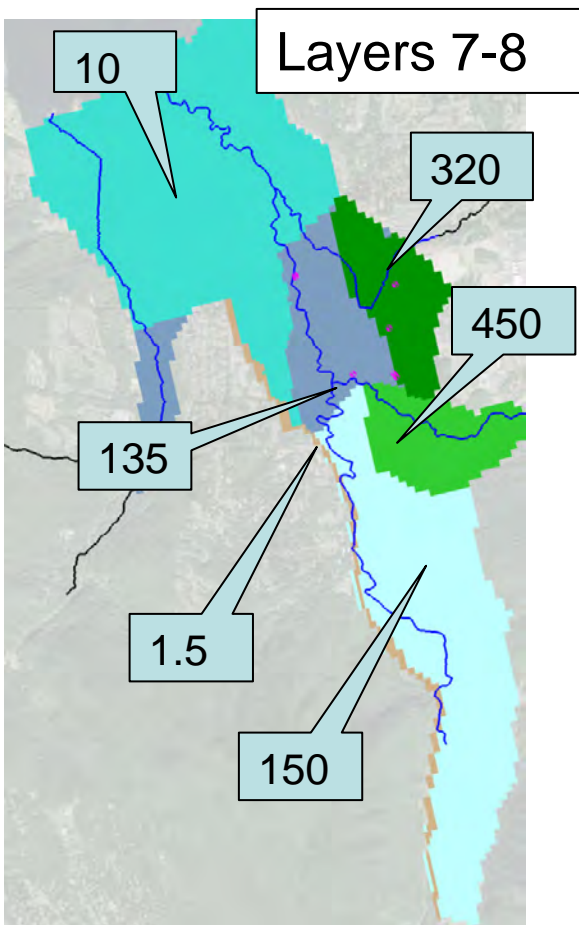
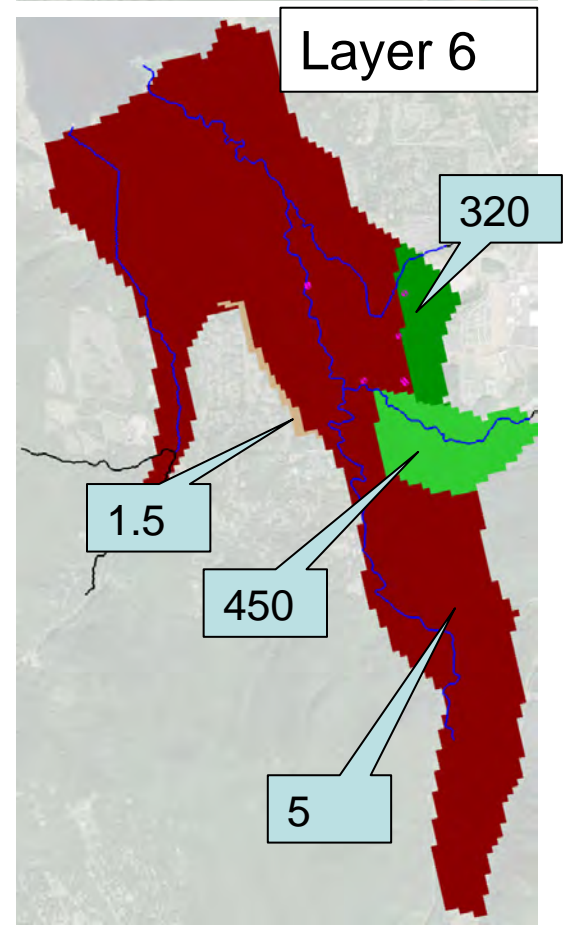
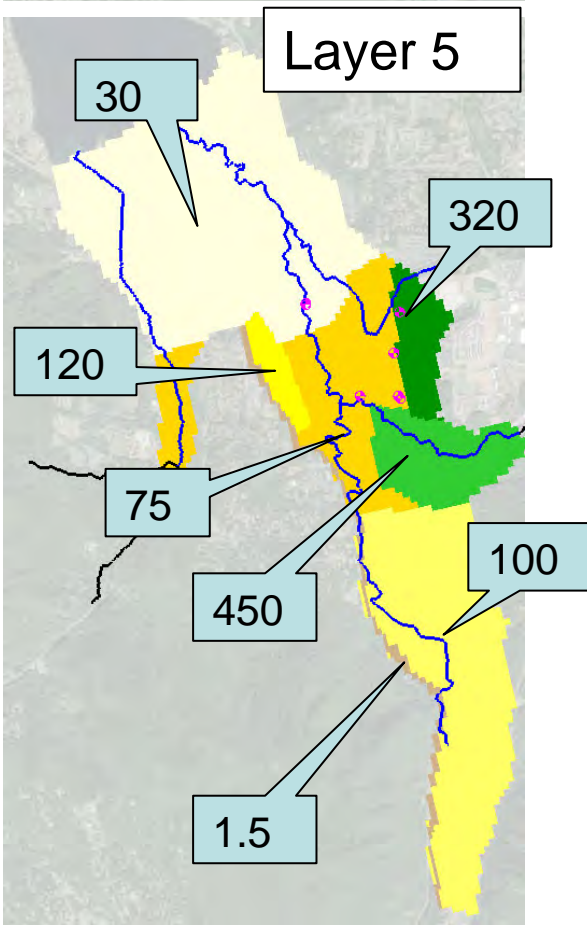
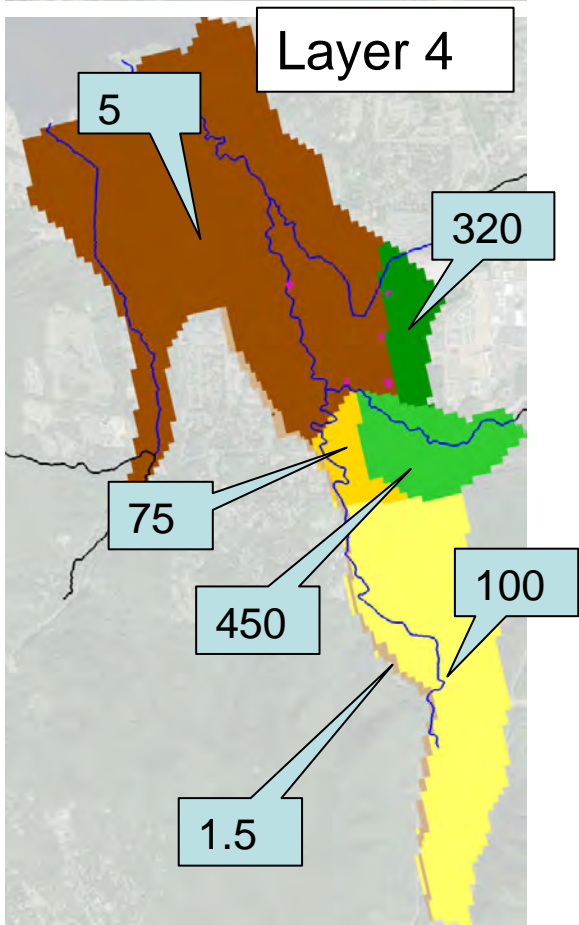
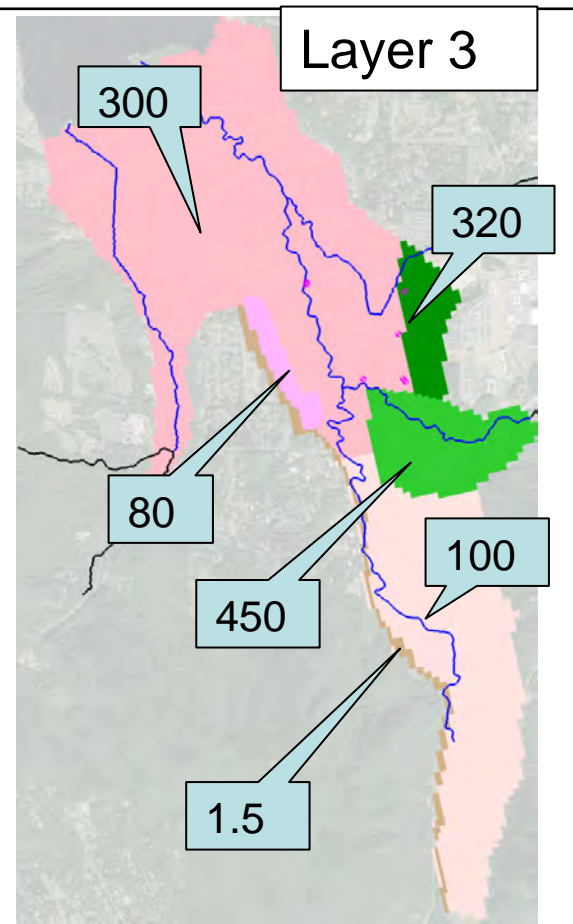
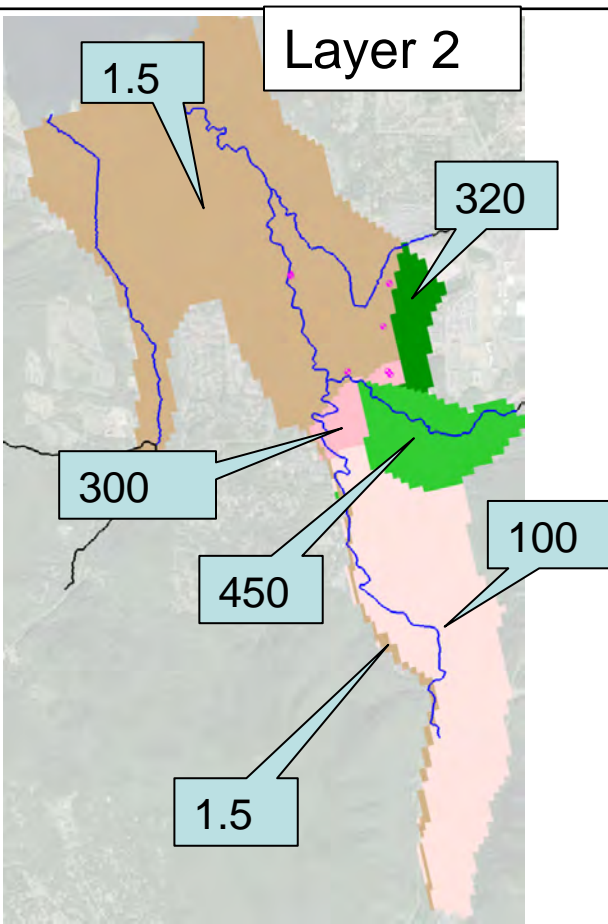
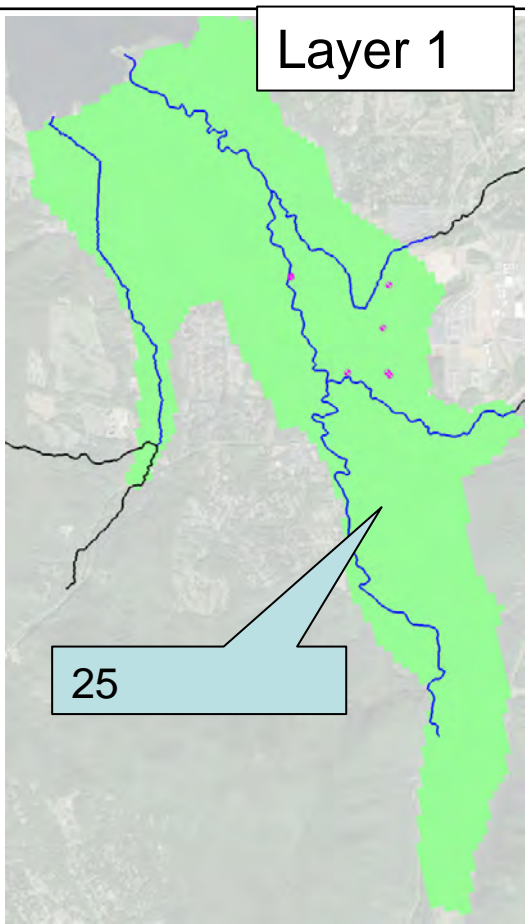


**Figure**

**2-9**

PNG0989

May 2022



MODFLOW Layers	Hydrostratigraphic Unit	Depth to Top of Layer (Range in Area of Interest) in Feet
1	Shallow Aquifer (including Aquitard 1)	10 - 50
2		20 - 50
3		60 - 100
4	Shallow Aquitard (Aquitard 2)	60 - 110
5	A Zone Aquifer	70 - 110
6	Deep Aquitard	110 - 160
7 and 8	B Zone Aquifer and B/C Zone Aquifer	190 - 200
9	Lower Deep Aquitard	300 - 420

Notes:  
 Specific yield = 0.2  
 Specific storage =  $10^{-5}$  feet<sup>-1</sup>  
 Hydraulic conductivity of layer 9 is 0.1

Kh in feet per day  
 $K_v = K_h/10$

**Hydraulic Properties**

Lower Issaquah Valley  
 Issaquah, Washington

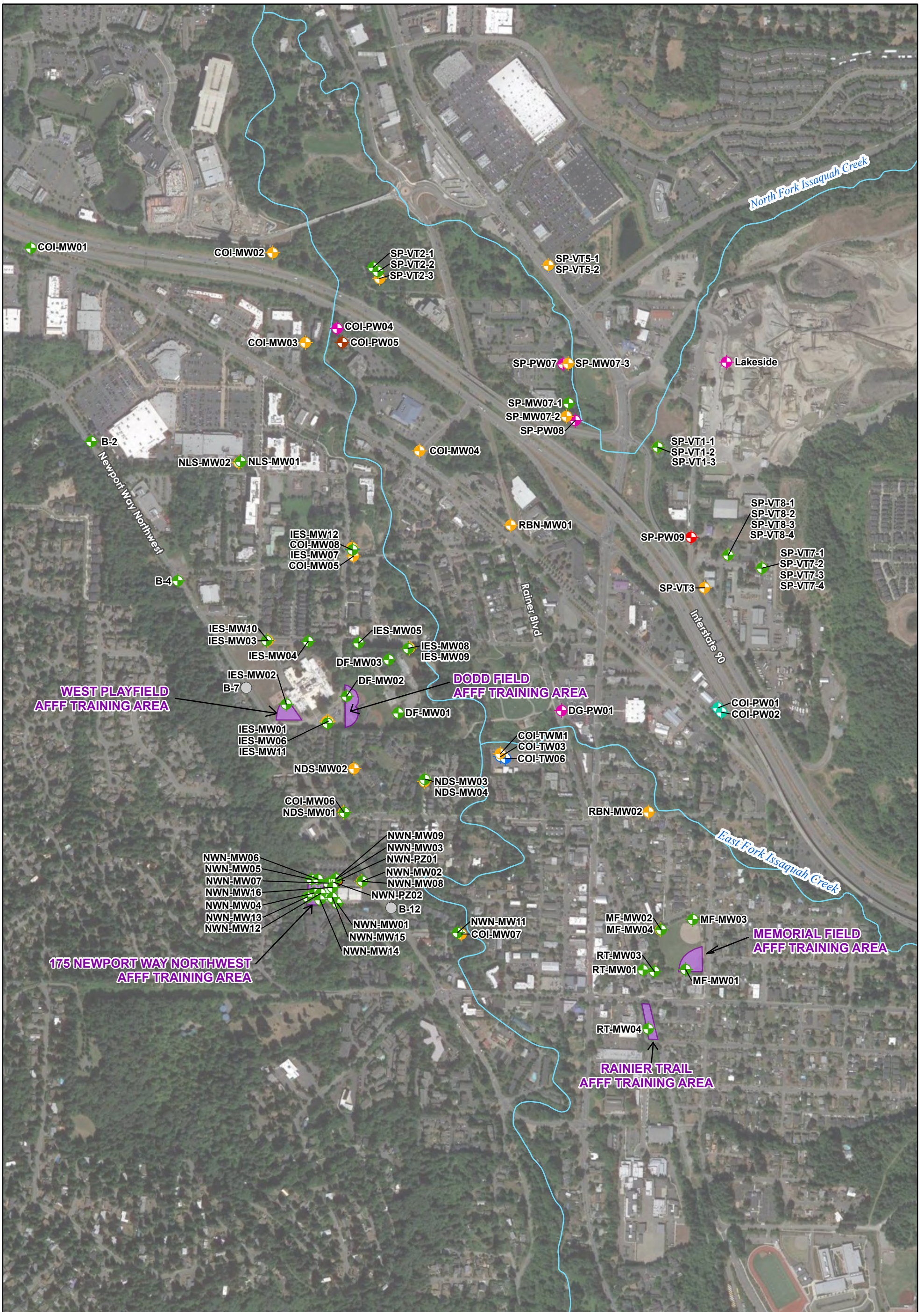
**Geosyntec**  
 consultants

PNG0989

November 2022

**Figure**  
**2-10**

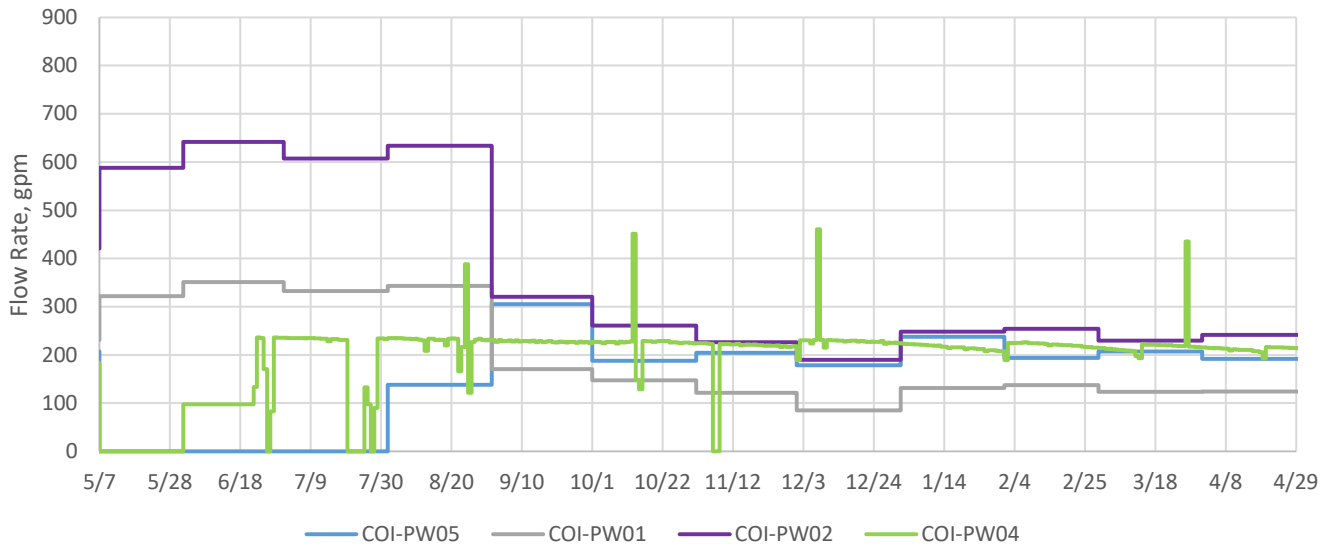




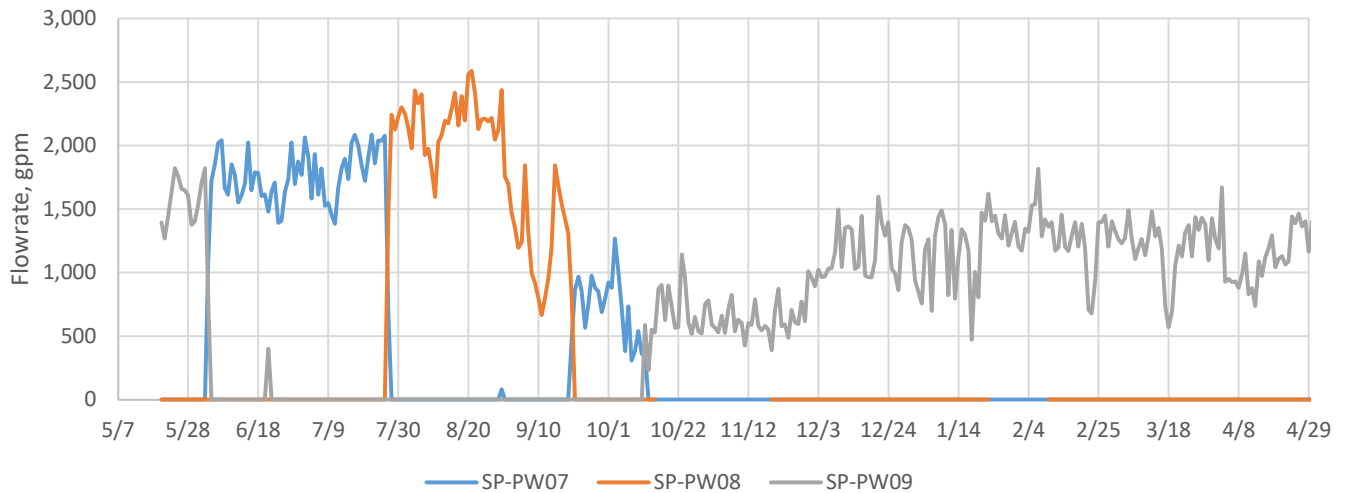
<b>Legend</b> <ul style="list-style-type: none"> <li><span style="color: green;">◆</span> Shallow Zone Monitoring Well</li> <li><span style="color: orange;">◆</span> A Zone Monitoring Well</li> <li><span style="color: blue;">◆</span> B Zone Monitoring Well</li> <li>○ Temporary Well</li> <li><span style="color: orange;">●</span> Piezometer</li> <li><span style="color: green;">◆</span> Shallow Zone Production Well</li> <li><span style="color: pink;">◆</span> A Zone Production Well</li> <li><span style="color: brown;">◆</span> B Zone Production Well</li> <li><span style="color: red;">◆</span> C Zone Production Well</li> <li>■ AFFF Training Area</li> <li>— Issaquah Creek</li> </ul>		<b>Notes:</b> Aerial imagery source: Google Earth Pro, August 2020.	N  0 680 Feet	<b>Observation Locations</b> Lower Issaquah Valley Issaquah, Washington	
<b>Geosyntec</b> consultants		<b>Figure</b> <b>3-1</b>			



### COI Production Wells



### SPWD Production Wells



gpm = gallons per minute

#### Pumping Rates at Production Wells During May 2016 through April 2017

Lower Issaquah Valley  
Issaquah, Washington

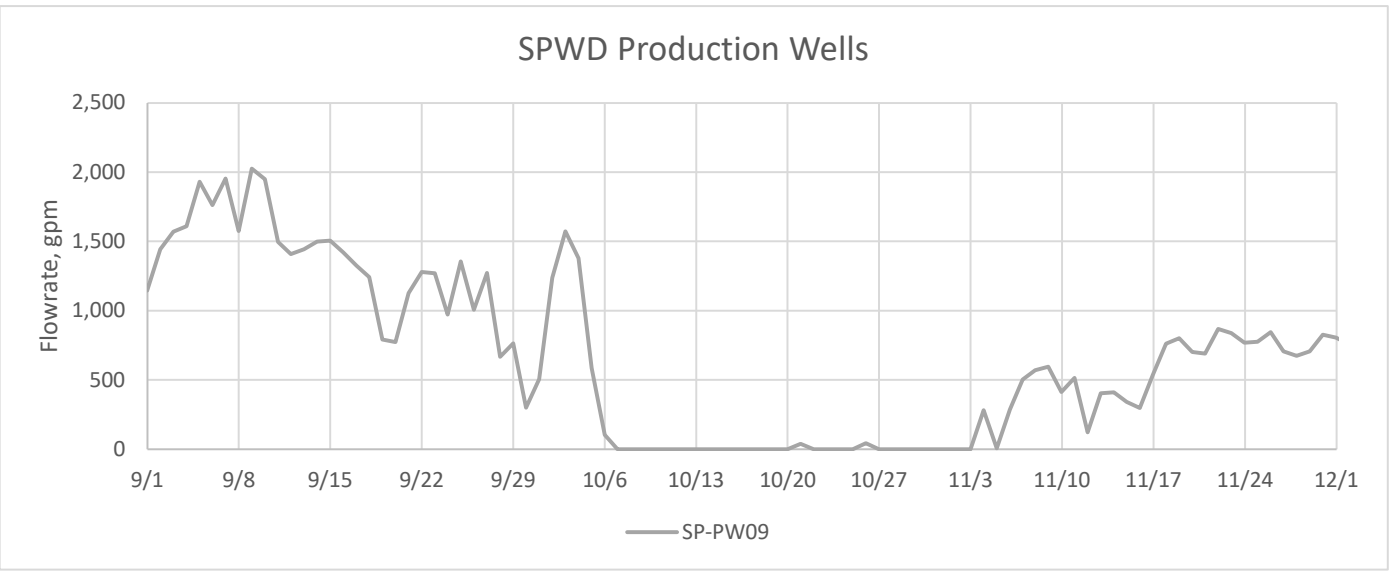
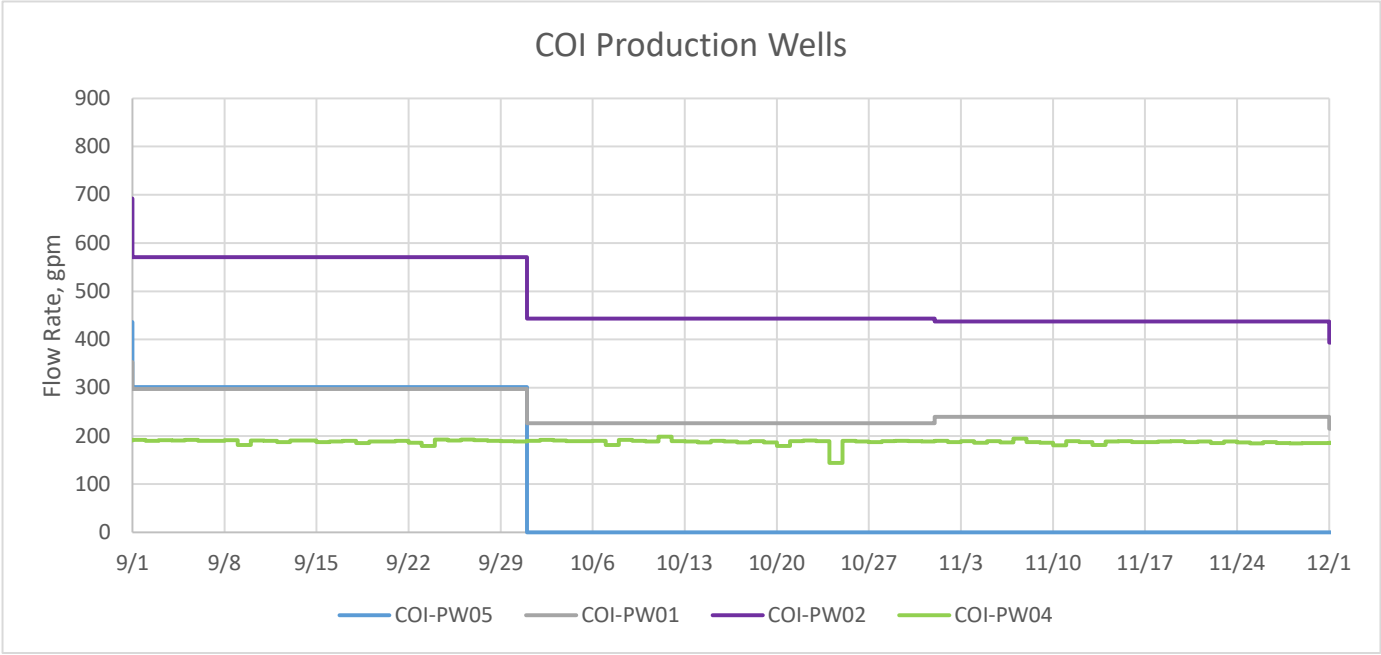


**Figure  
3-2A**

PNG0989

May 2023

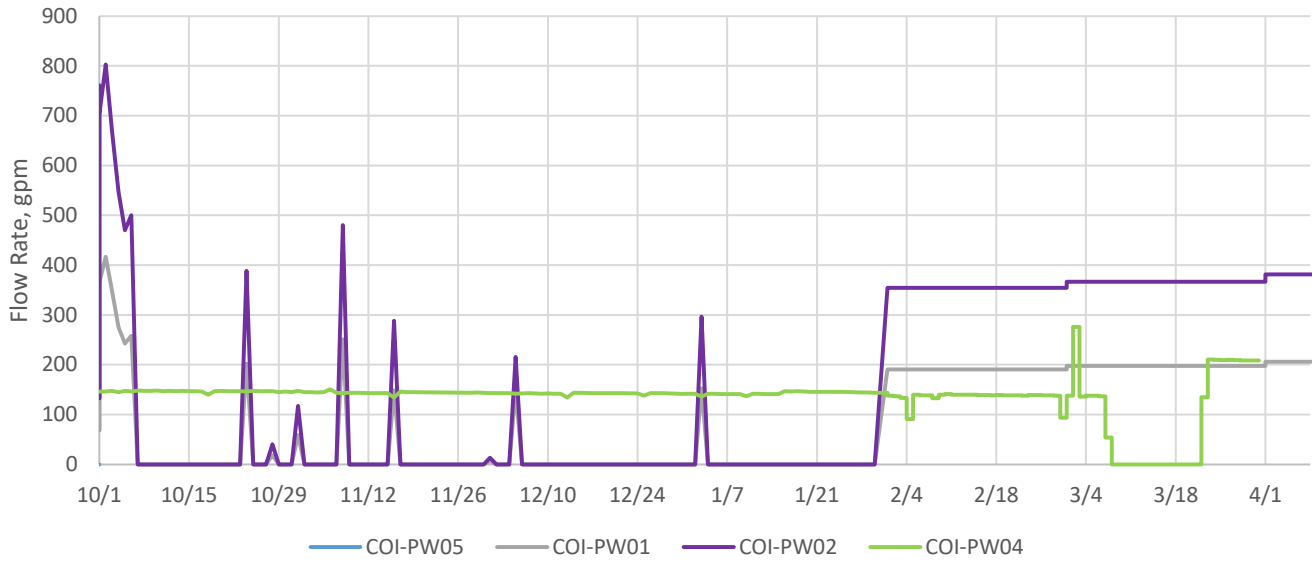




gpm = gallons per minute

<b>Pumping Rates at Production Wells During September through November 2021</b>	
Lower Issaquah Valley Issaquah, Washington	
PNG0989	May 2023
<b>Figure 3-2B</b>	

### COI Production Wells



### SPWD Production Wells



gpm = gallons per minute

#### Pumping Rates at Production Wells During October 2022 through April 2023

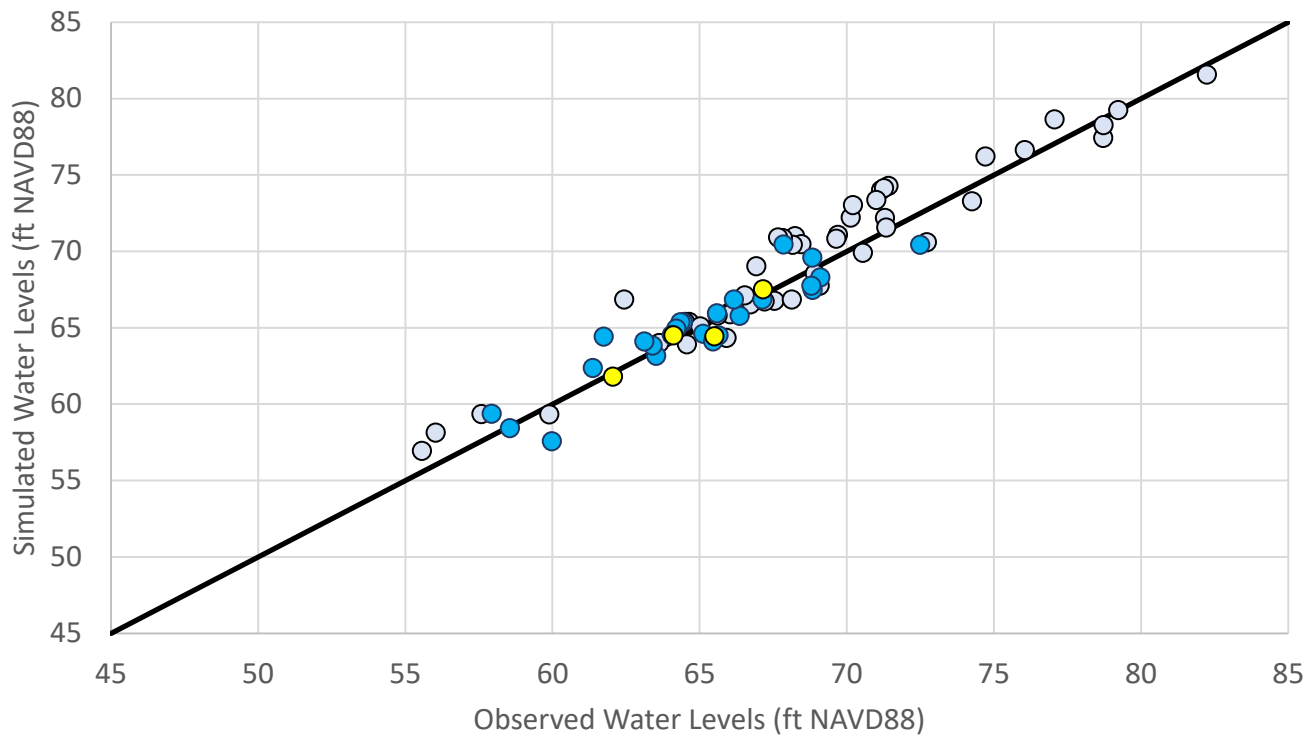
Lower Issaquah Valley  
Issaquah, Washington



**Figure  
3-2C**

PNG0989

May 2023



○ Shallow Zone Aquifer    ● A Zone Aquifer    ● B and B/C Zone Aquifers

	All	Shallow Zone Aquifer	A Zone Aquifer	B and B/C Zone Aquifers
Number of Observations	78	49	25	4
Min Head (ft)	55.6	55.6	57.9	62.0
Max Head (ft)	82.2	82.2	72.5	67.2
Range (ft)	26.7	26.7	14.6	5.1
Mean Residual (ft)	-0.5	-0.8	-0.1	0.1
RMSE (ft)	1.5	1.7	1.3	0.6
% RMSE	6%	6%	9%	12%
R <sup>2</sup>	0.90	0.90	0.86	0.90

**Note:**

ft = feet

RMSE = Root mean square error

R<sup>2</sup> = coefficient of determination

**Simulated vs. Observed Groundwater Levels for Steady State Simulation**

Lower Issaquah Valley  
Issaquah, Washington



**Figure**

PNG0989

August 2023

**3-3**





**Legend**

- Groundwater Elevation Contour (ft msl) - 10 ft Interval
- Groundwater Elevation Contour (ft msl) - 2 ft Interval
- Shallow Zone Production Well
- Model Domain

**Shallow Well Residual (feet)**

- < -2.5
- 2.5 - -1
- 1 - 0
- 0 - 1
- 1 - 2.5
- > 2.5

**Notes:**  
 ft msl = feet above mean sea level  
 Aerial imagery source: Esri, July 2022.

**Simulated Groundwater Elevation Contours (Steady-State) in Shallow Aquifer**

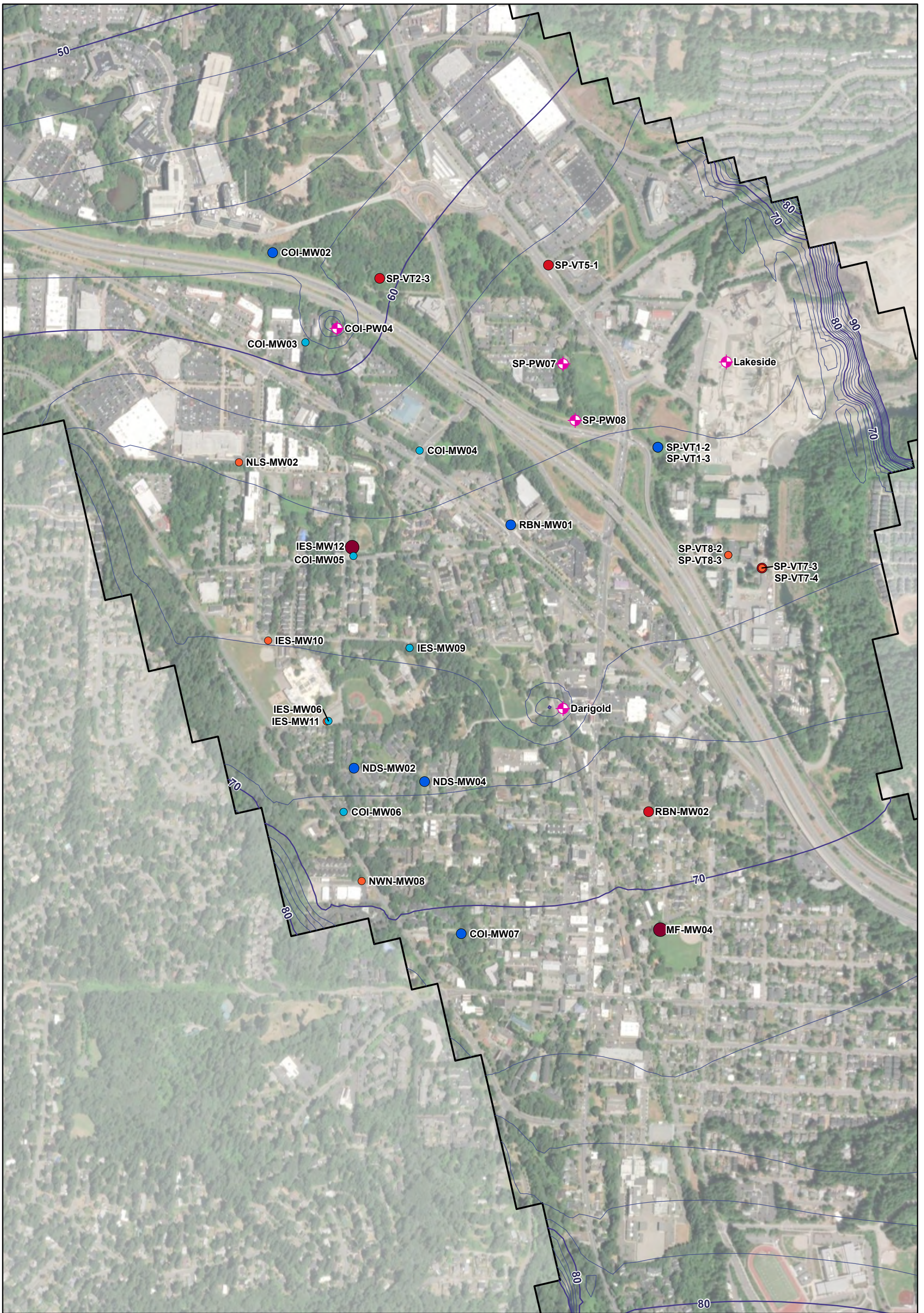
Lower Issaquah Valley  
Issaquah, Washington

**Geosyntec**  
consultants

**Figure 3-4a**

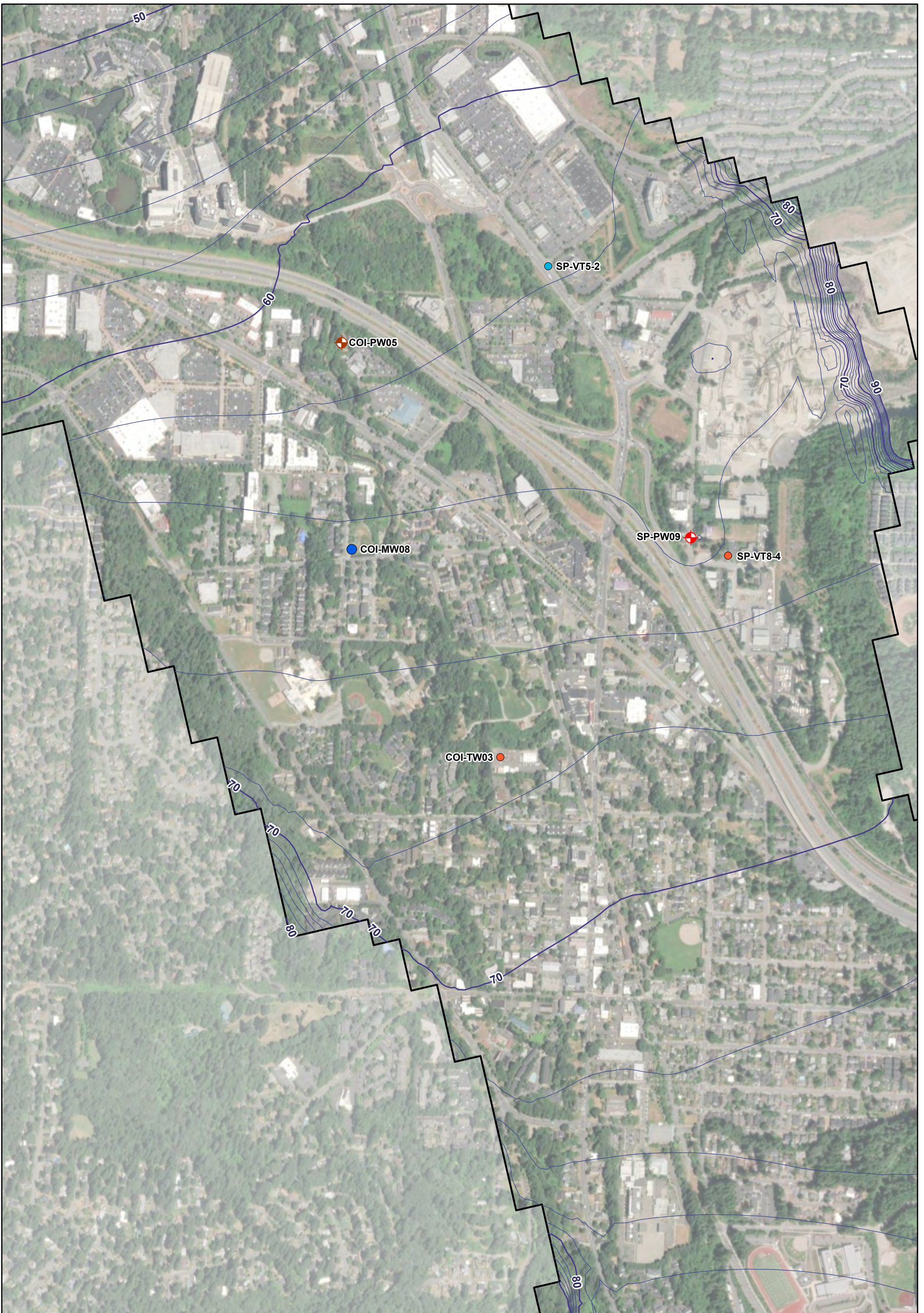
PNG0989 August 2023





<b>Legend</b> Groundwater Elevation Contour (ft msl) - 10 ft Interval Groundwater Elevation Contour (ft msl) - 2 ft Interval A Zone Production Well Model Domain		<b>A Well Residual (feet)</b> < -2.5 -2.5 - -1 -1 - 0 0 - 1 1 - 2.5 > 2.5	<b>Notes:</b> ft msl = feet above mean sea level Aerial imagery source: Esri, July 2022.	<b>Simulated Groundwater Elevation Contours (Steady-State) in A Aquifer</b> Lower Issaquah Valley Issaquah, Washington
				<b>Figure</b> <b>3-4b</b>
			PNG0989	August 2023





**Legend**

- Groundwater Elevation Contour (ft msl) - 10 ft Interval
- Groundwater Elevation Contour (ft msl) - 2 ft Interval
- B Zone Production Well
- C Zone Production Well
- Model Domain

**B/C Well Residual (feet)**

- < -2.5
- 2.5 - -1
- 1 - 0
- 0 - 1
- 1 - 2.5
- > 2.5

**Notes:**  
 ft msl = feet above mean sea level  
 Aerial imagery source: Esri, July 2022.

N  
  
 0 680  
 Feet

**Simulated Groundwater Elevation Contours  
(Steady-State) in B and B/C Aquifers**

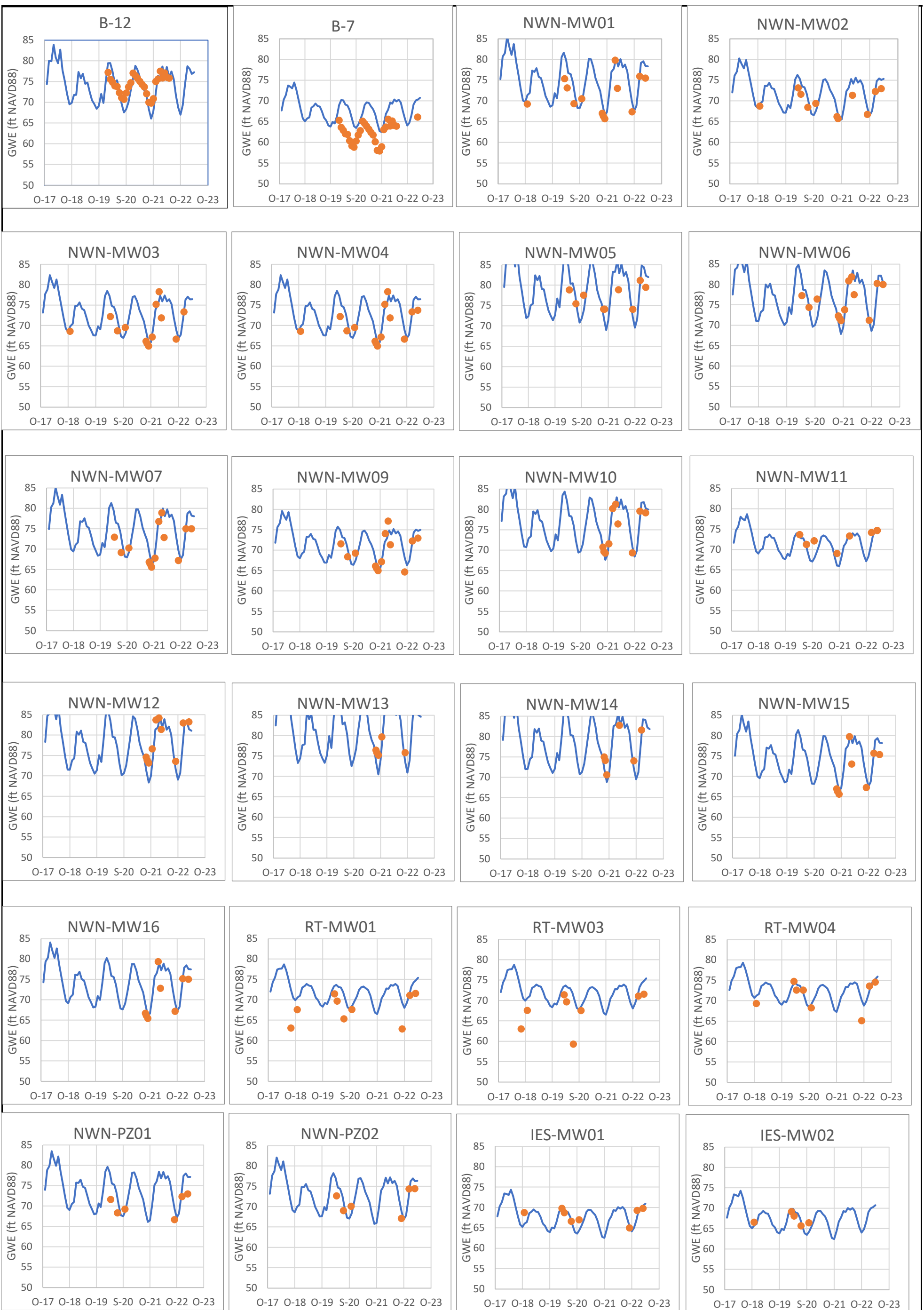
Lower Issaquah Valley  
Issaquah, Washington

**Geosyntec**  
consultants

**Figure  
3-4c**

PNG0989 August 2023





● Observed — Simulated

Measured water levels for temporary well B-7 are uncertain as the elevation of the top of casing is not based on surveyed data.

**Hydrographs of Observed and Simulated Water Levels - Shallow Aquifer (1 of 2)**

Lower Issaquah Valley  
Issaquah, Washington



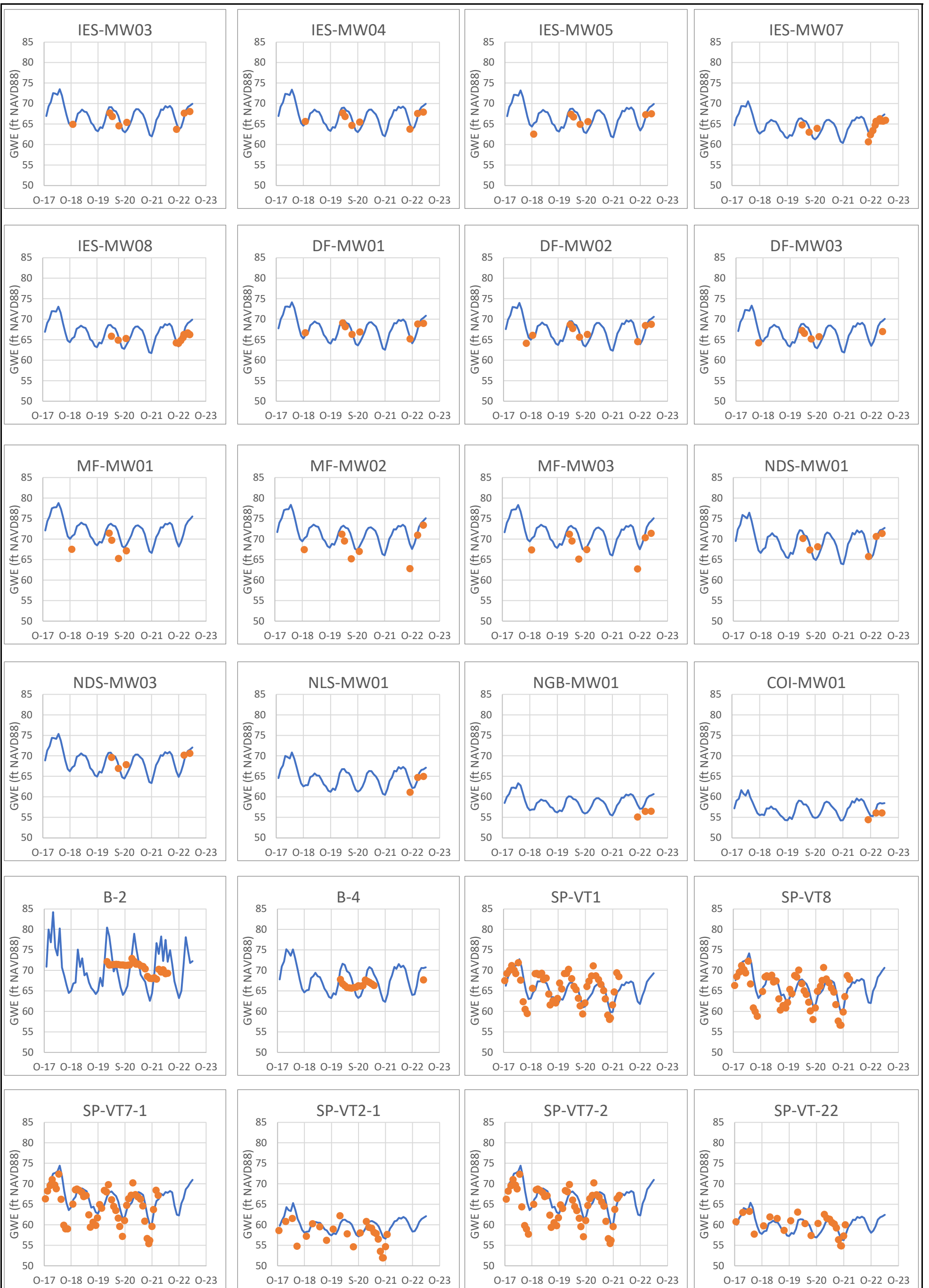
**Figure**

PNG0989

August 2023

**3-5a**





● Observed — Simulated

**Hydrographs of Observed and Simulated Water Levels - Shallow Aquifer (2 of 2)**

Lower Issaquah Valley  
Issaquah, Washington

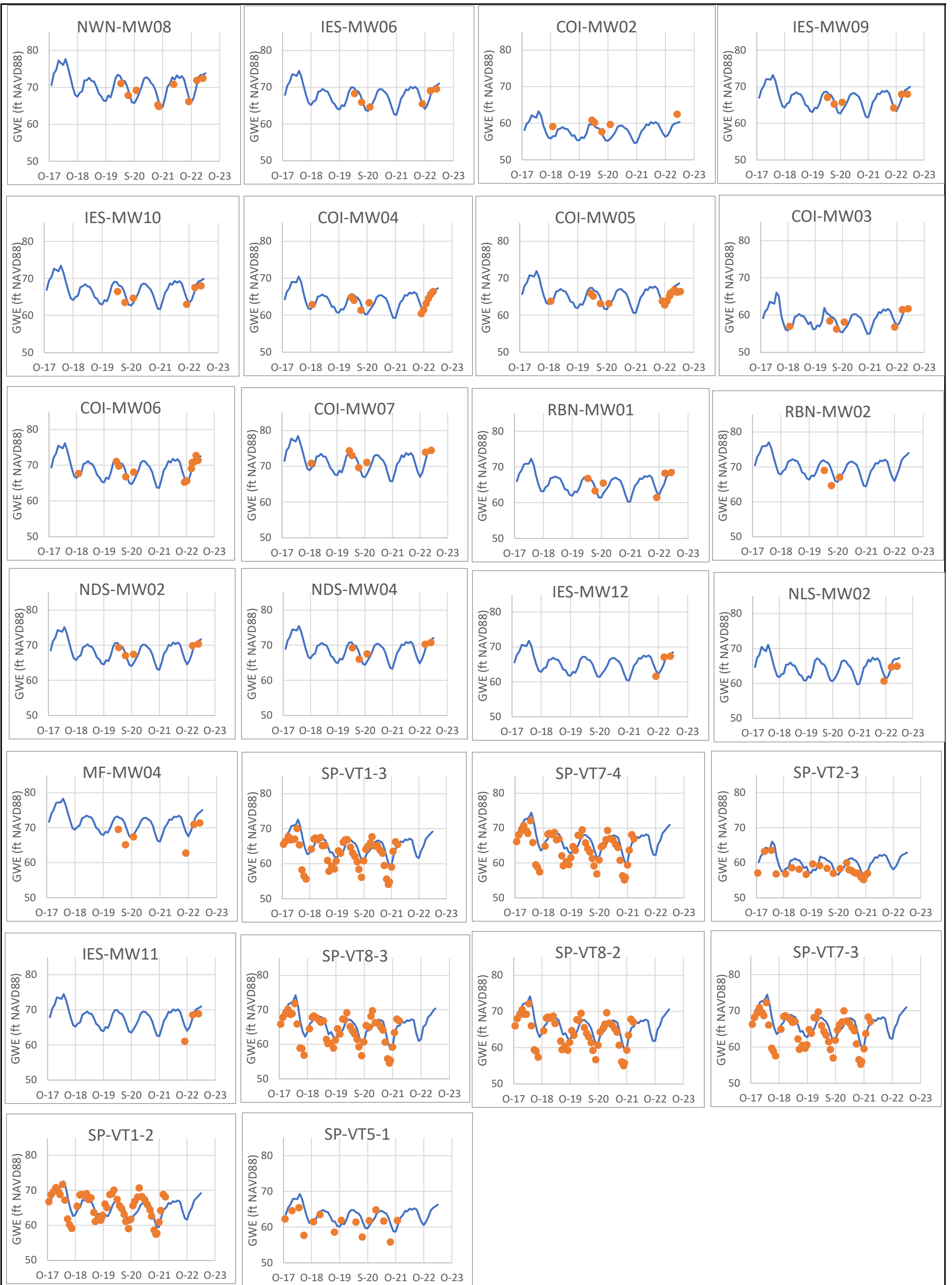


**Figure**

PNG0989

August 2023

**3-5b**



● Observed — Simulated

**Hydrographs of Observed and Simulated Water Levels - A Aquifer**

Lower Issaquah Valley  
Issaquah, Washington



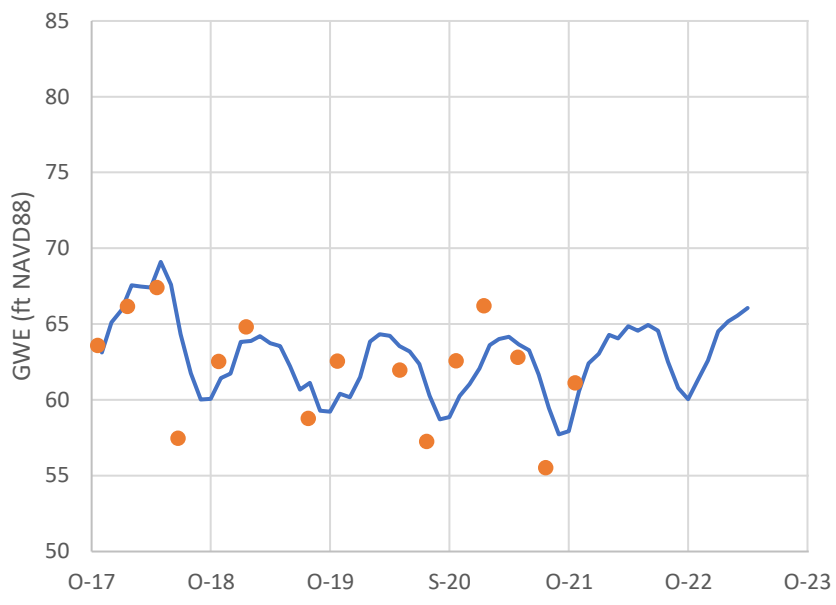
**Figure**

PNG0989

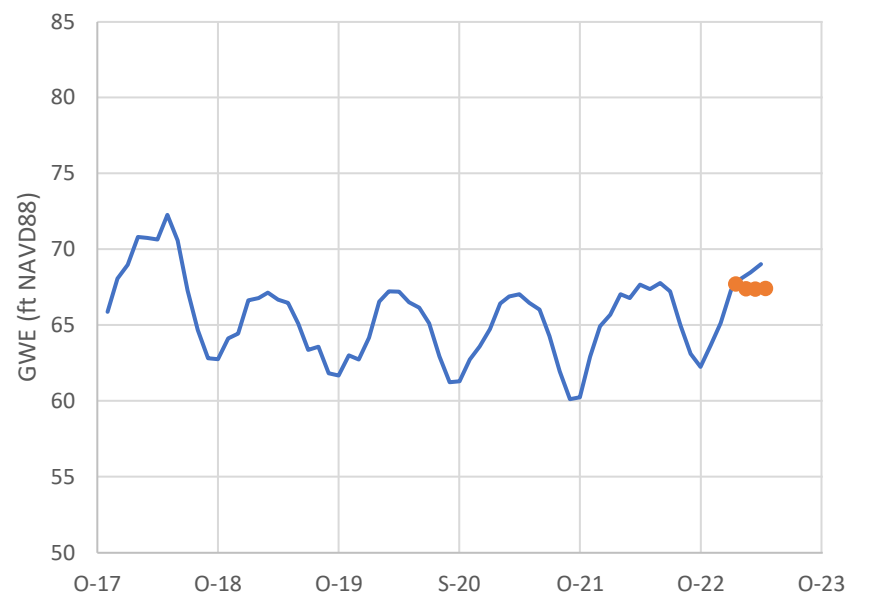
August 2023

**3-5c**

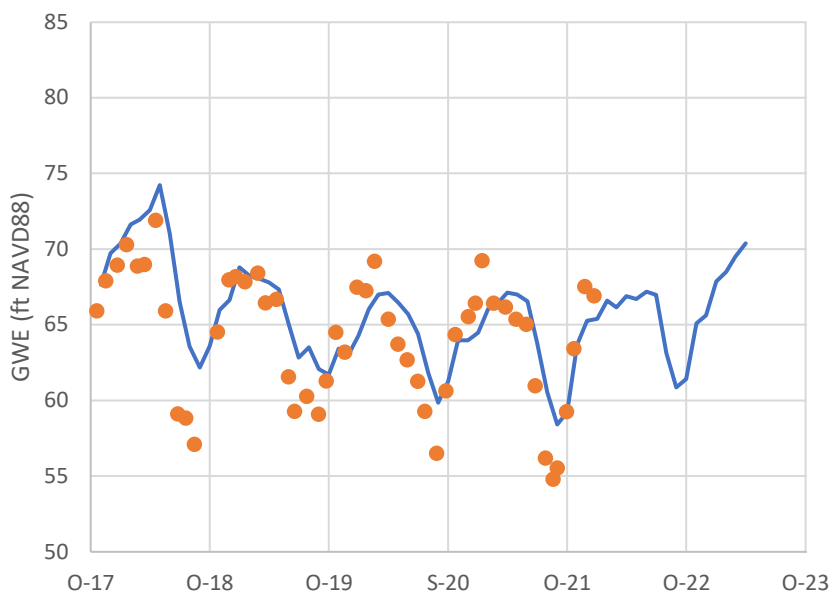
SP-VT5-2



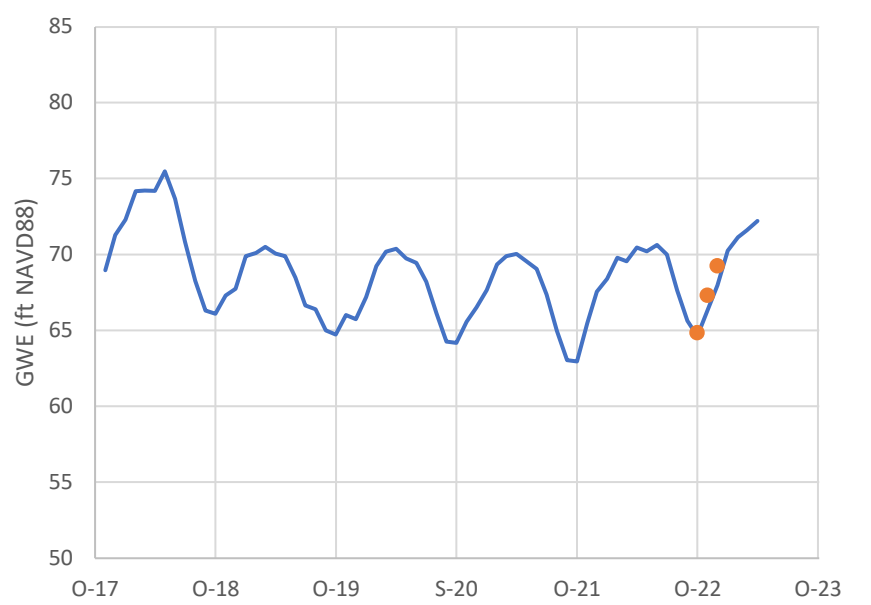
COI-MW08



SP-VT8-4



COI-TW03



● Observed — Simulated

**Hydrographs of Observed and Simulated Water Levels - B and B/C Aquifers**

Lower Issaquah Valley  
Issaquah, Washington



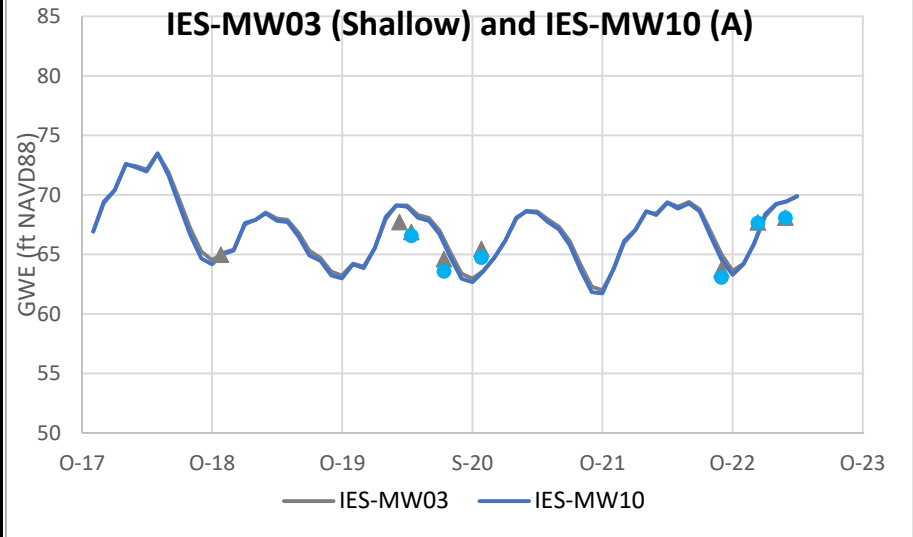
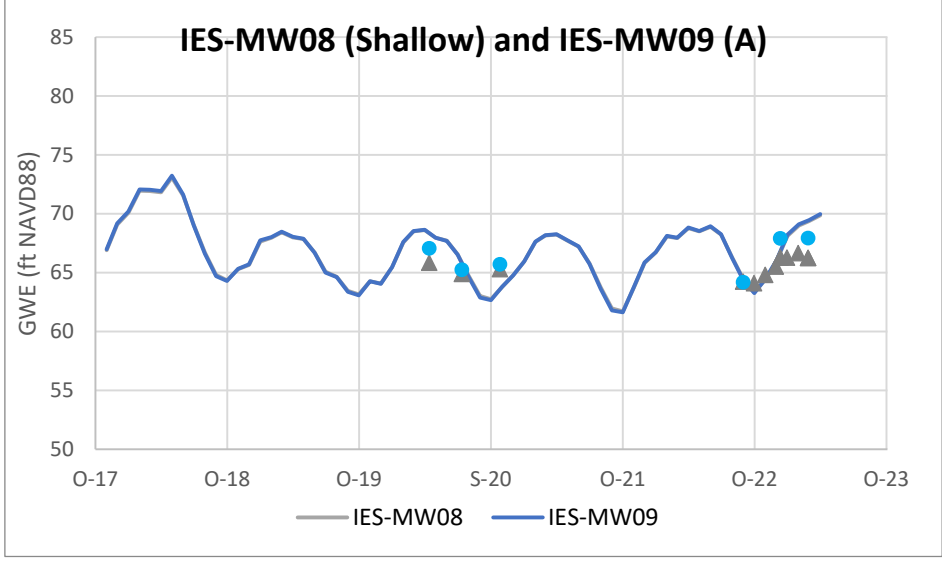
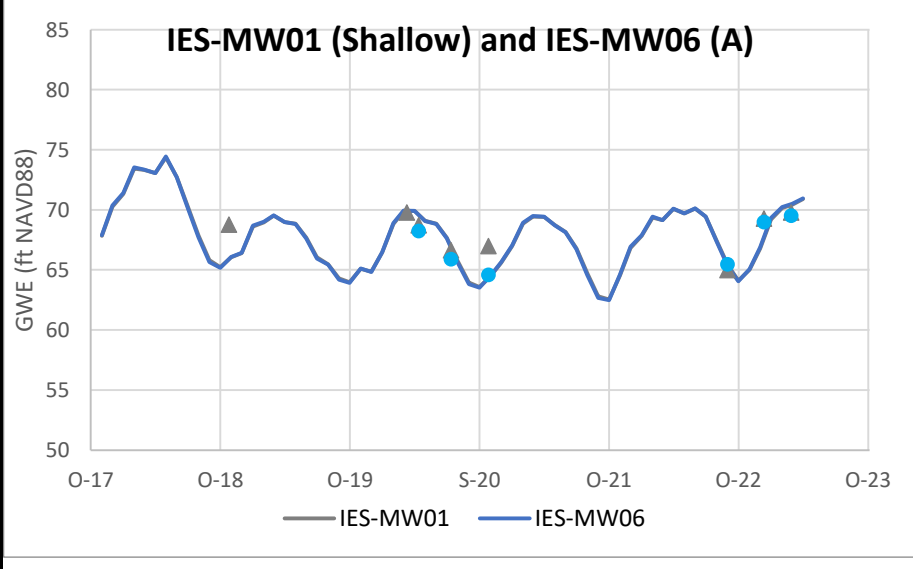
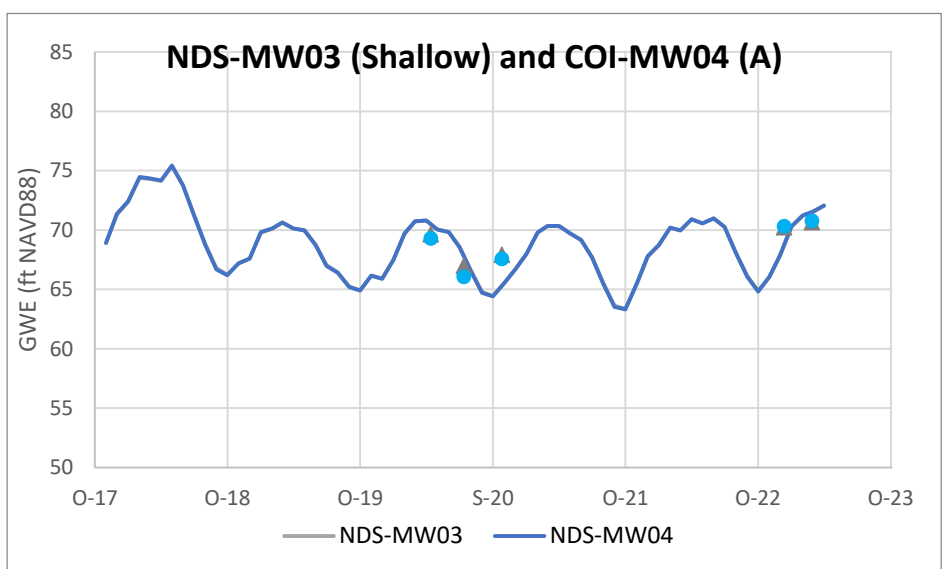
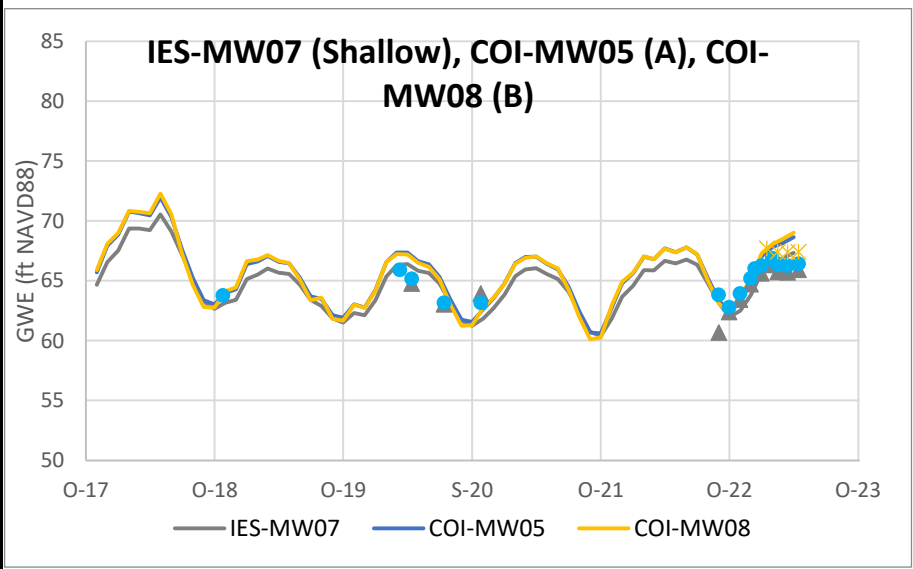
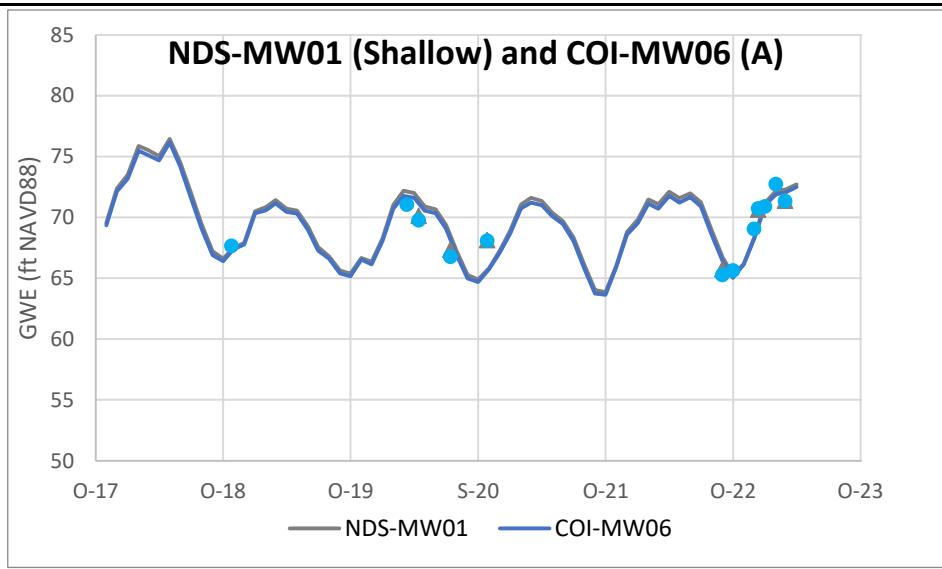
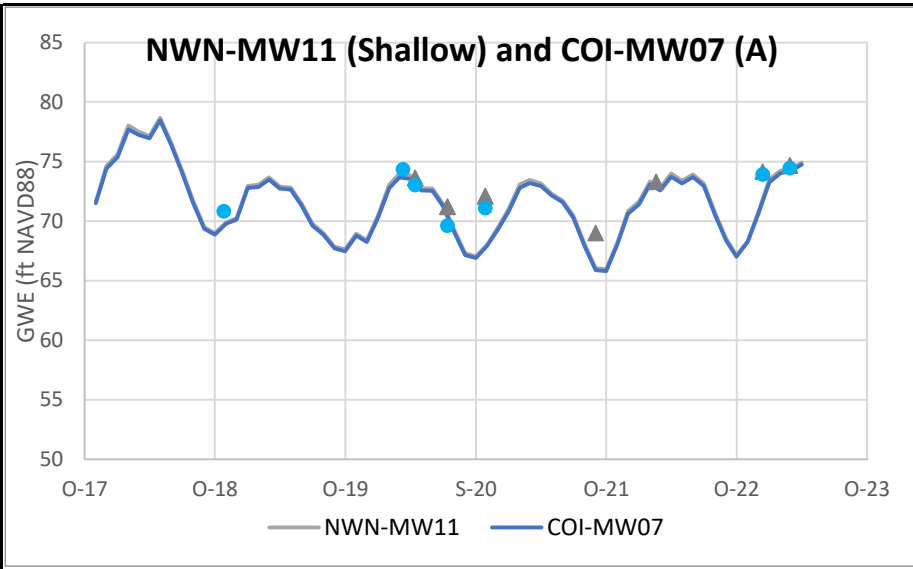
**Figure**

PNG0989

August 2023

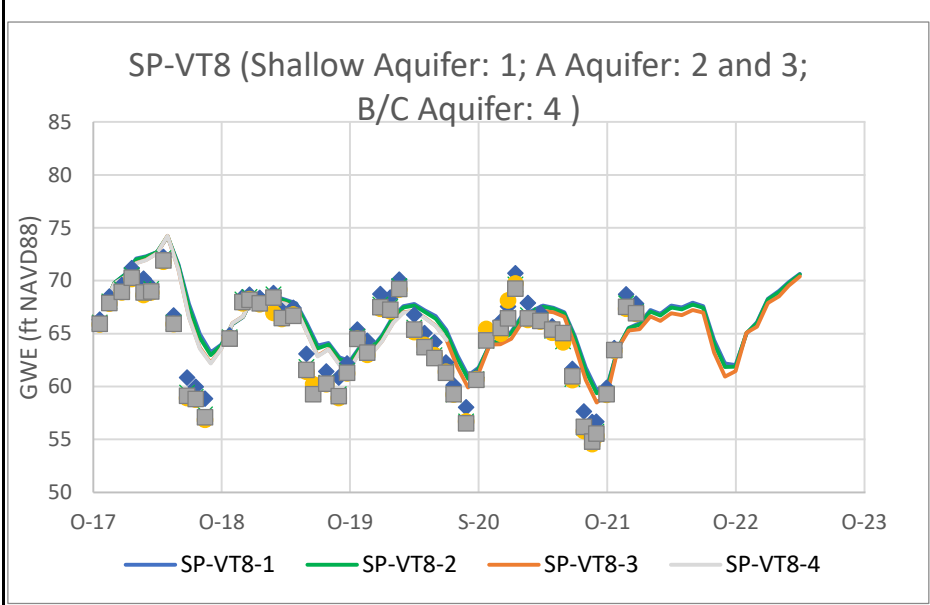
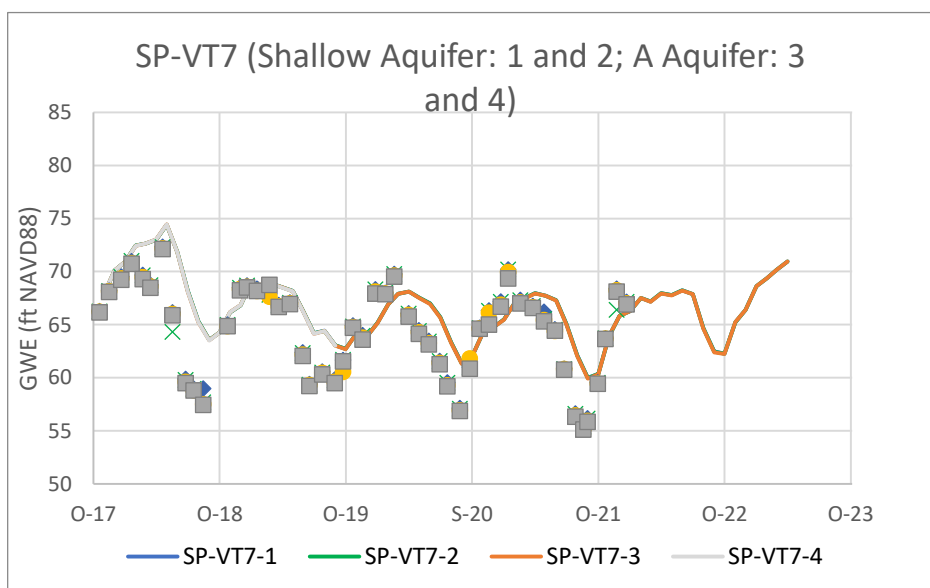
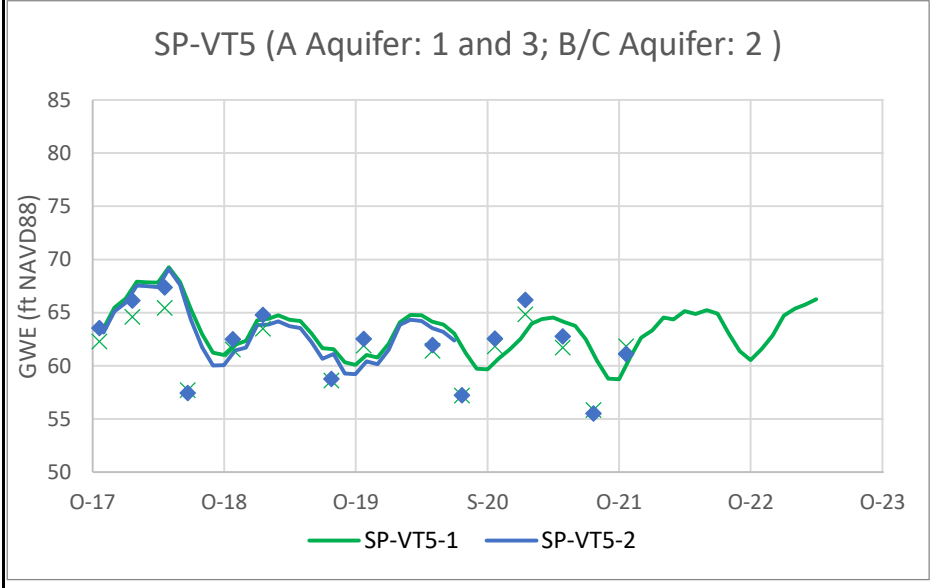
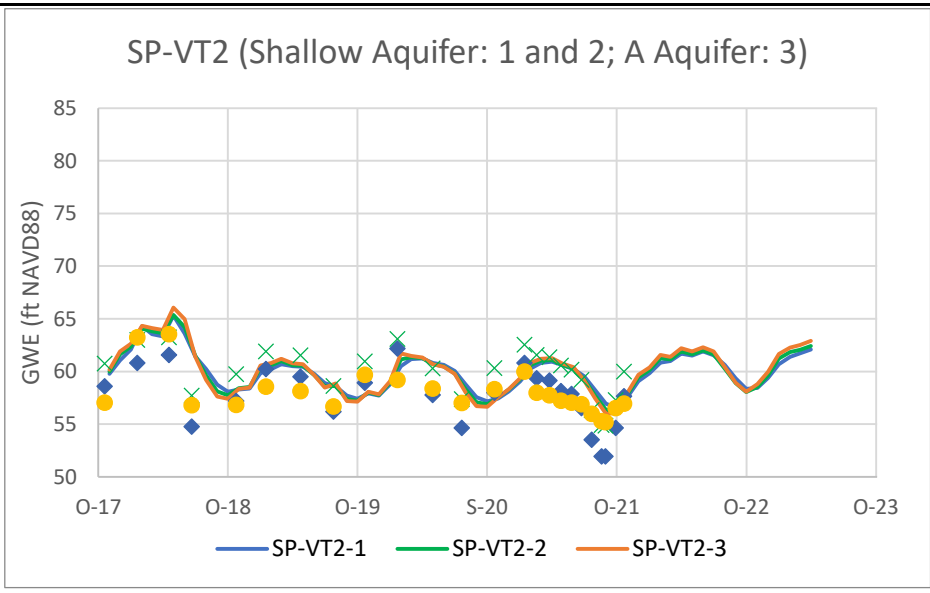
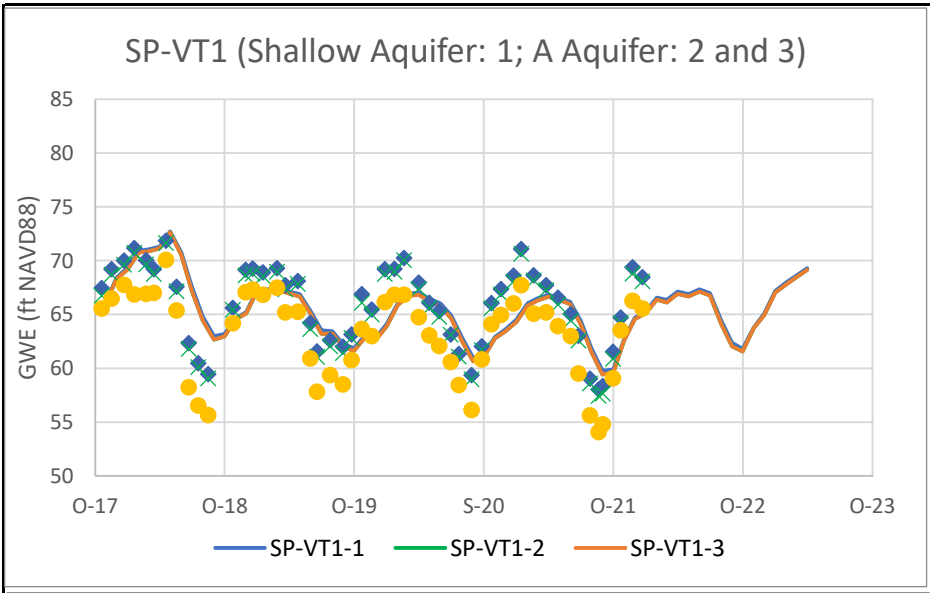
**3-5d**





**Note:**  
Solid lines and scatter points indicate simulated and observed water levels, respectively.

<b>Hydrographs of Observed and Simulated Water Levels at Cluster Wells - Central/Western Wells</b>	
Lower Issaquah Valley Issaquah, Washington	
PNG0989	August 2023
<b>Figure 3-6a</b>	

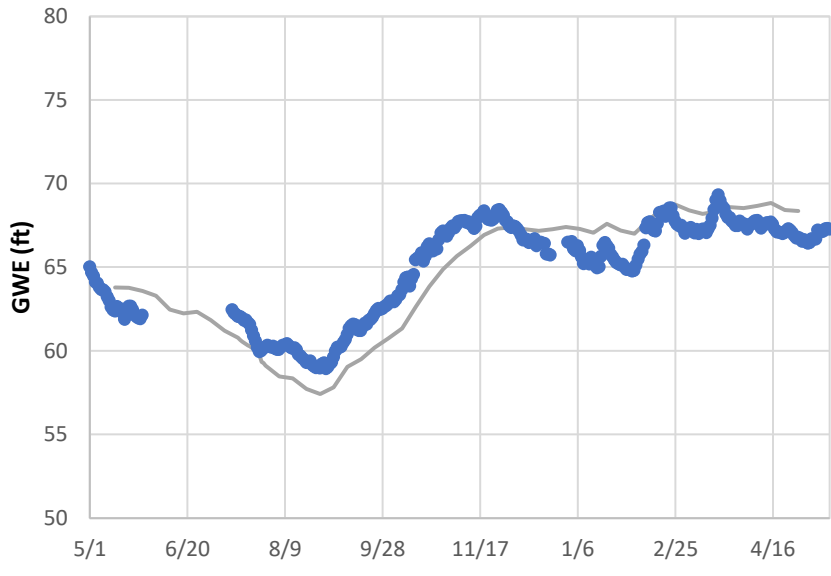


**Note:**  
Solid lines and scatter points indicate simulated and observed water levels, respectively.

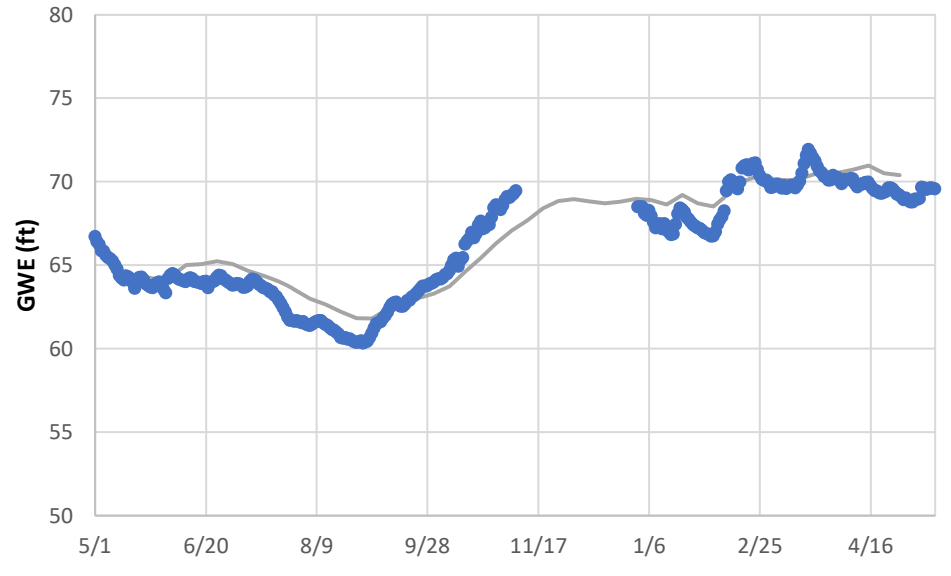
<b>Hydrographs of Observed and Simulated Water Levels at Cluster Wells - Eastern Wells</b>	
Lower Issaquah Valley Issaquah, Washington	
PNG0989	August 2023
<b>Figure 3-6b</b>	



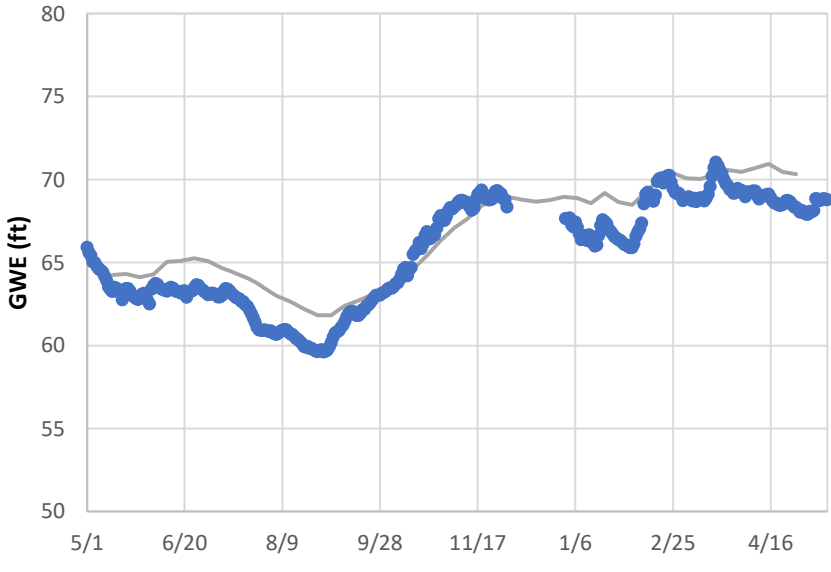
VT1-3



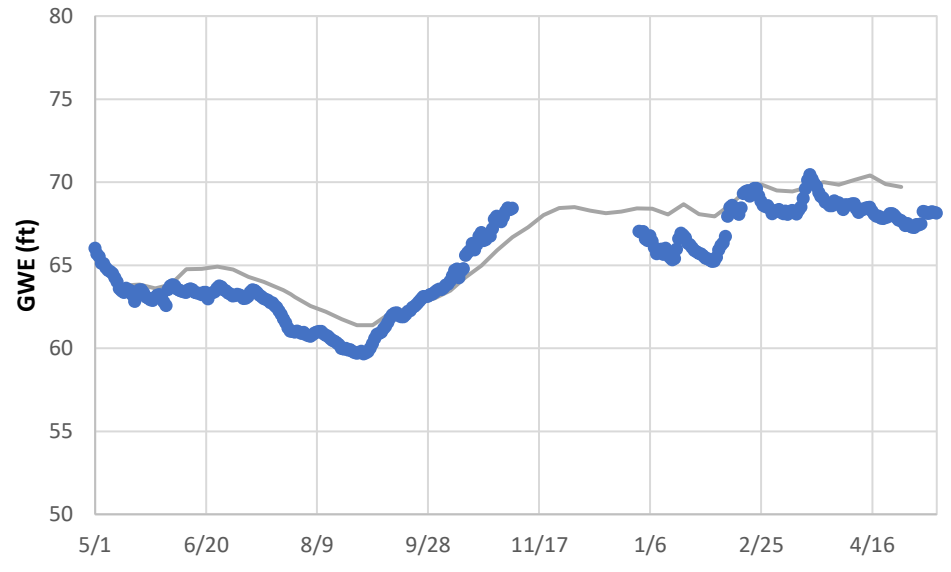
VT7-1



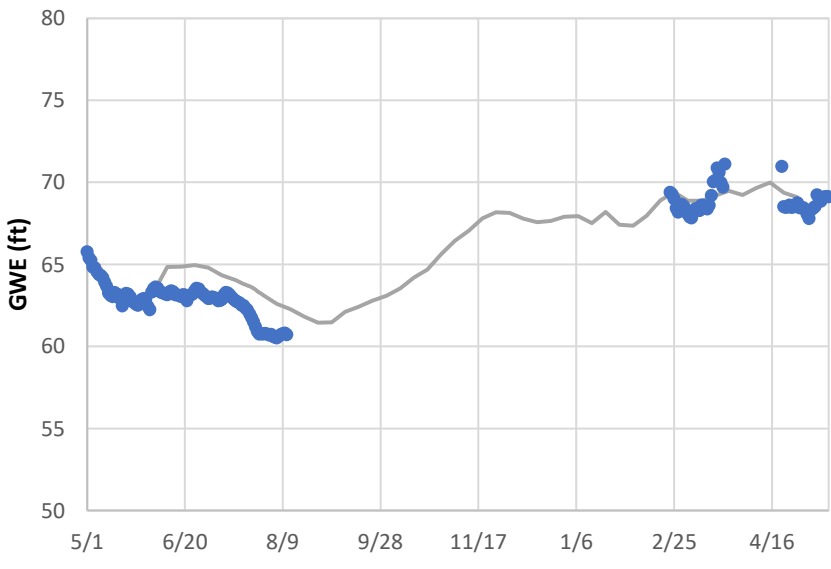
VT7-4



VT8-2



VT8-3



**Note:**  
Scatter points and lines indicate observed and simulated water levels, respectively.

**Simulated and Observed Water Levels at COI Wells between May 2016 and April 2017**

Lower Issaquah Valley  
Issaquah, Washington



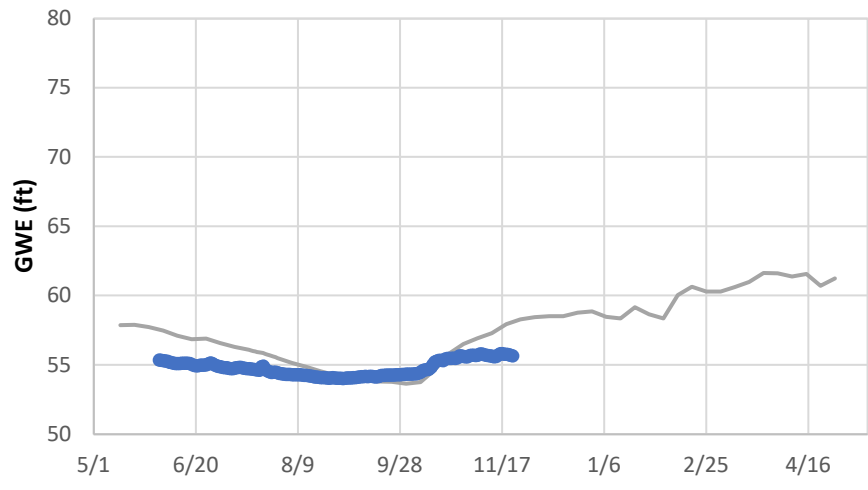
PNG0989

May 2023

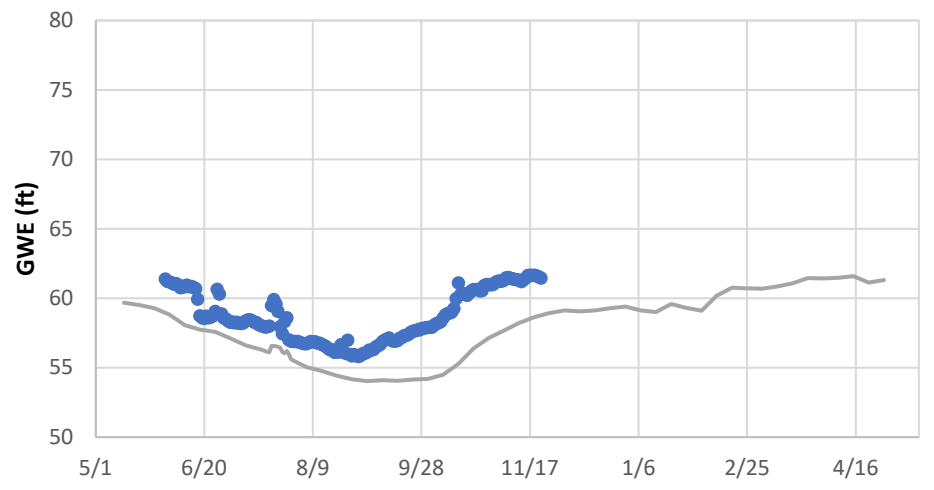
**Figure  
3-7a**



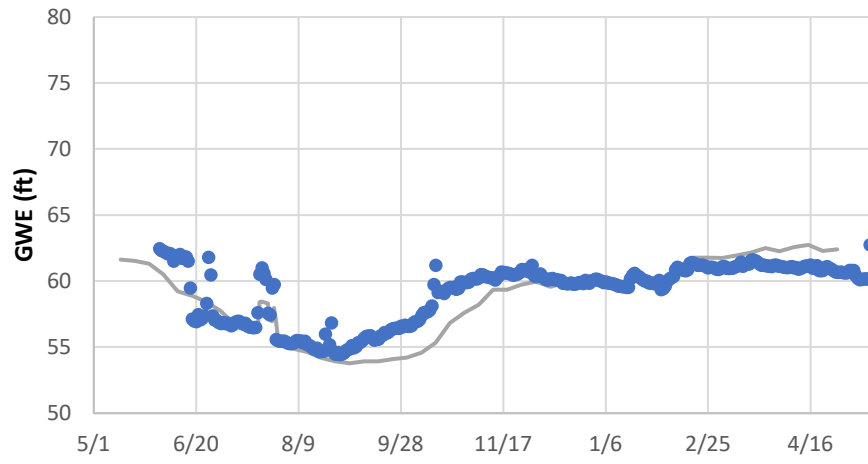
**COI-MW01**



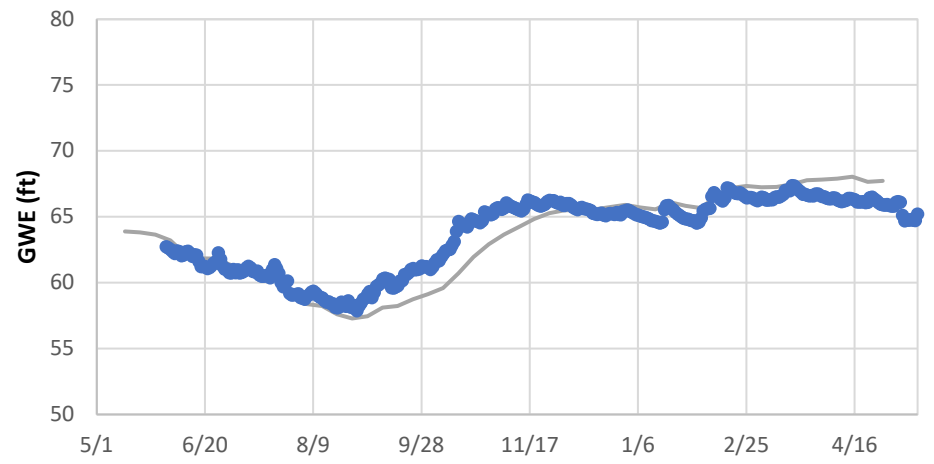
**COI-MW02**



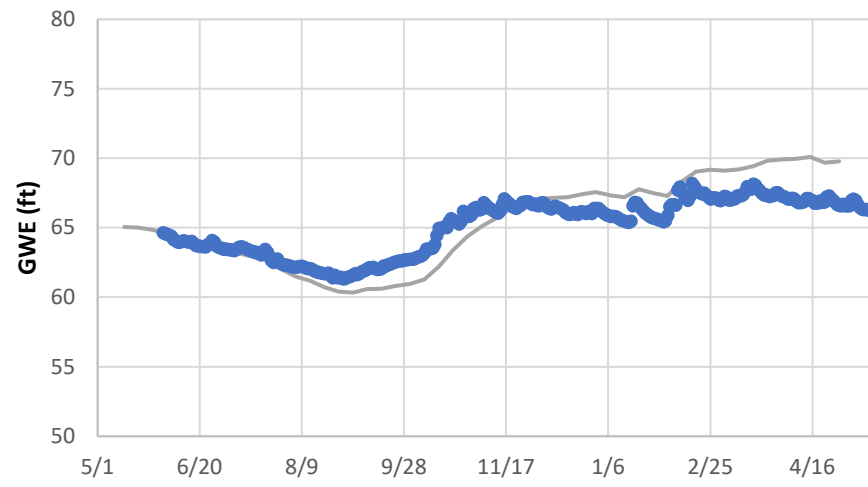
**COI-MW03**



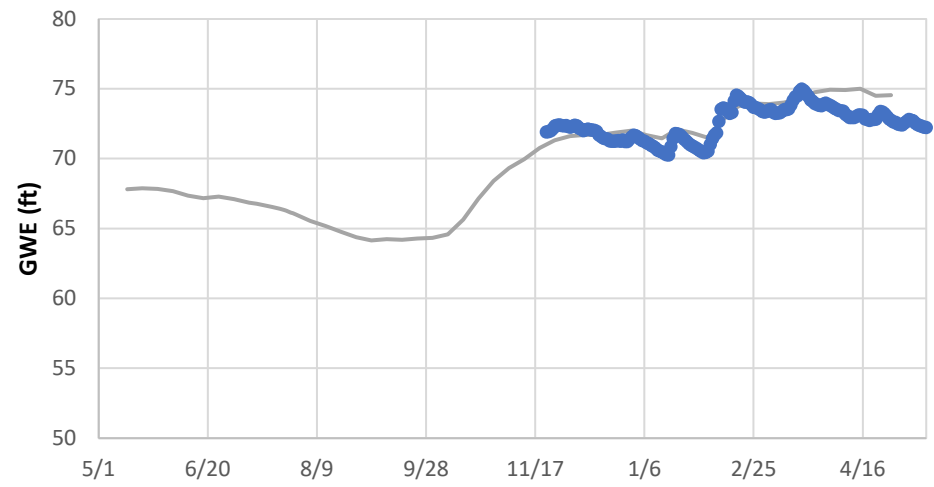
**COI-MW04**



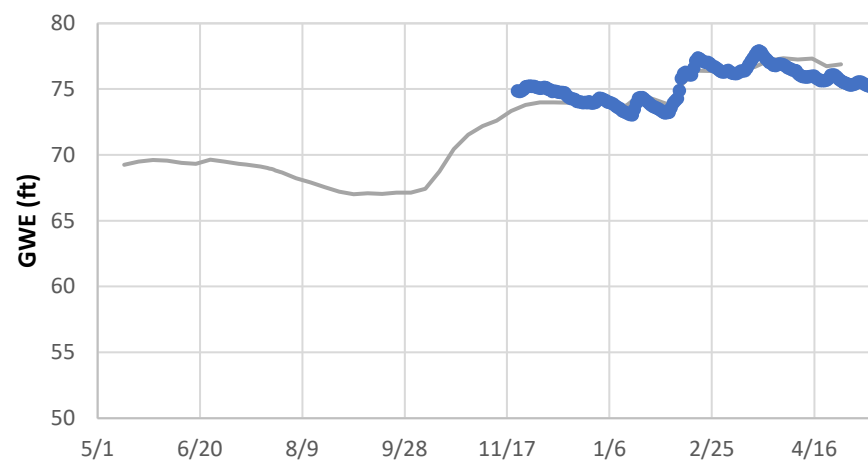
**COI-MW05**



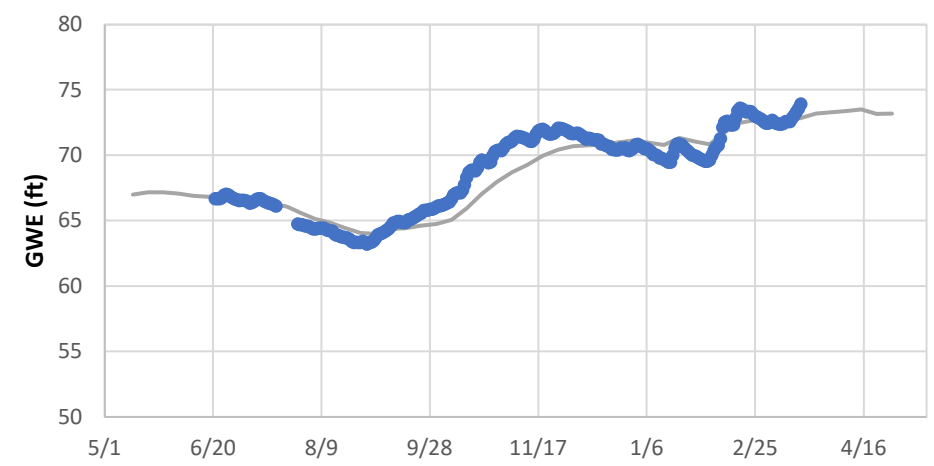
**COI-MW06**



**COI-MW07**



**COI-TW03**



**Note:**  
Open symbols are non-detects,

**Simulated and Observed Water Levels at COI Wells between May 2016 and April 2017**

Lower Issaquah Valley  
Issaquah, Washington



**Figure**

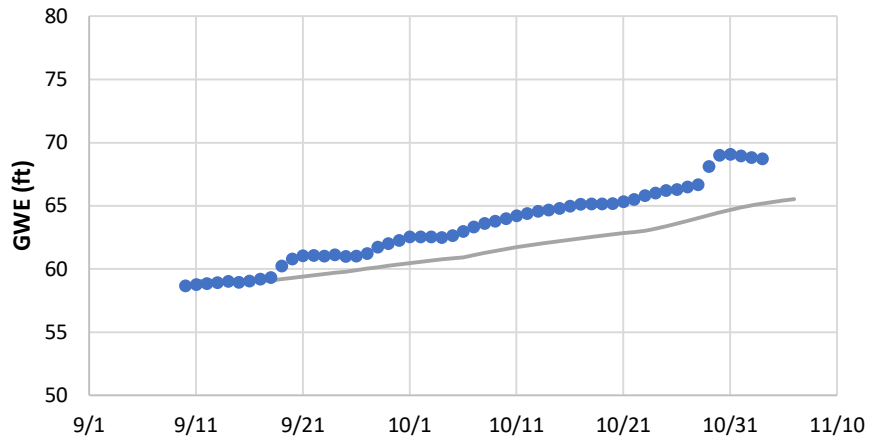
PNG0989

May 2023

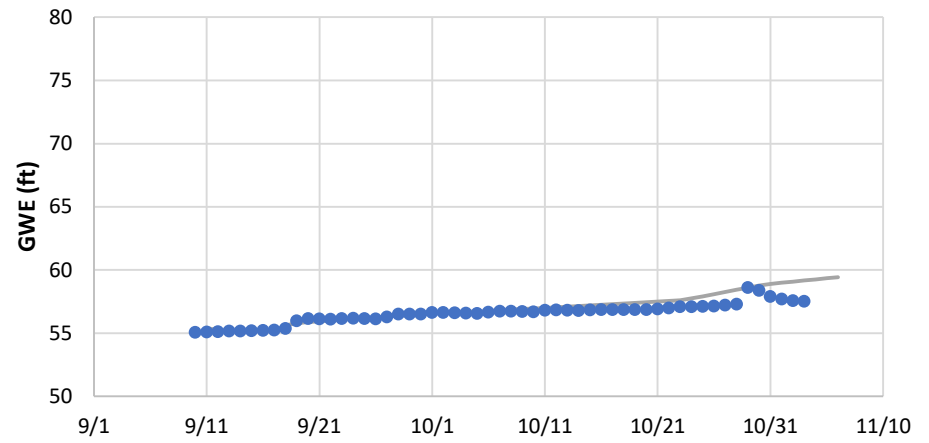
**3-7b**



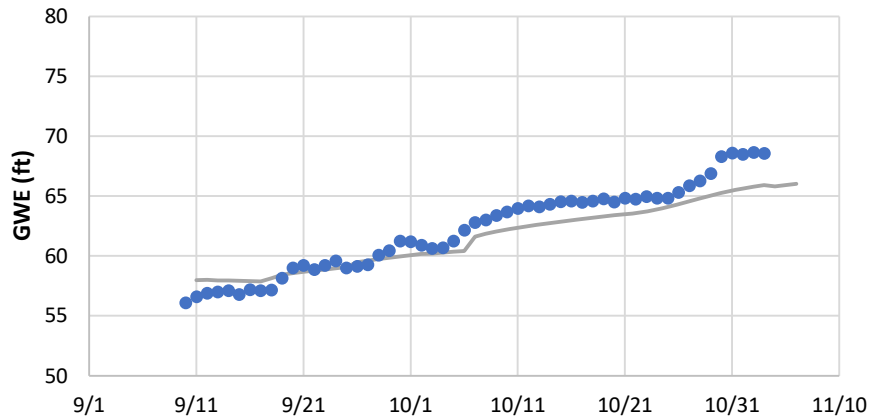
**VT1-1**



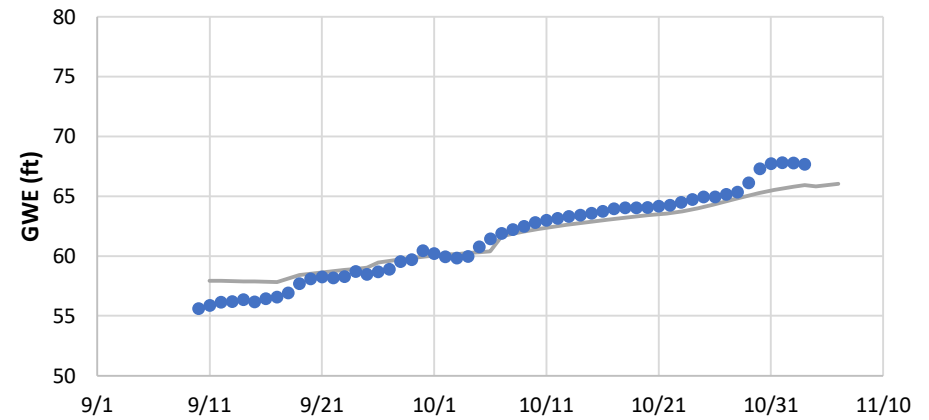
**VT2-3**



**VT8-3**



**VT8-4**



**Note:**  
Scatter points and lines indicate observed and simulated water levels, respectively.

**Simulated and Observed Water Levels at SPWD between  
September and November, 2021**

Lower Issaquah Valley  
Issaquah, Washington



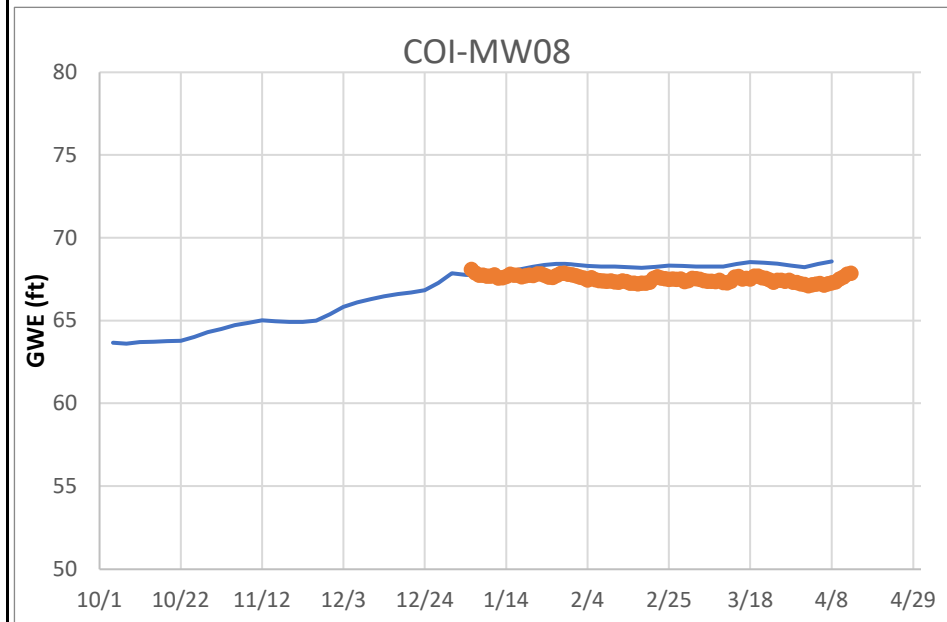
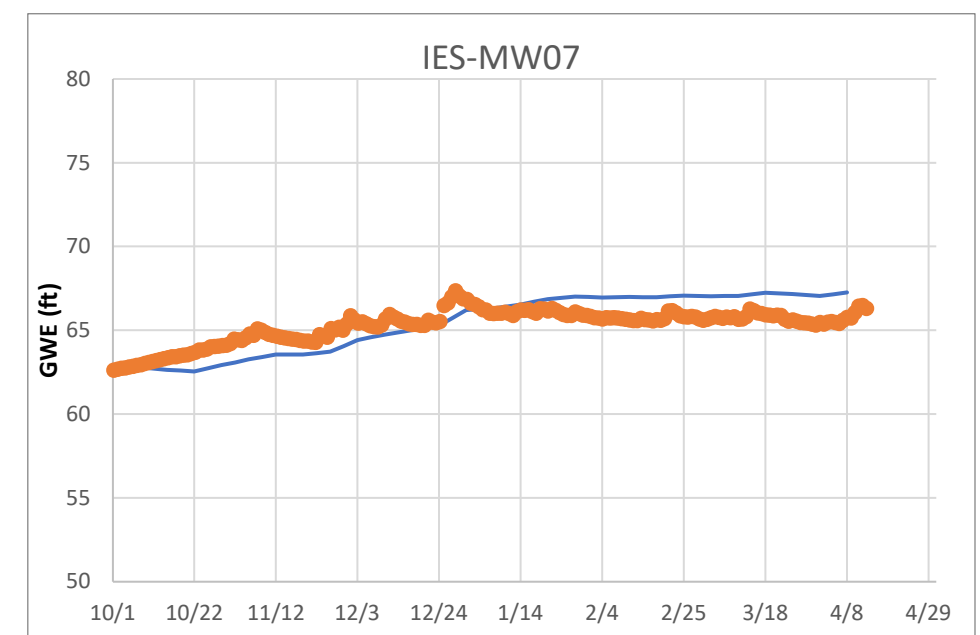
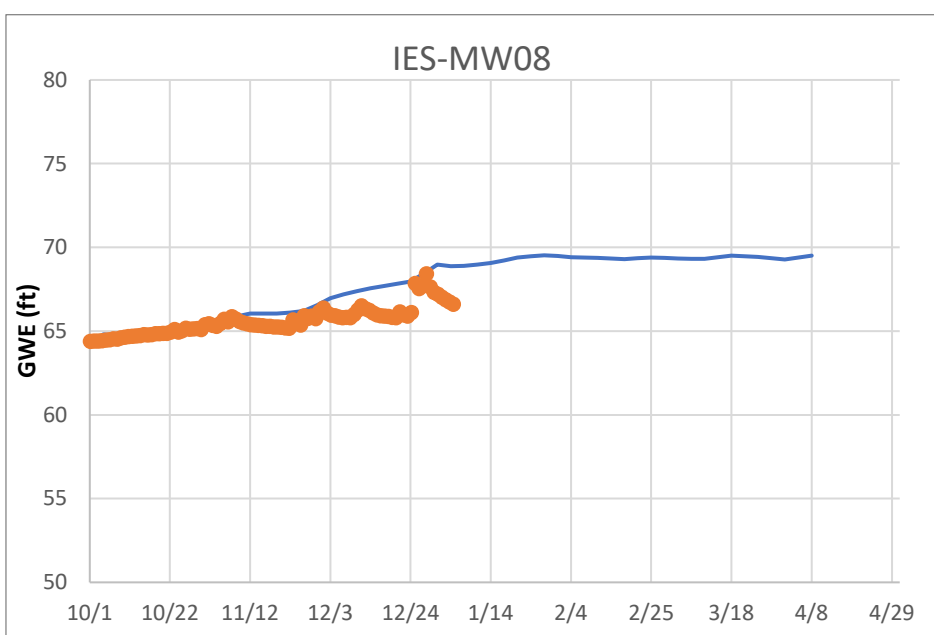
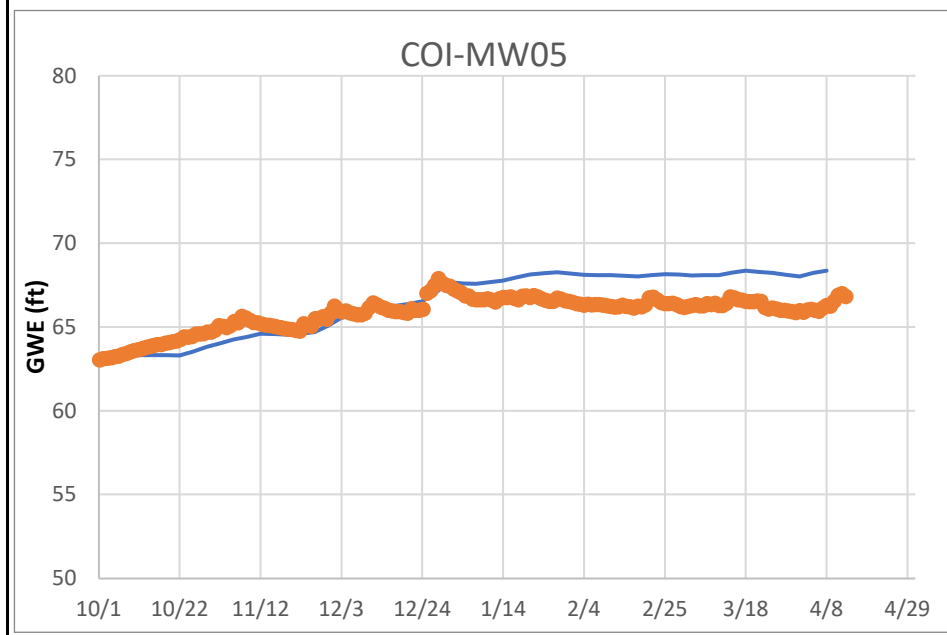
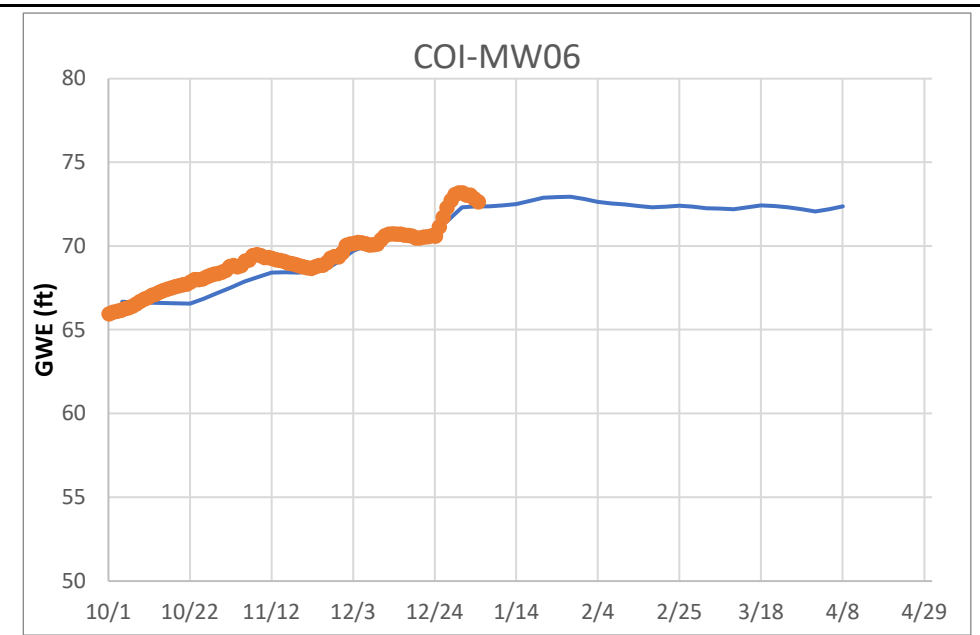
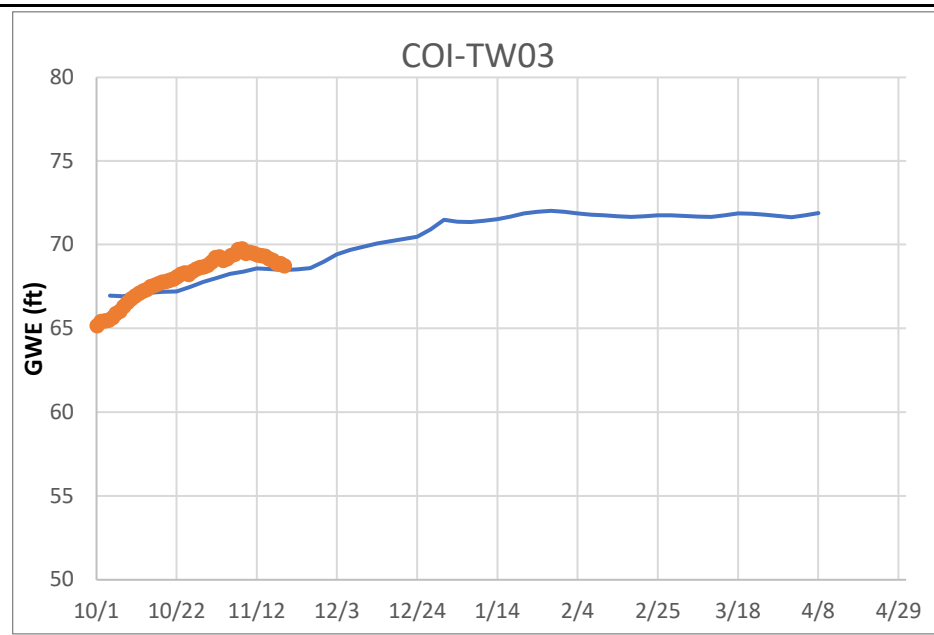
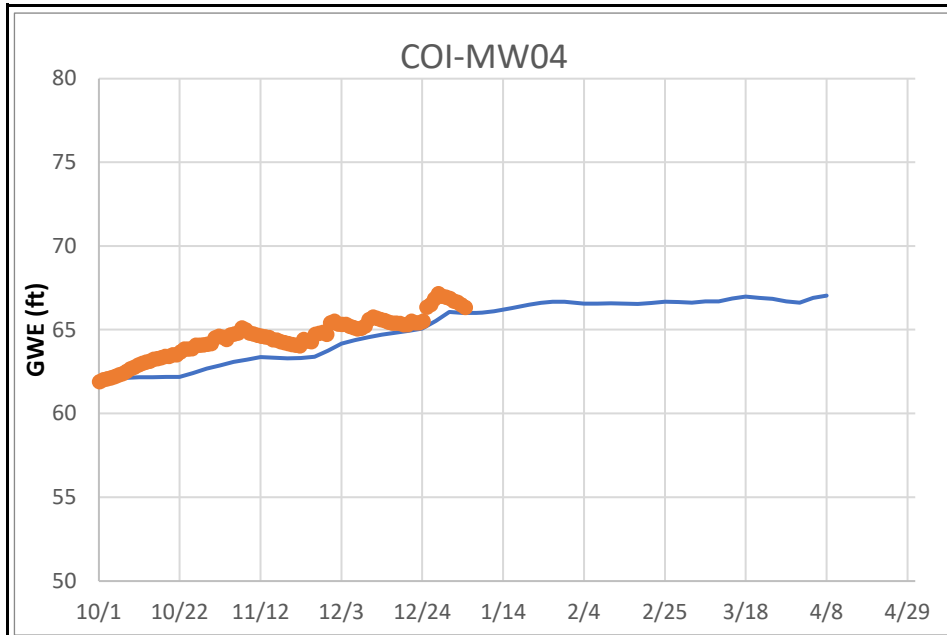
**Figure**

**3-8**

PNG0989

May 2023

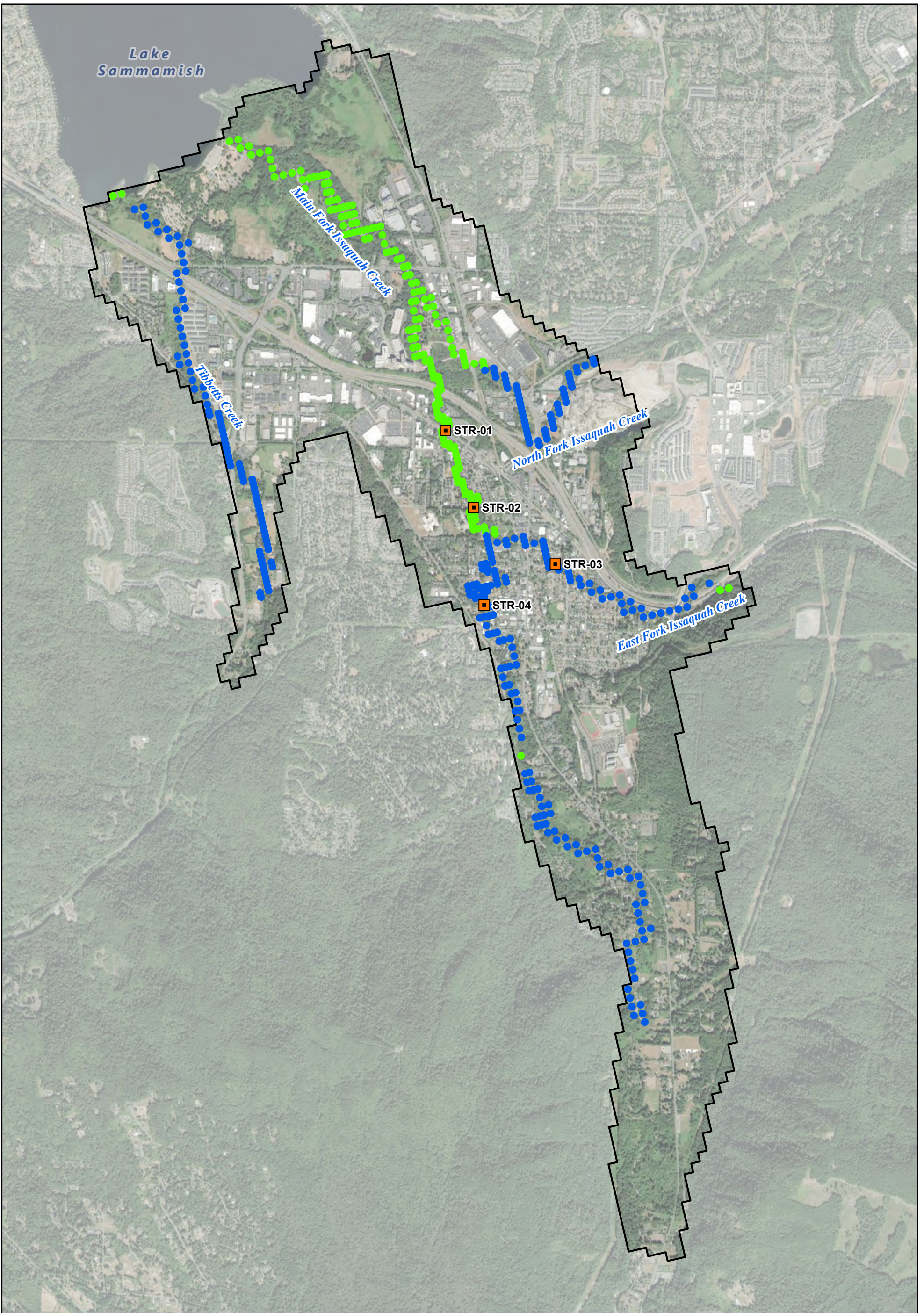




● Observed — Simulated

<b>Hydrographs of Observed and Simulated Water Levels between October 2022 and April 2023</b>	
Issaquah, WA	
PNG0989	May 2023
<b>Figure 3-9</b>	





**Legend**

**Simulated Stream/Aquifer Interaction**

- Gaining Stream
- Losing Stream

Stream Gauging Station

Model Domain

**Notes:**  
Aerial imagery source: Esri, July 2022.

**Simulated River Leakage  
(Steady-State Simulation)**

Lower Issaquah Valley  
Issaquah, Washington



0 2,000  
Feet

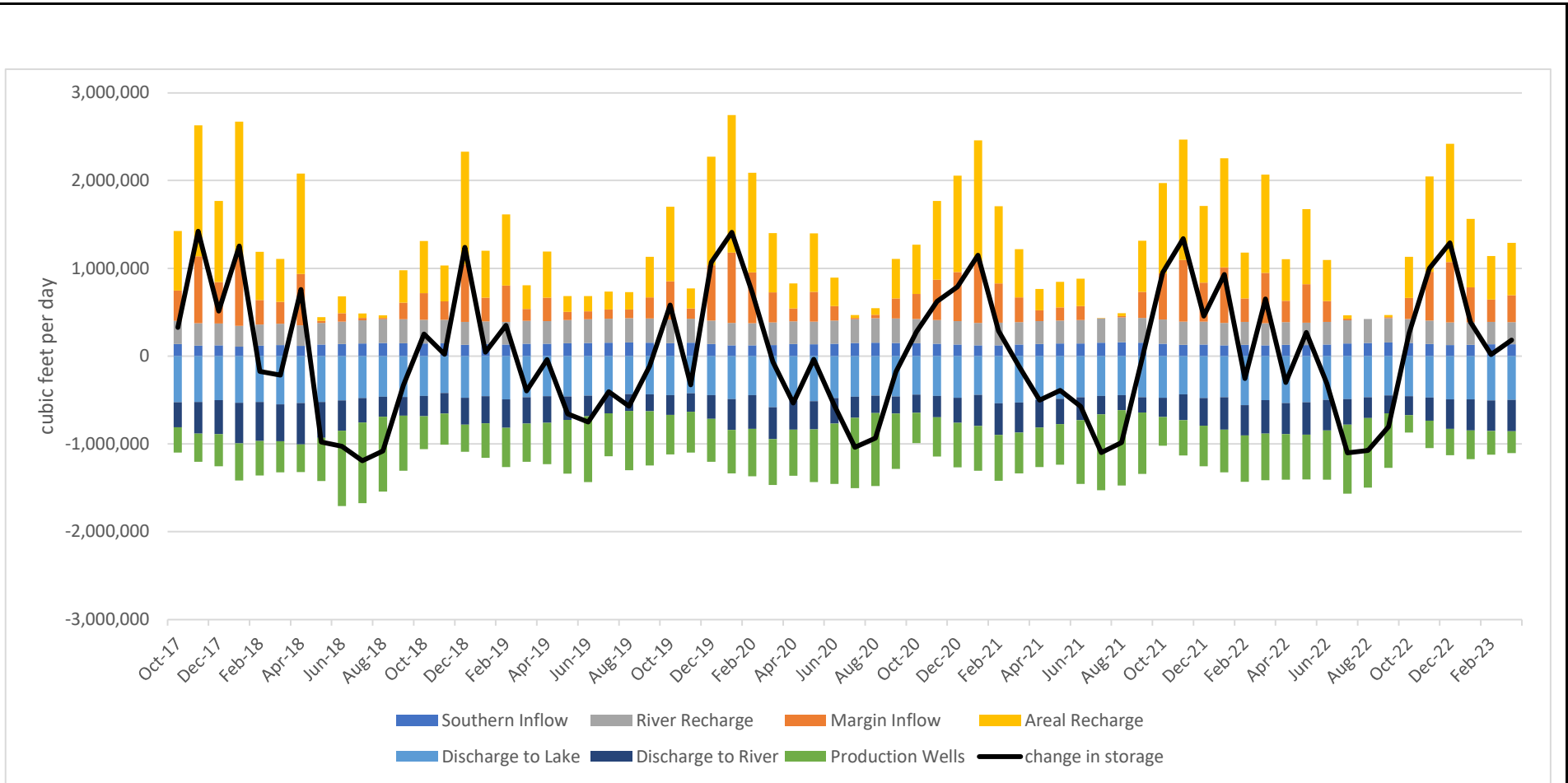
**Geosyntec**  
consultants

**Figure**  
**4-1**

PNG0989

August 2023





**Water Balance for Historical Simulation**

Lower Issaquah Valley  
Issaquah, Washington



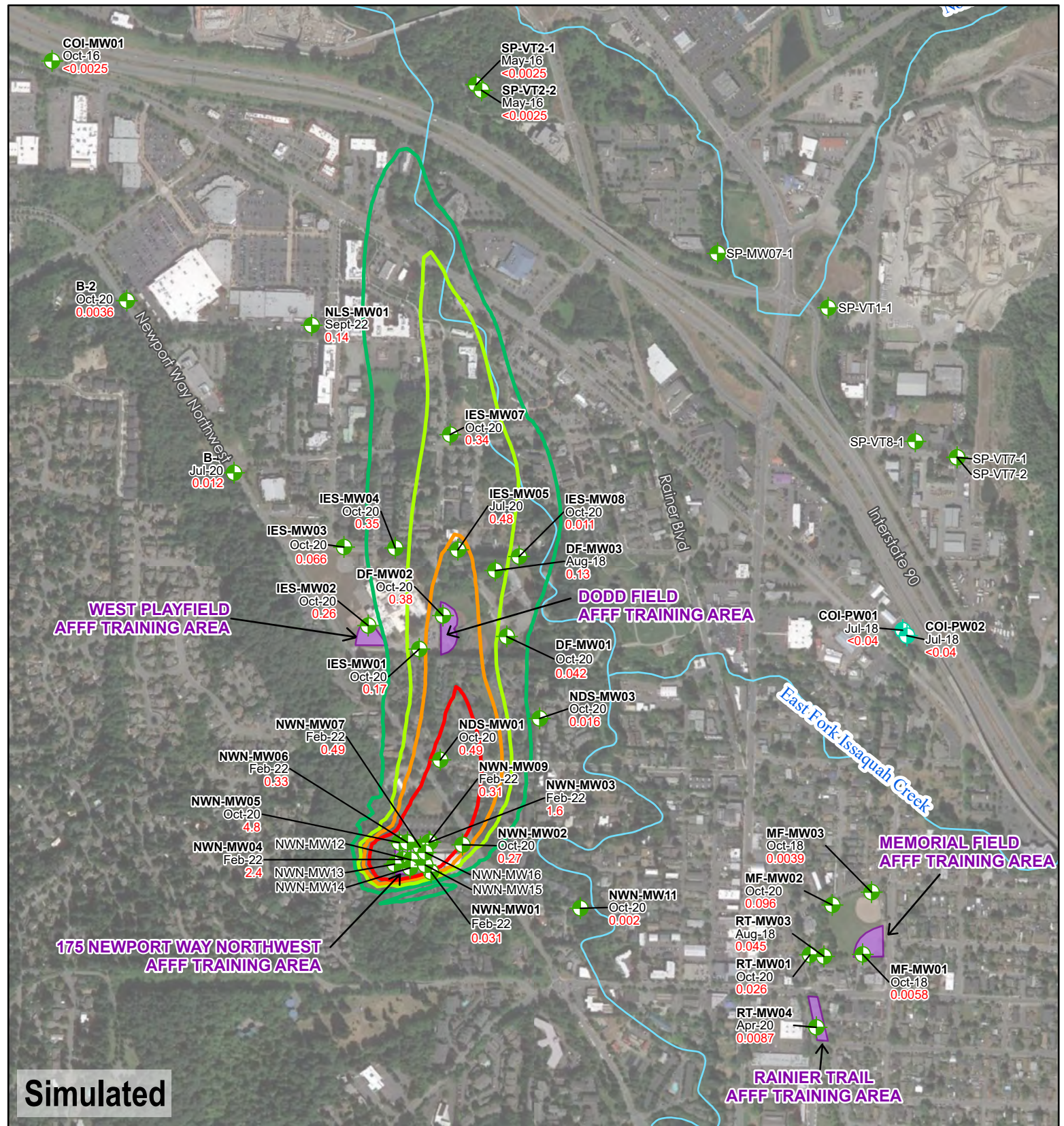
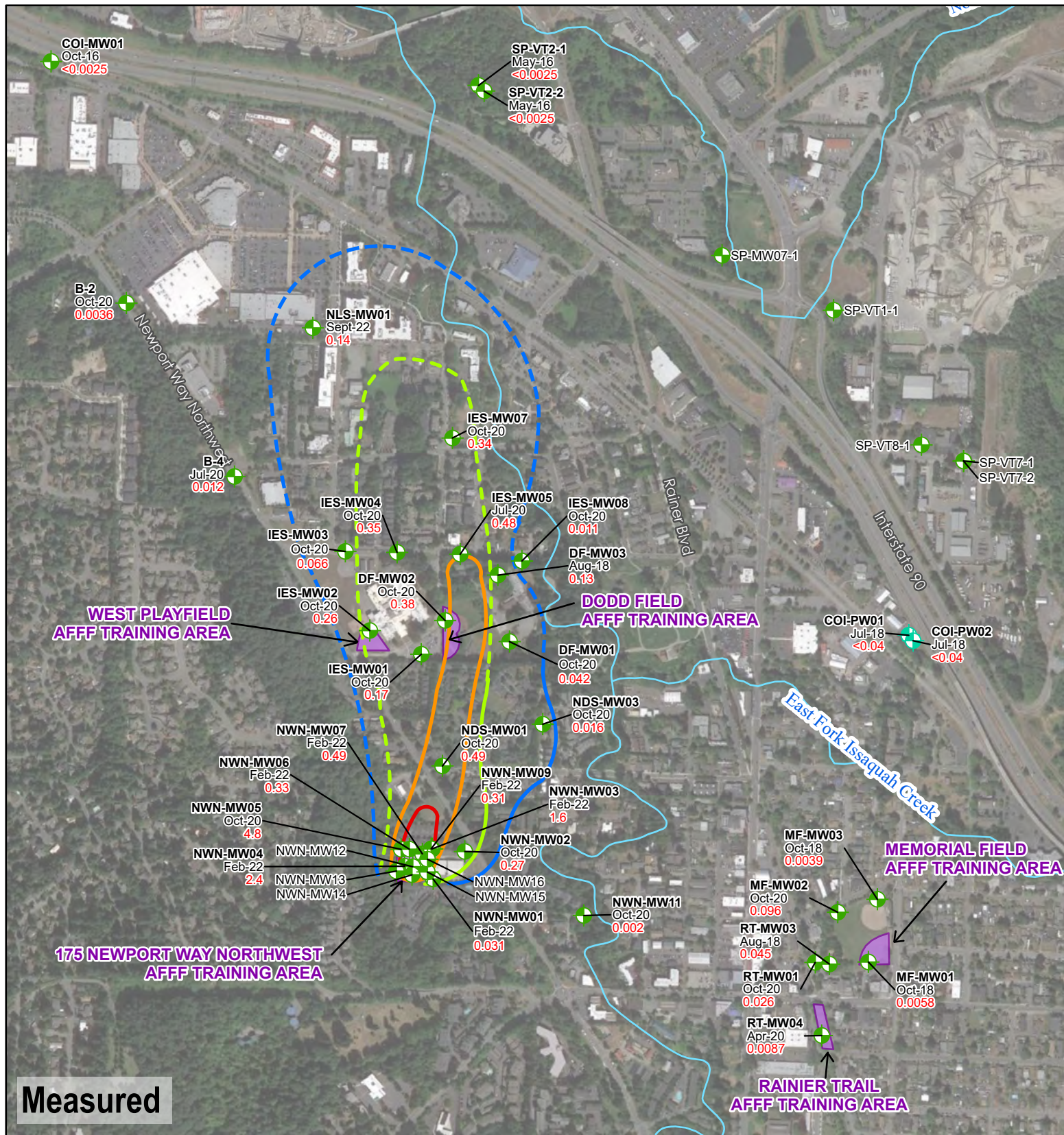
**Figure**

PNG0989

August 2023

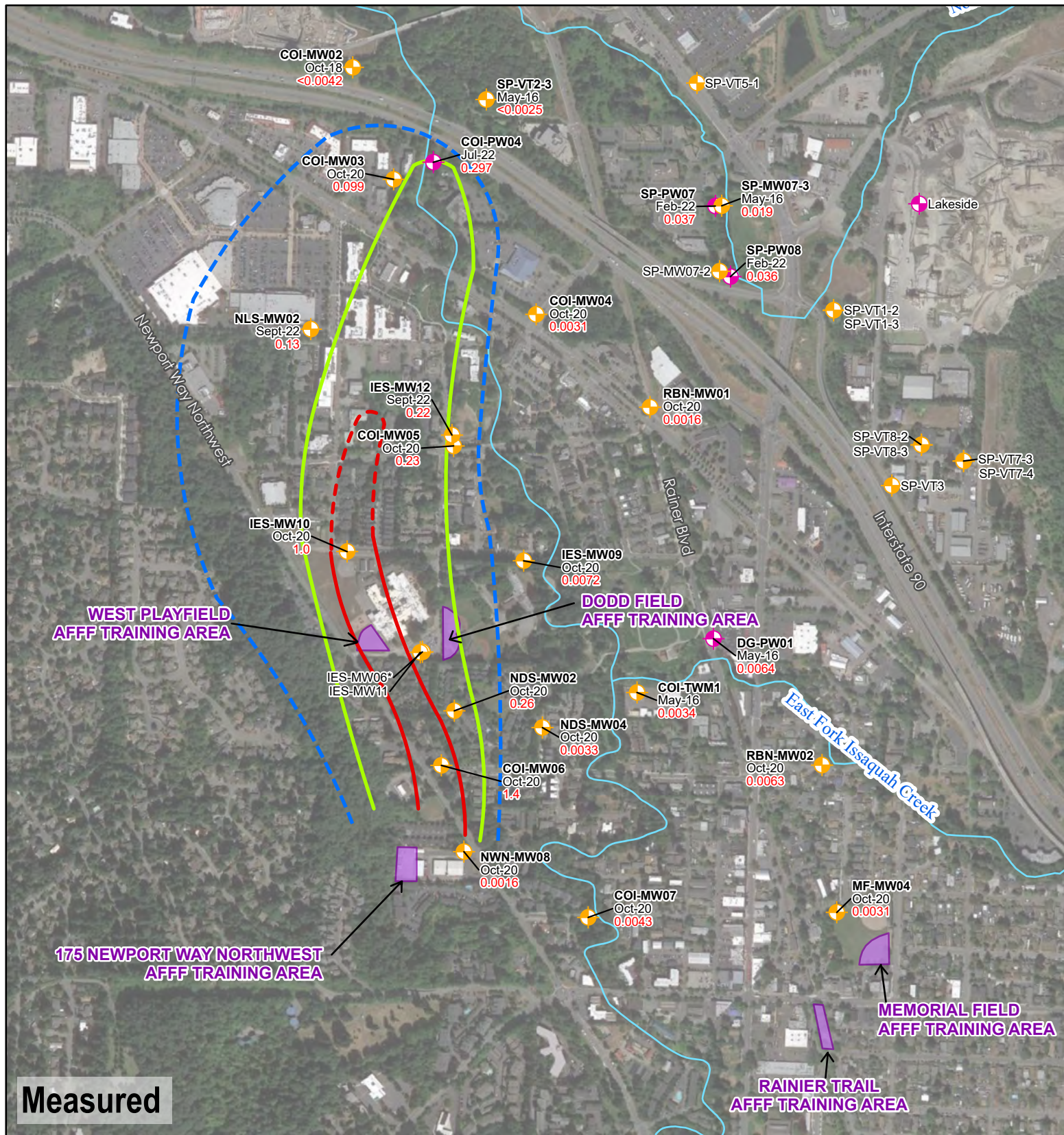
**4-2**



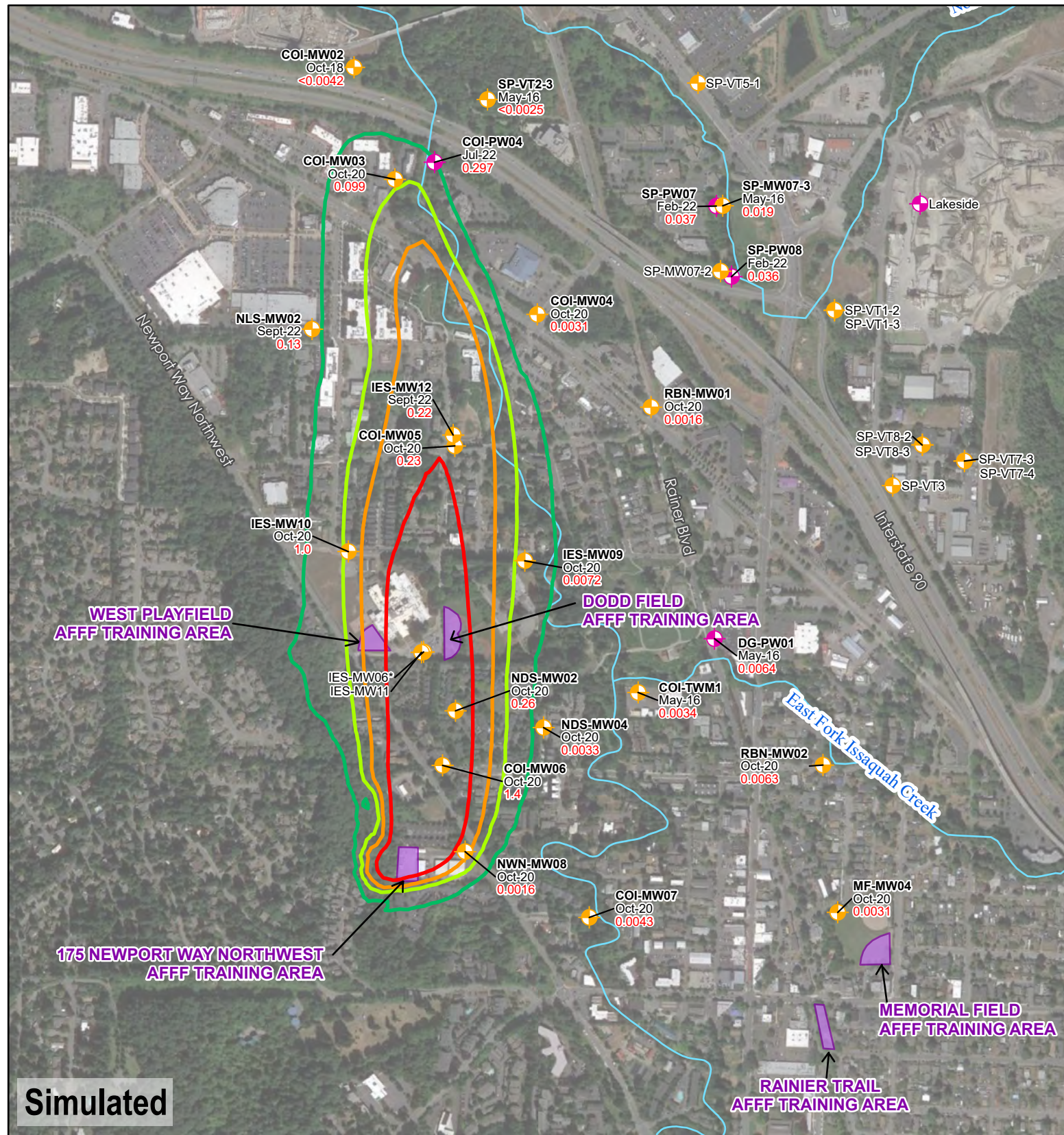


<b>Legend</b> Shallow Zone Monitoring Well Shallow Zone Production Well <b>Interpolated PFOS Concentration Contours</b> 0.015 µg/L 0.05 µg/L 0.25 µg/L 0.5 µg/L 1 µg/L <i>Dashed where inferred</i> AFFF Training Area Issaquah Creek <b>PFOS Concentration (Model Output)</b> 0.05 µg/L 0.25 µg/L 0.50 µg/L 1.0 µg/L		<b>Notes:</b> µg/L = micrograms per liter - Aerial imagery source: Google Earth Pro, August 2020.	<b>Measured and Simulated PFOS Concentrations in Shallow Aquifer</b> Lower Issaquah Valley Issaquah, Washington Geosyntec consultants PNG0989 August 2023	<b>Figure</b> <b>6-1</b>
---	--	---	---	-----------------------------





**Measured**



**Simulated**

**Legend**

- A Zone Monitoring Well
  - A Zone Production Well
  - Interpolated PFOS Concentration Contours**
    - 0.015 µg/L
    - 0.05 µg/L
    - 0.25 µg/L
    - 0.5 µg/L
    - 1 µg/L
    - Dashed where inferred*
  - AFFF Training Area
  - Issaquah Creek
- COI-MW07 – Location ID  
 Oct-20 – Most Recent Sample Date (Month and Year)  
 0.0043 – PFOS Concentration (µg/L)

**PFOS Concentration (Model Output)**

- 0.05 µg/L
- 0.25 µg/L
- 0.50 µg/L
- 1.0 µg/L

**Notes:**  
 µg/L = micrograms per liter  
 \* Data from IES-MW06 not used in contour interpretation. October 2020 concentration was 0.0018 µg/L.  
 - Aerial imagery source: Google Earth Pro, August 2020.



**Measured and Simulated PFOS Concentrations in A Zone Aquifer**

Lower Issaquah Valley  
 Issaquah, Washington



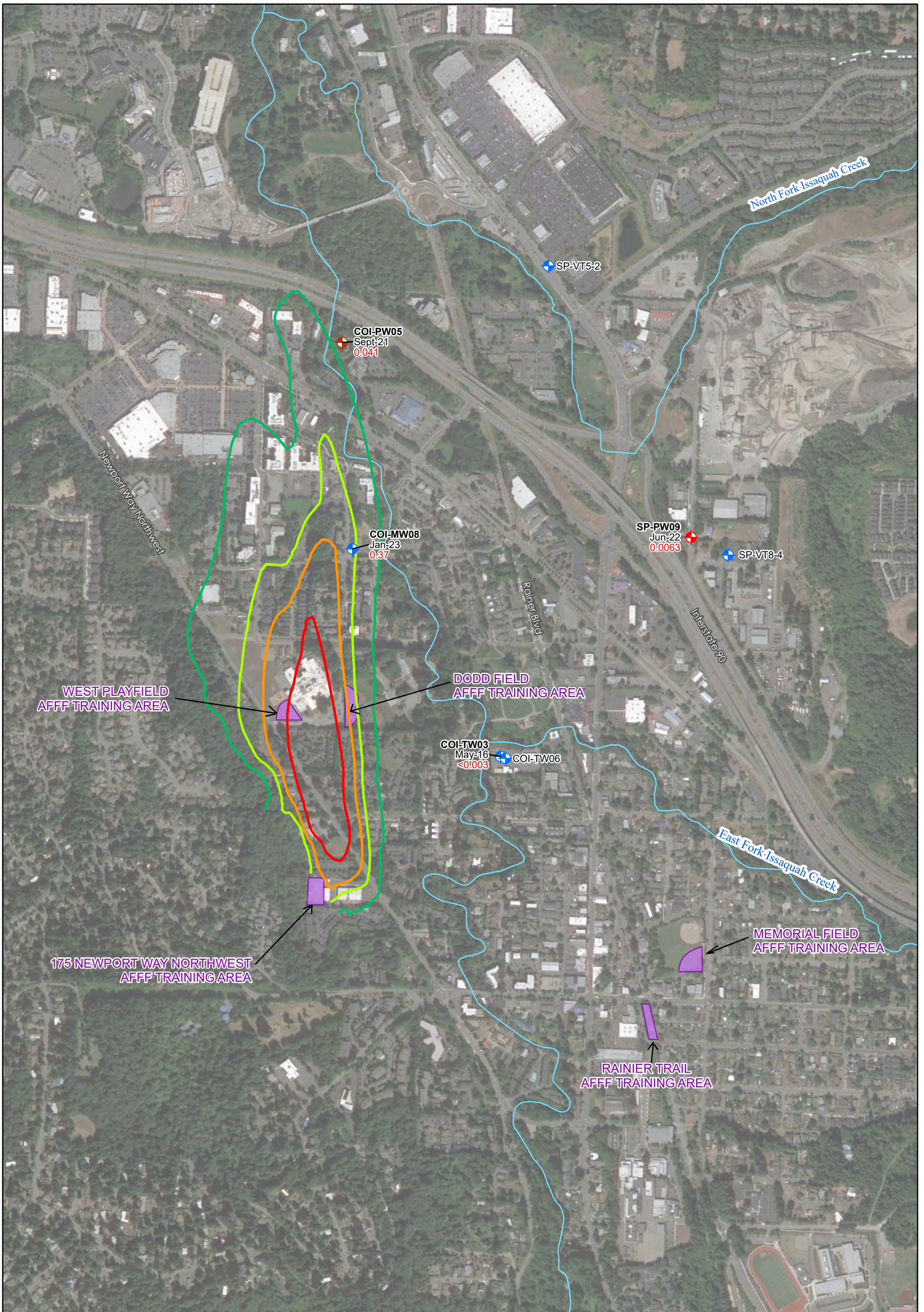
PNG0989

August 2023

**Figure**

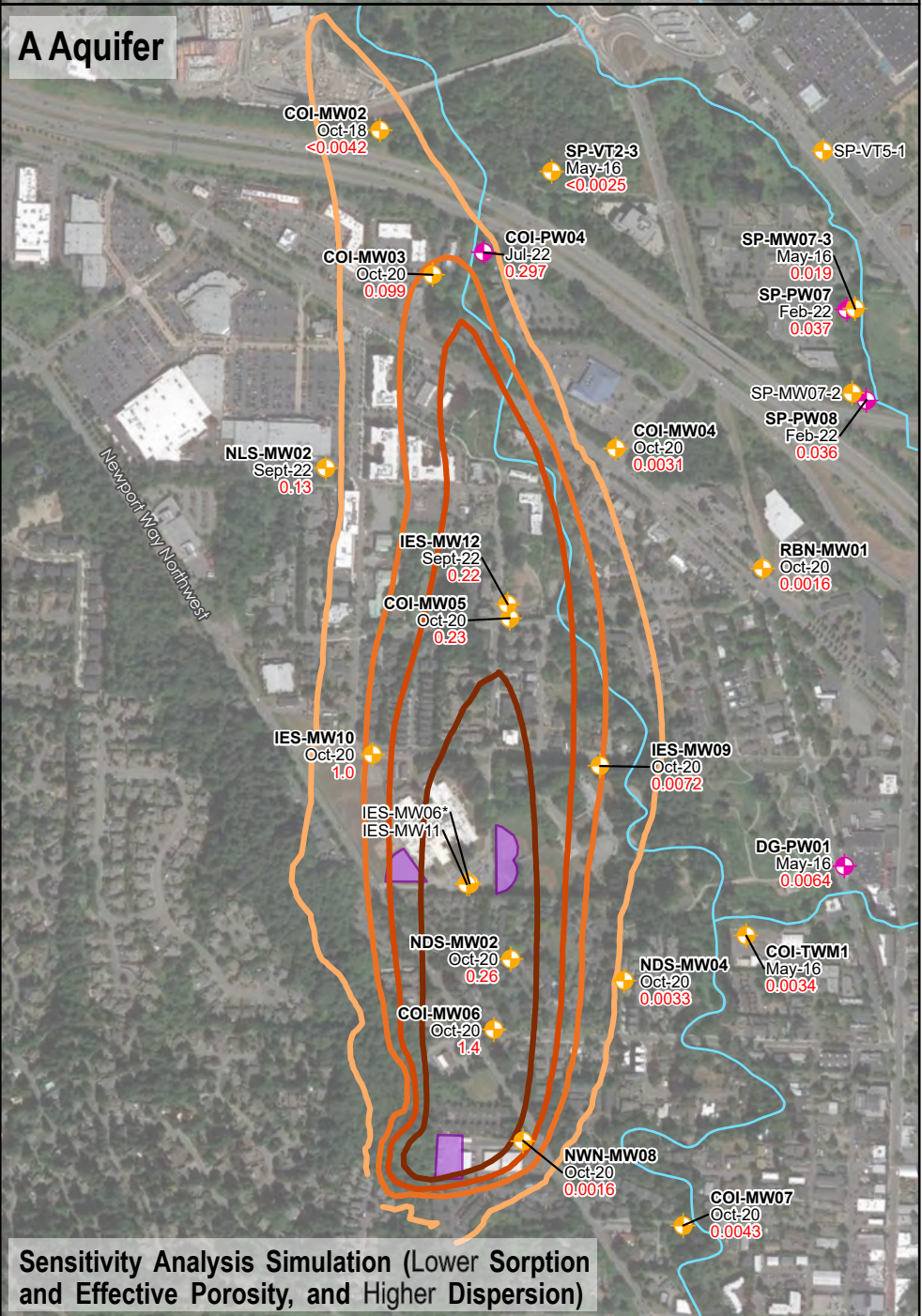
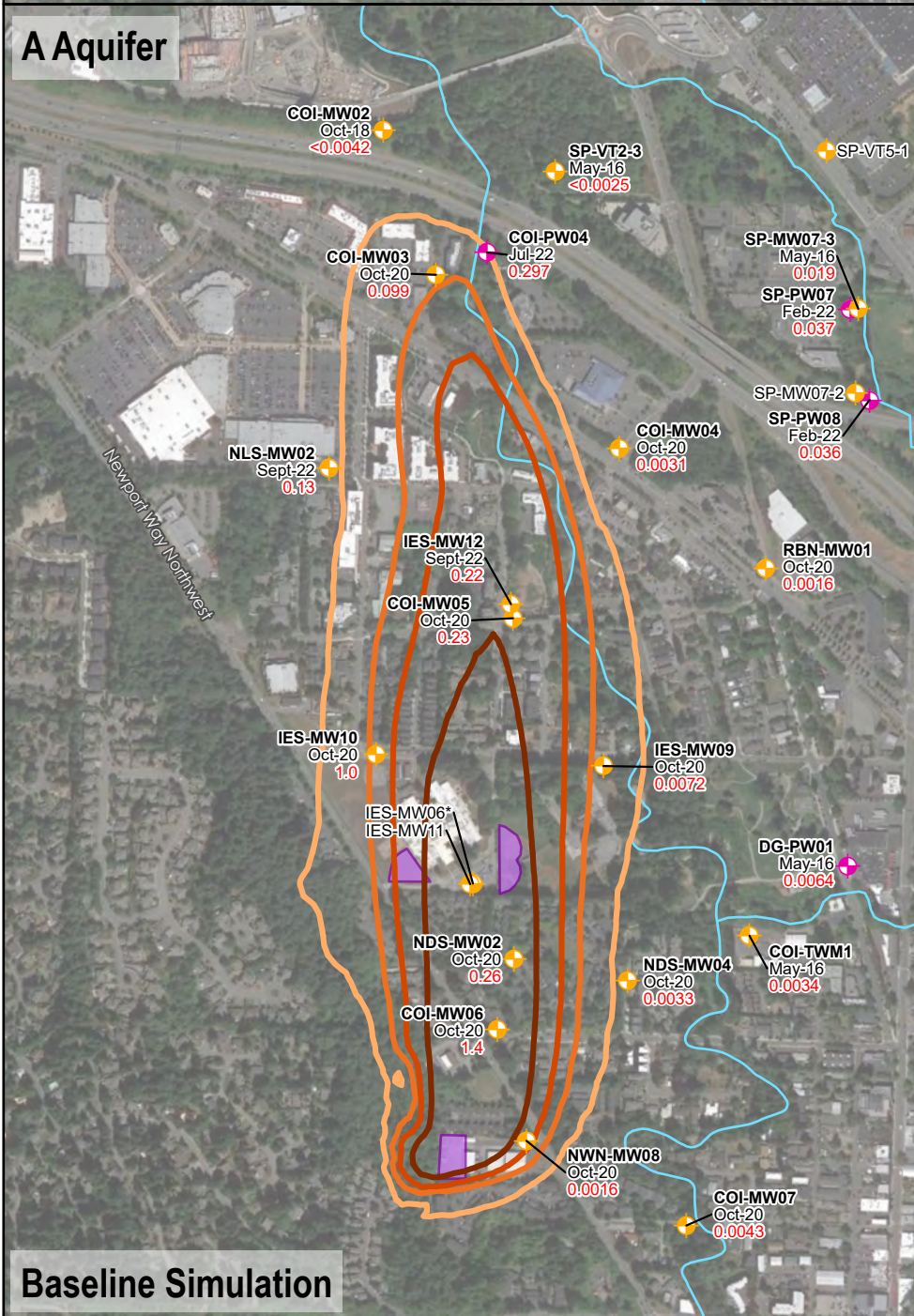
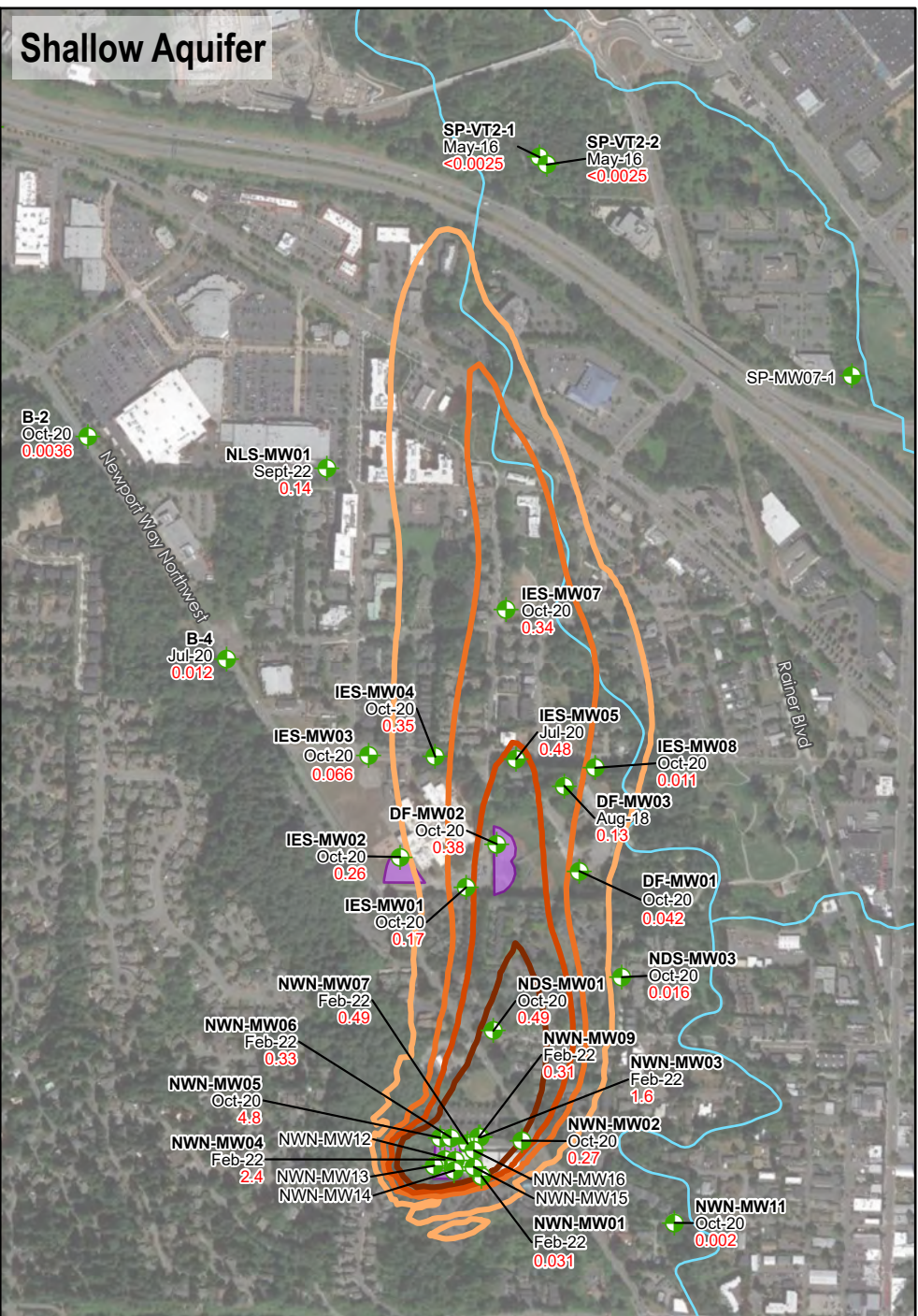
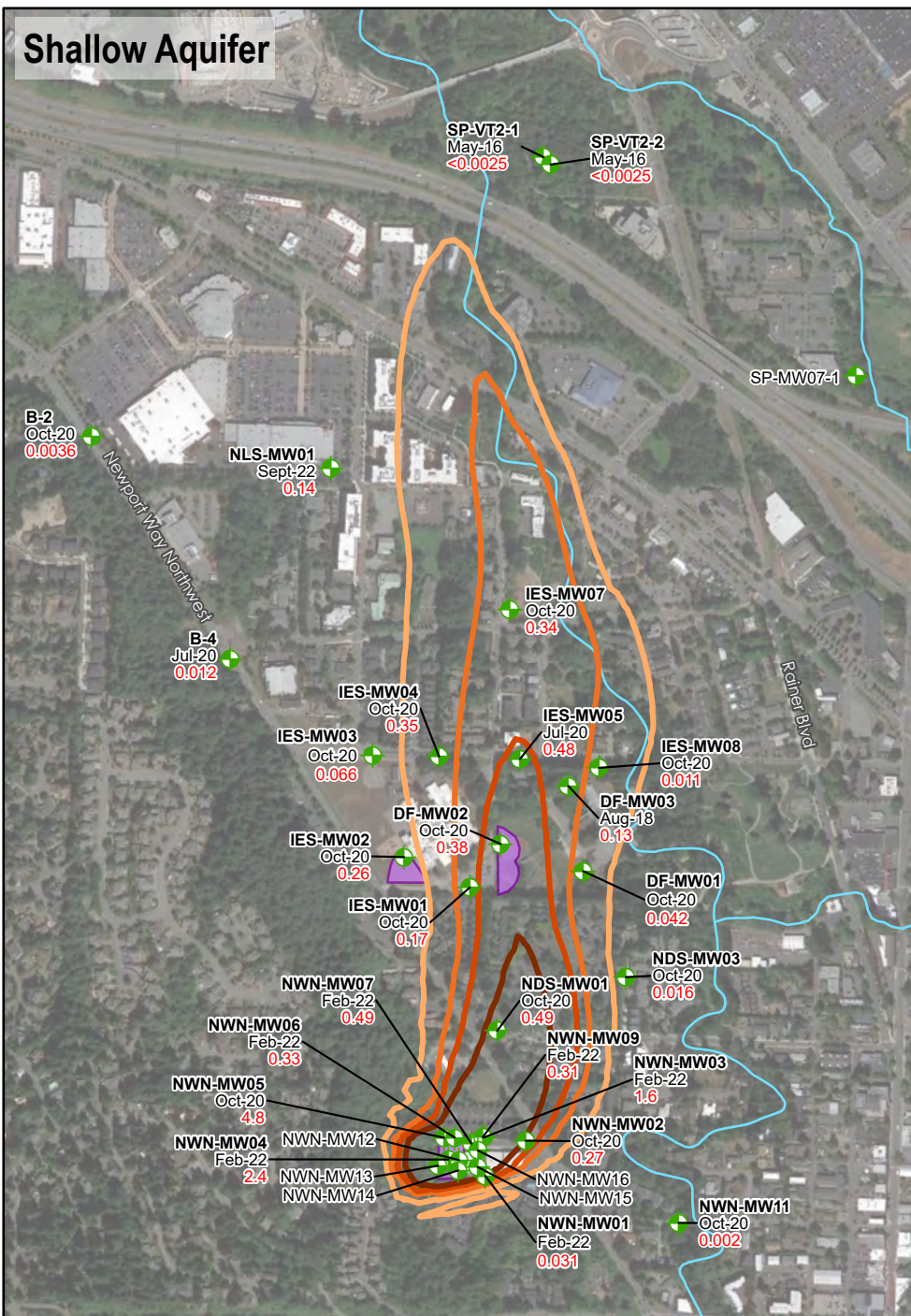
**6-2**





<b>Legend</b> B Zone Monitoring Well B Zone Production Well C Zone Production Well		<b>PFOS Concentration (Model Output)</b> 0.05 µg/L 0.25 µg/L 0.50 µg/L 1.0 µg/L		AFFF Training Area Issaquah Creek  <b>COI-TW03</b> – Location ID May-16 – Most Recent Sample Date (Month and Year) <0.003 – PFOS Concentration (µg/L)		<b>Notes:</b> µg/L = micrograms per liter - Aerial imagery source: Google Earth Pro, August 2020.		<b>Simulated PFOS Concentration B Zone Aquifer</b> Lower Issaquah Valley Issaquah, Washington	
				N 0 680 Feet		Geosyntec consultants		<b>Figure</b> <b>6-3</b>	
						PNG0989		August 2023	





**Legend**

- Shallow Zone Monitoring Well
- A Zone Monitoring Well
- Shallow Zone Production Well
- A Zone Production Well

**PFOS Concentration (Model Output)**

- 0.05 μg/L
- 0.25 μg/L
- 0.50 μg/L
- 1.0 μg/L

**MAFF Training Area**

- Issaquah Creek

**MF-MW03** – Location ID  
 Oct-18 – Most Recent Sample Date (Month and Year)  
 0.0039 – PFOS Concentration (μg/L)

**Notes:**  
 μg/L = micrograms per liter  
 - Aerial imagery source: Google Earth Pro, August 2020.

**Sensitivity Assessment for Fate and Transport Model (Sensitivity 1)**

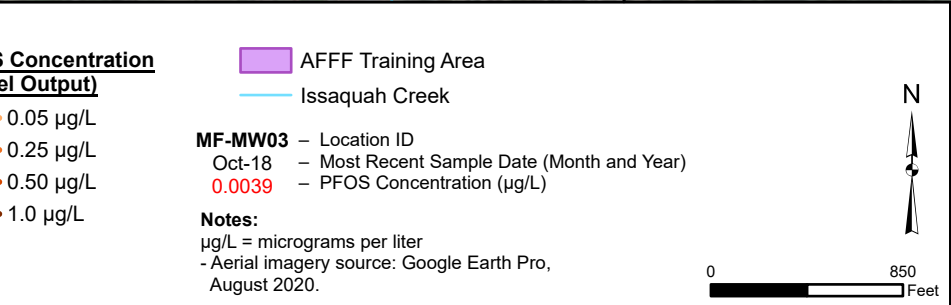
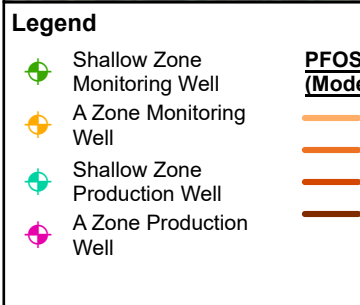
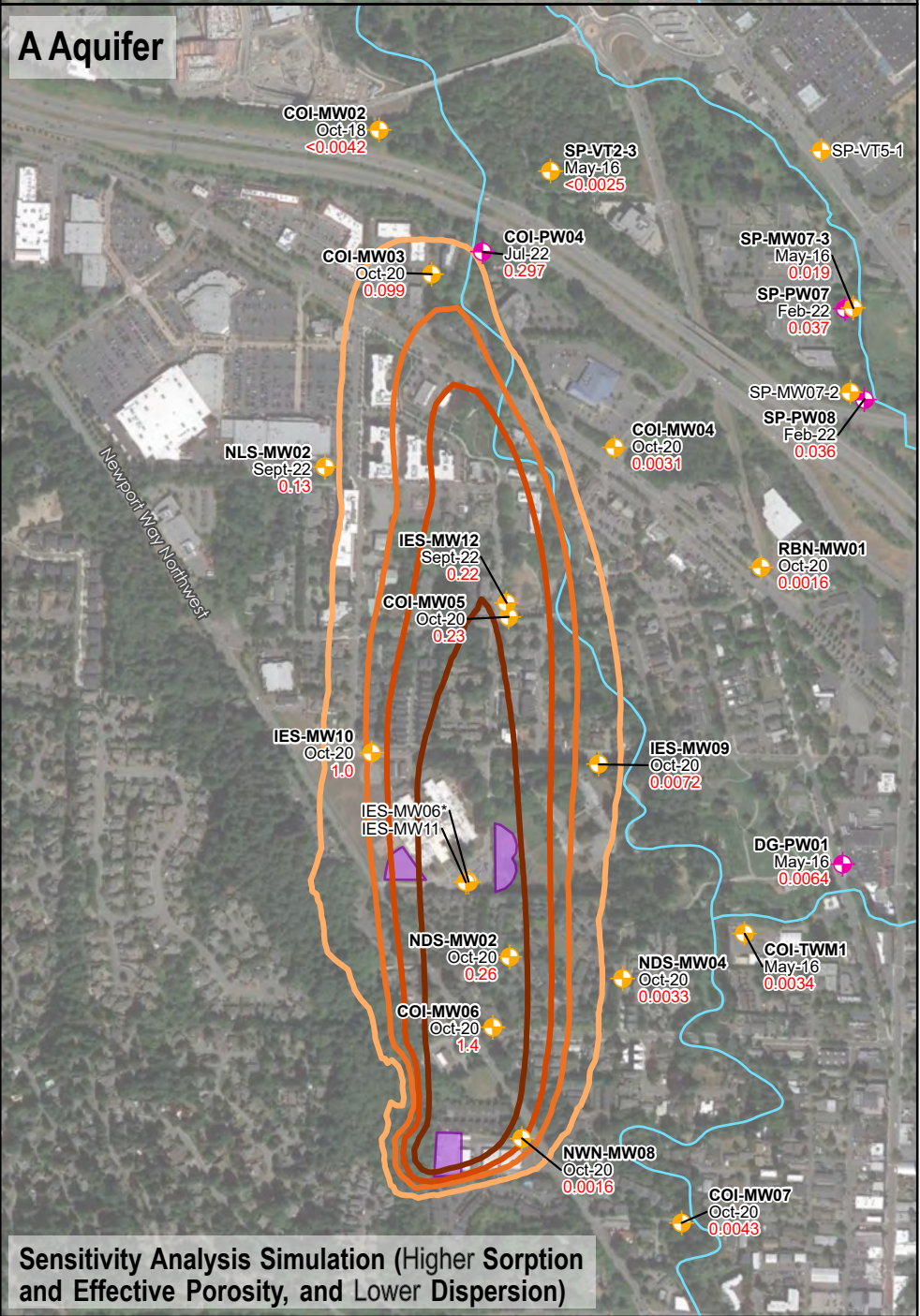
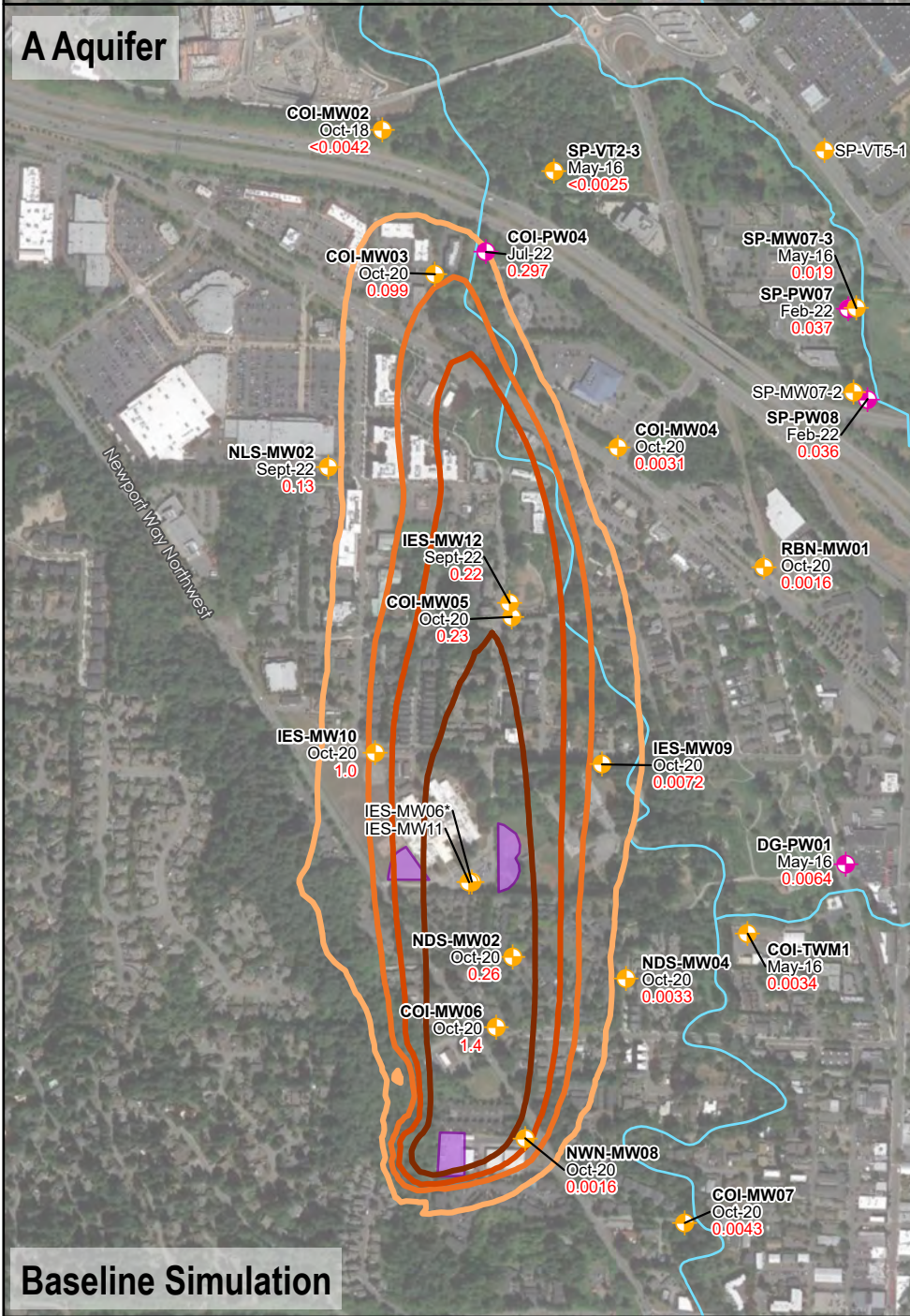
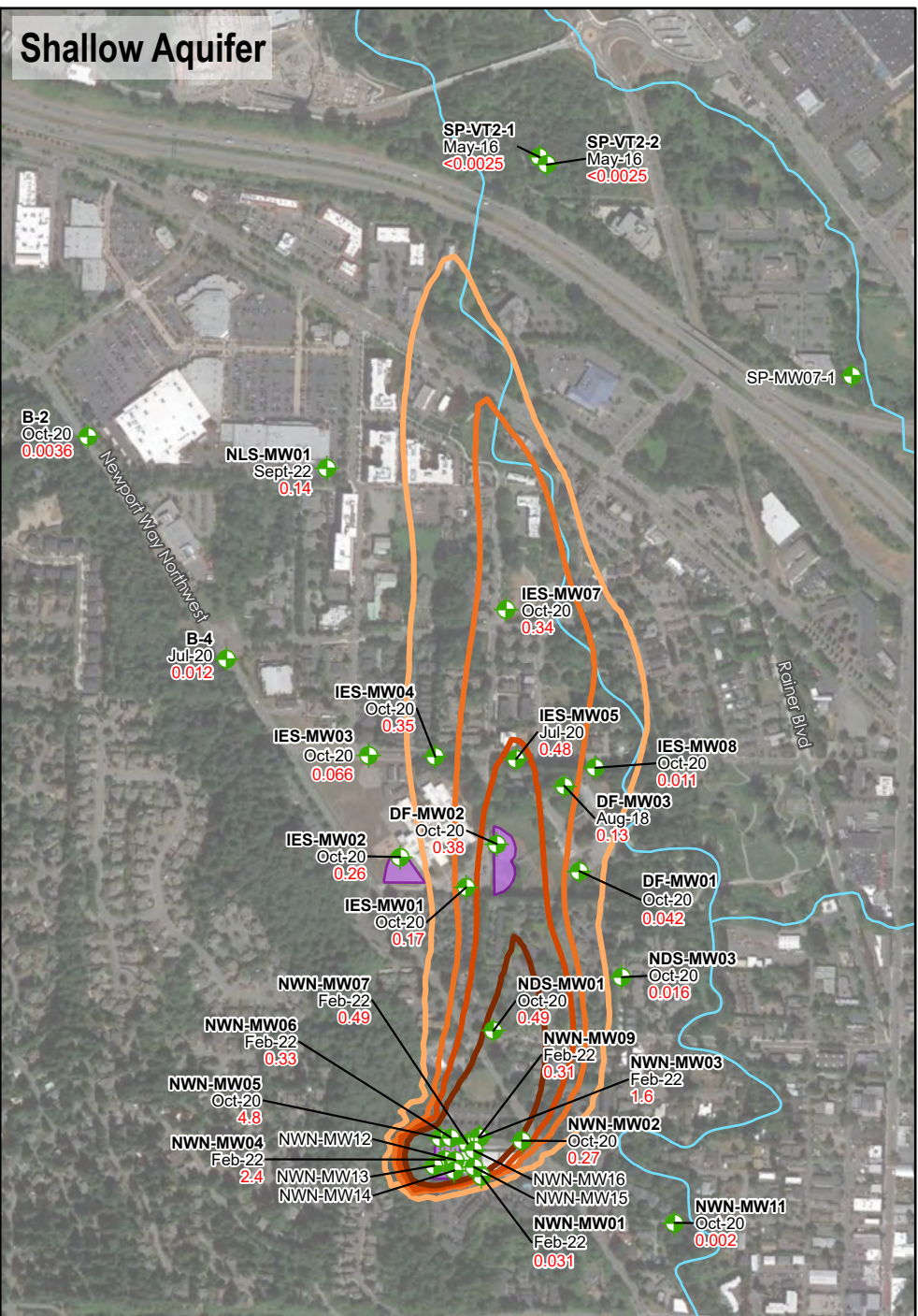
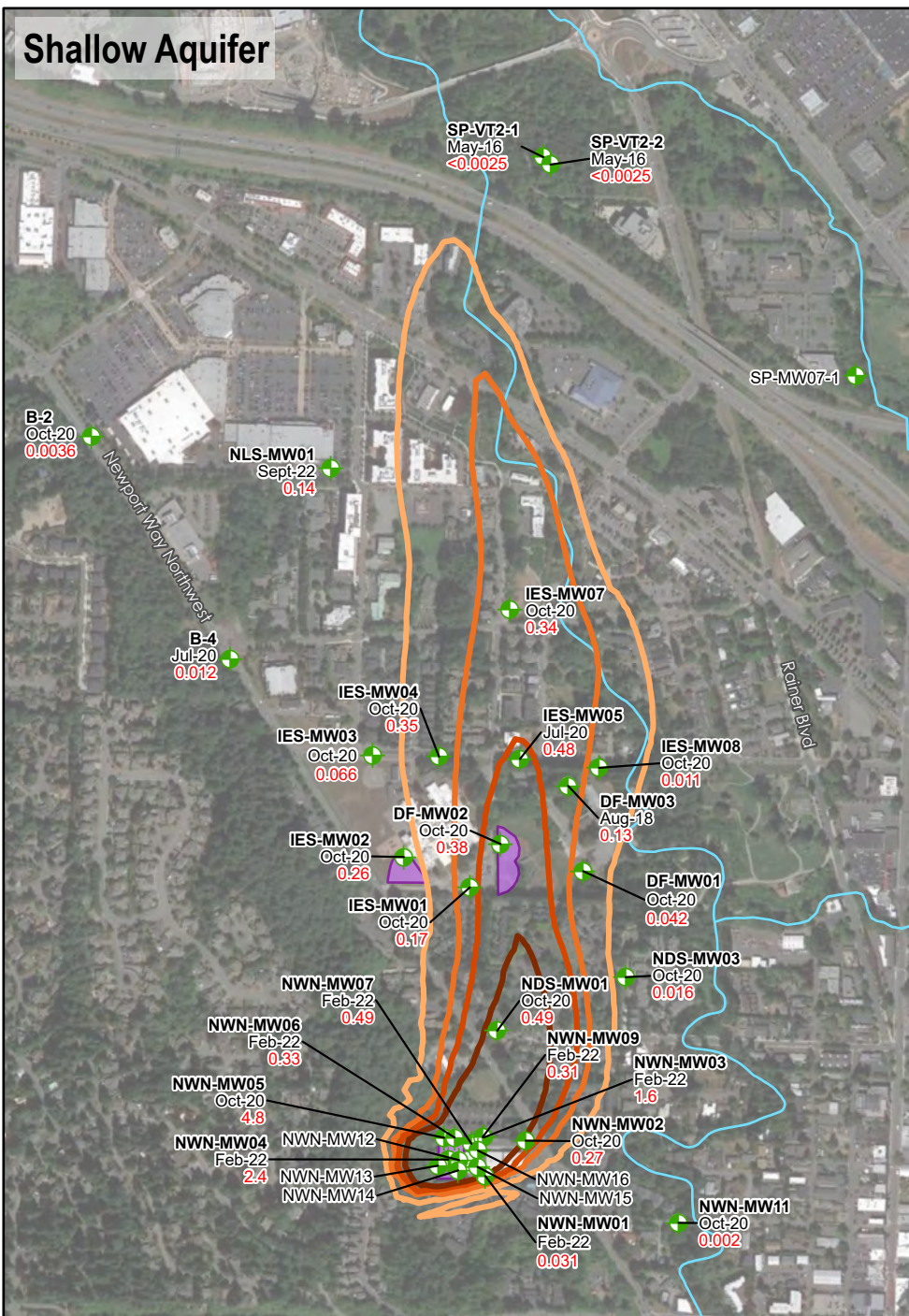
Lower Issaquah Valley  
Issaquah, Washington

**Geosyntec**  
consultants

**Figure 7-1a**

PNG0989 August 2023





### Sensitivity Assessment for Fate and Transport Model (Sensitivity 2)

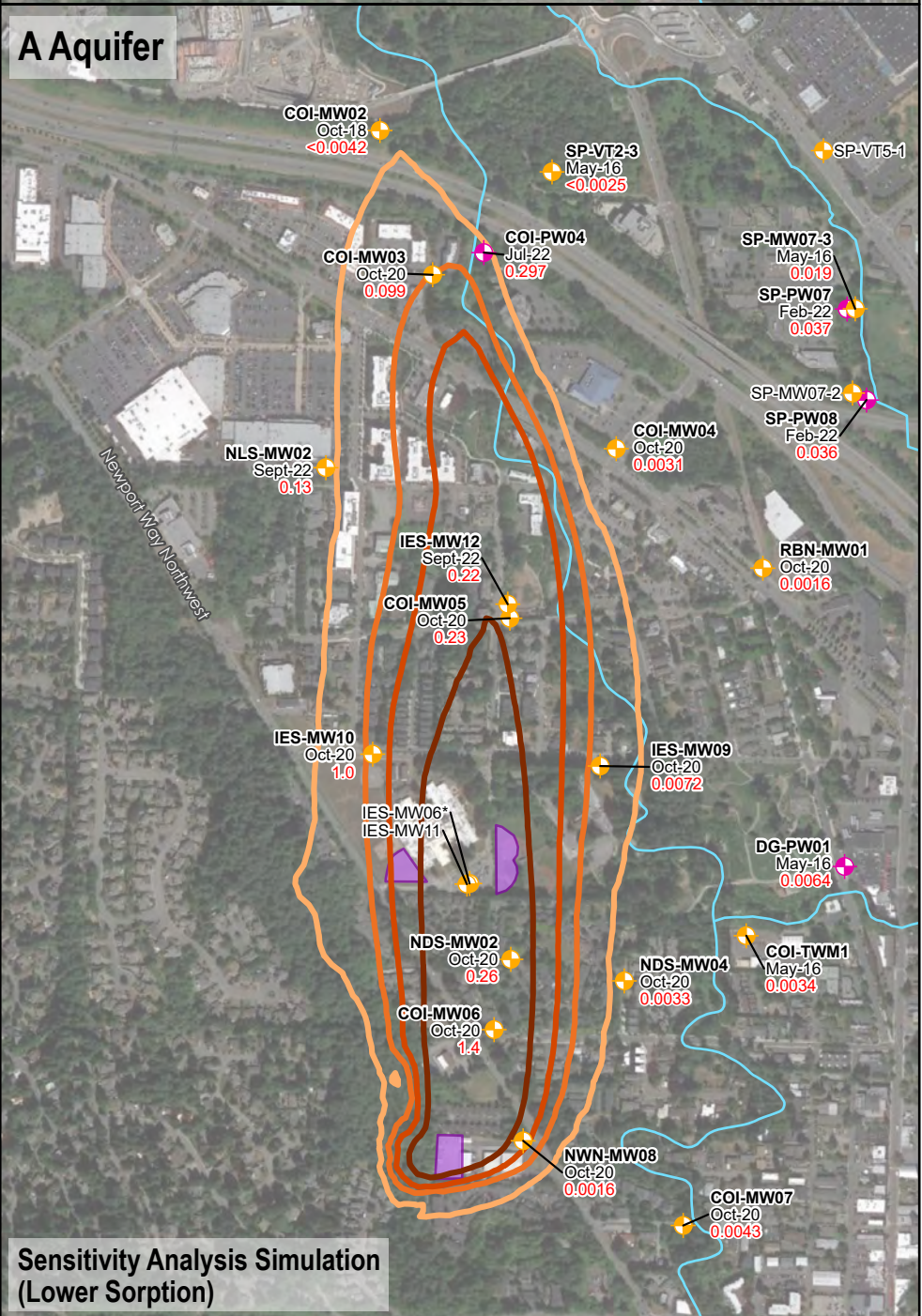
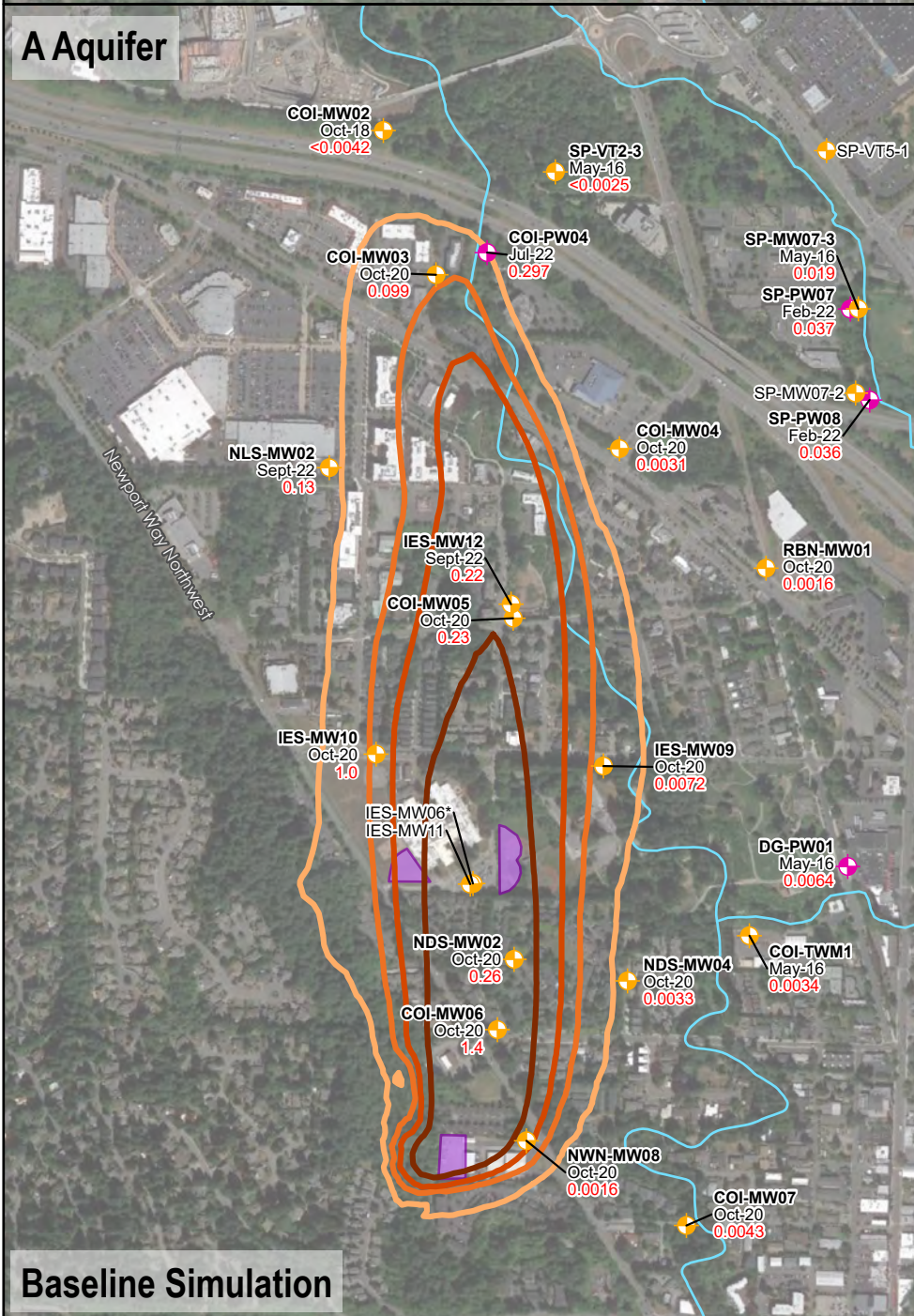
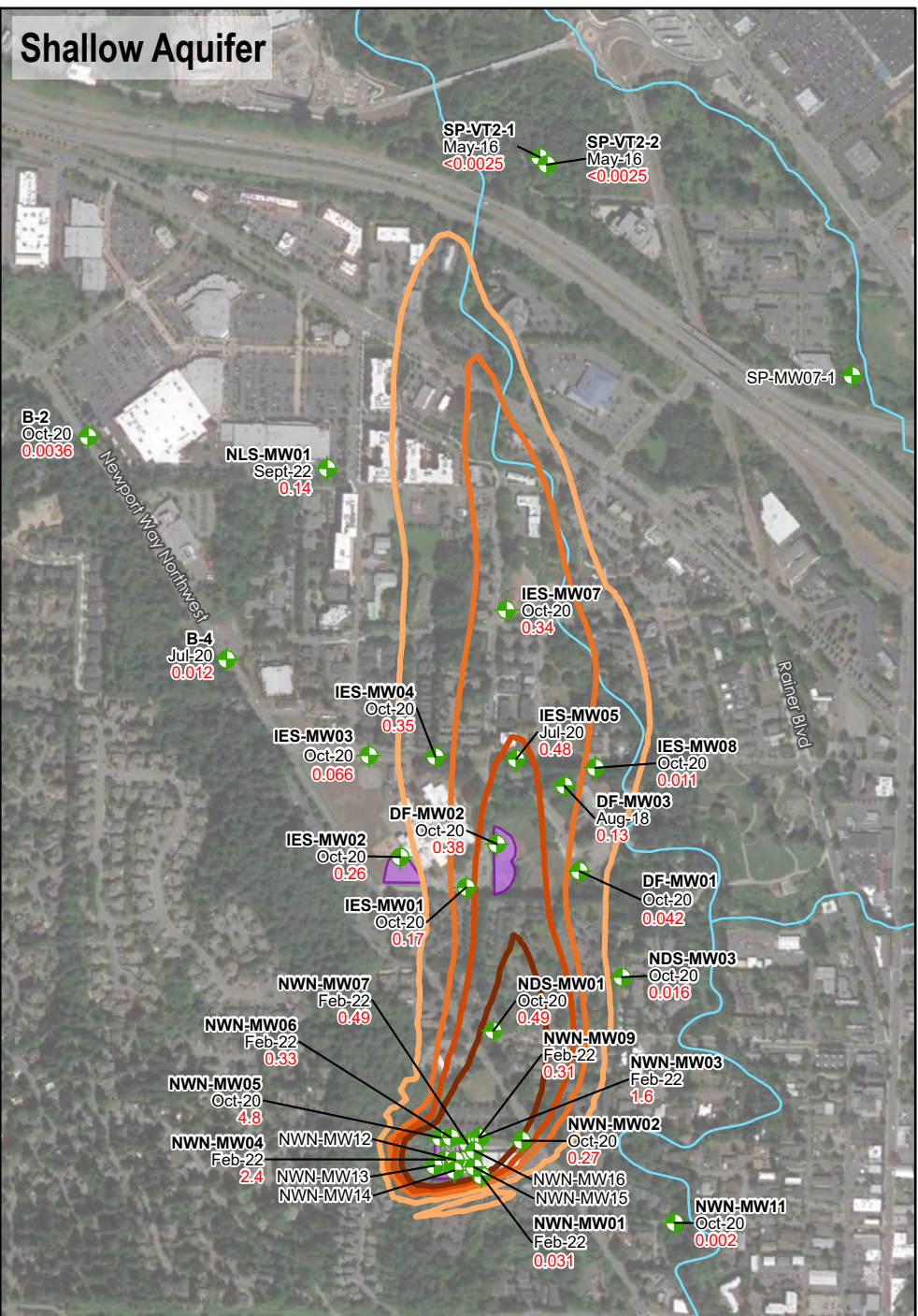
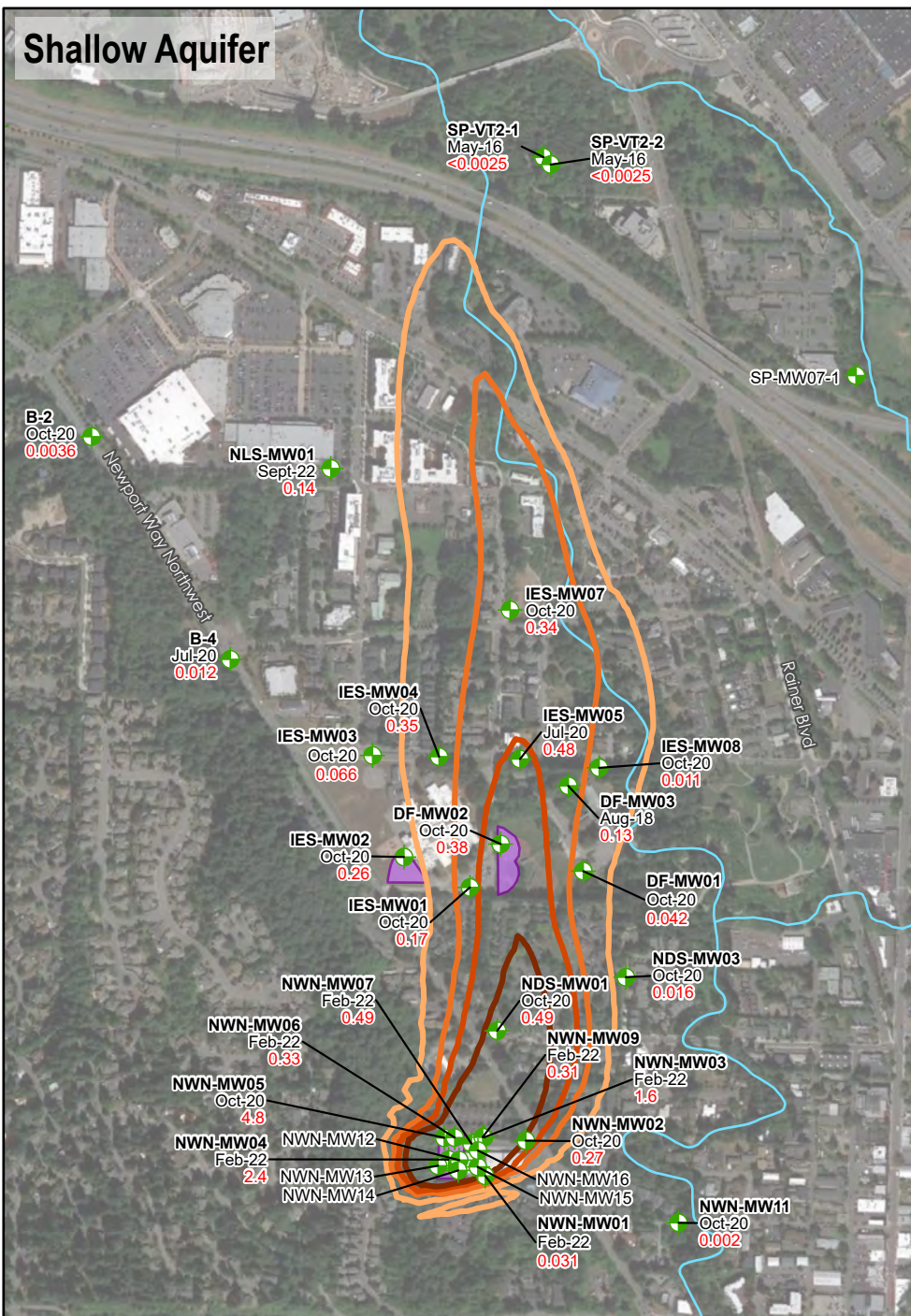
Lower Issaquah Valley  
Issaquah, Washington

**Geosyntec**  
consultants

**Figure 7-1b**

PNG0989 August 2023





**Legend**

- Shallow Zone Monitoring Well
- A Zone Monitoring Well
- Shallow Zone Production Well
- A Zone Production Well

**PFOS Concentration (Model Output)**

- 0.05 µg/L
- 0.25 µg/L
- 0.50 µg/L
- 1.0 µg/L

**MF-MW03** – Location ID  
 Oct-18 – Most Recent Sample Date (Month and Year)  
 0.0039 – PFOS Concentration (µg/L)

**Notes:**  
 µg/L = micrograms per liter  
 - Aerial imagery source: Google Earth Pro, August 2020.

AFFF Training Area  
 Issaquah Creek

**Sensitivity Assessment for Fate and Transport Model (Sensitivity 3)**

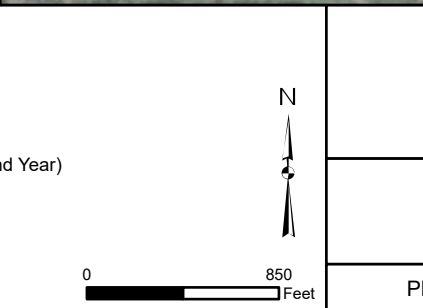
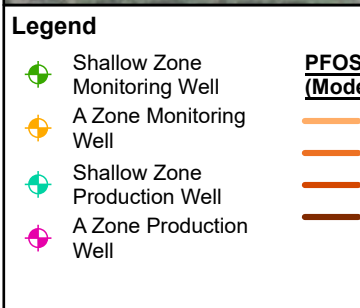
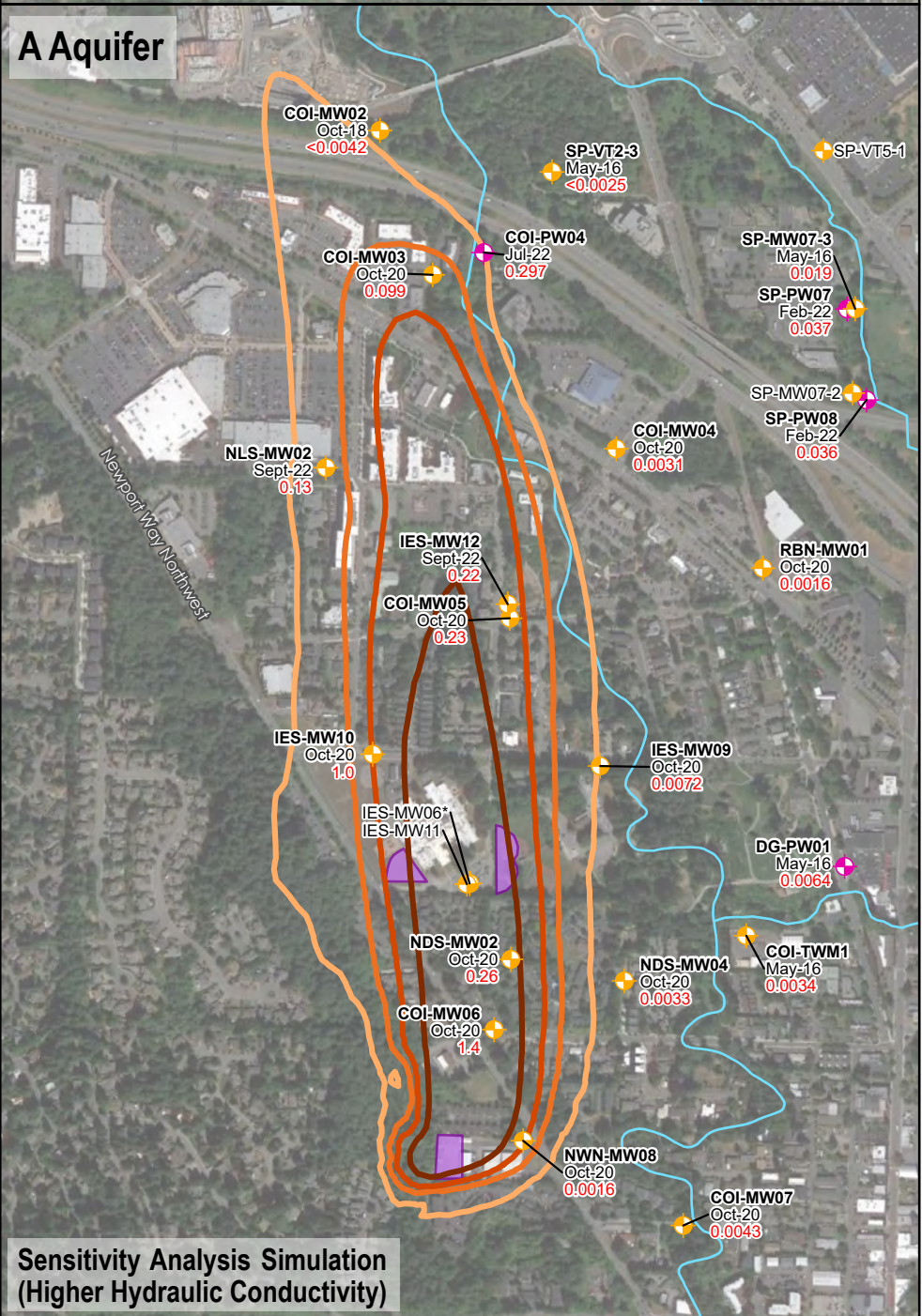
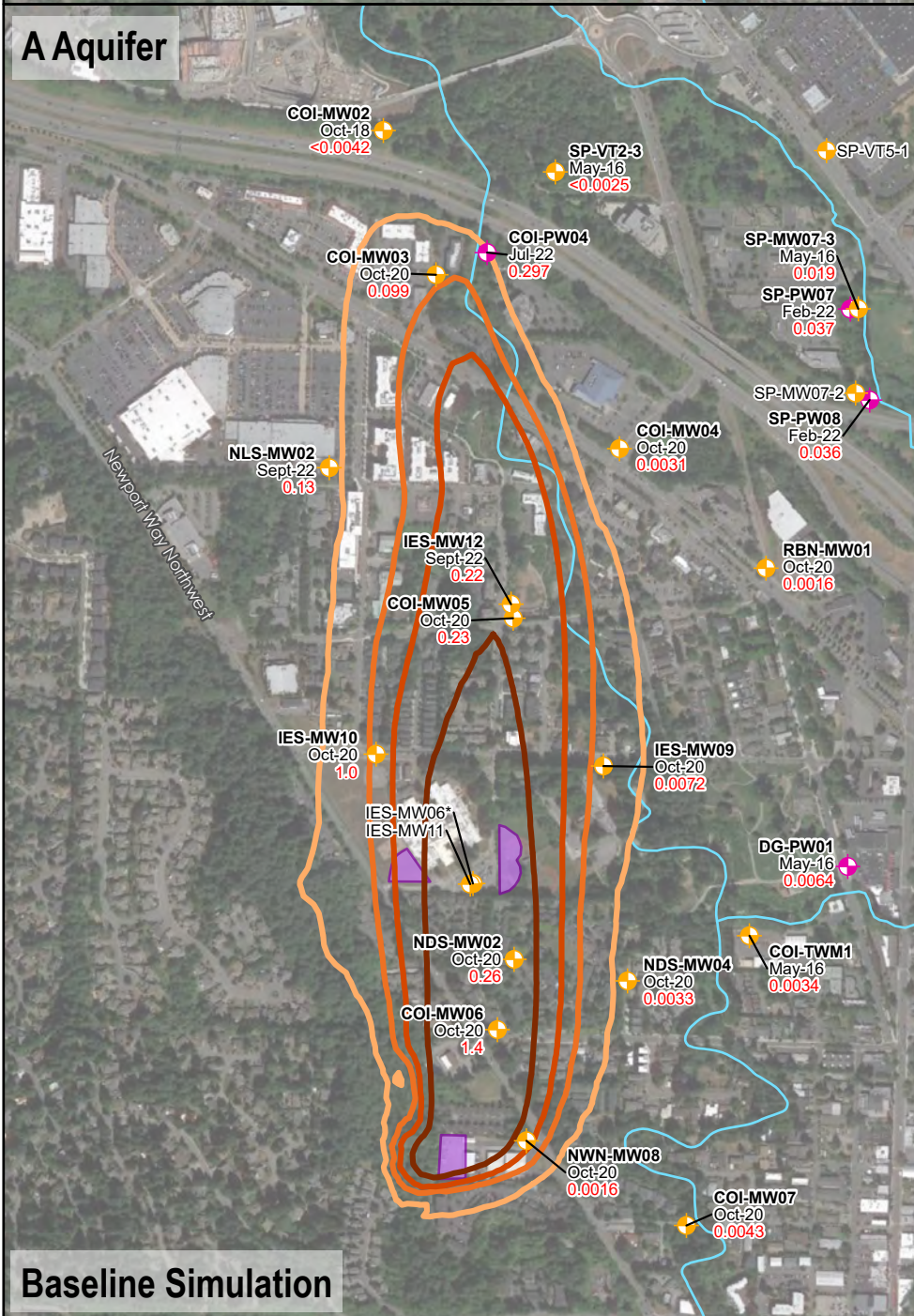
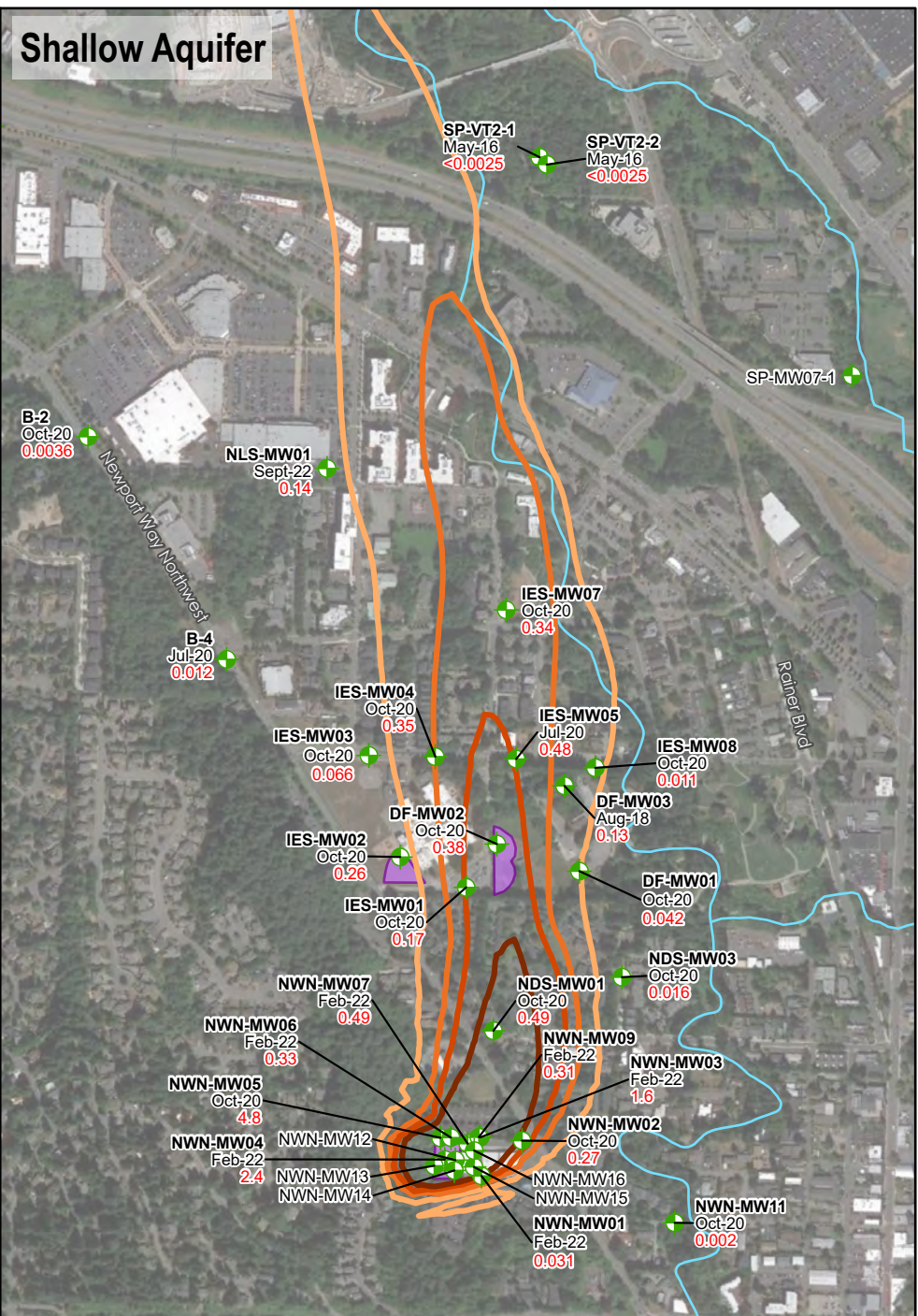
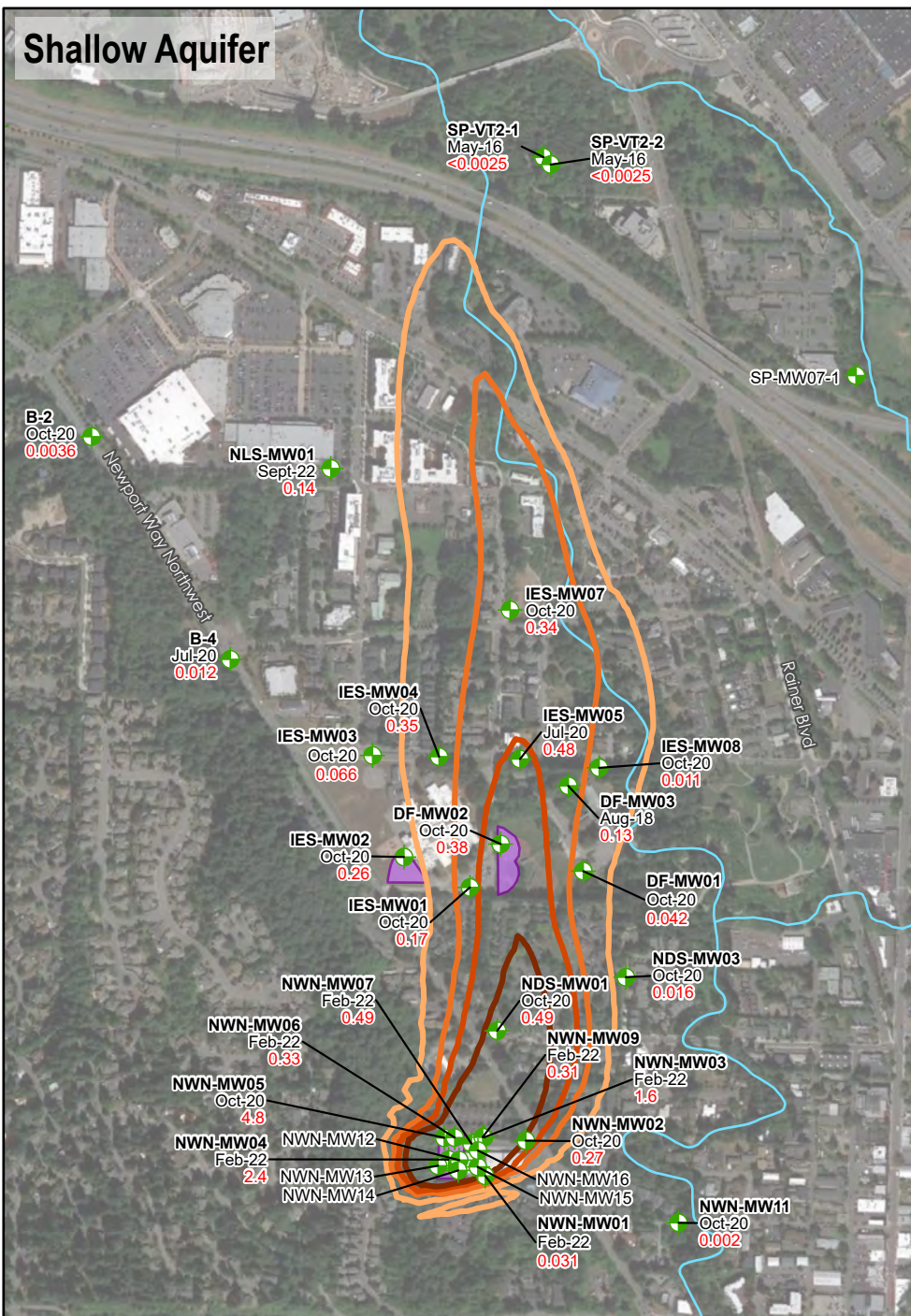
Lower Issaquah Valley  
Issaquah, Washington

**Geosyntec**  
consultants

**Figure 7-1c**

PNG0989 August 2023





<b>Legend</b> Shallow Zone Monitoring Well A Zone Monitoring Well Shallow Zone Production Well A Zone Production Well AFFF Training Area Issaquah Creek <b>PFOS Concentration (Model Output)</b> 0.05 μg/L 0.25 μg/L 0.50 μg/L 1.0 μg/L <b>MF-MW03</b> – Location ID Oct-18 – Most Recent Sample Date (Month and Year) 0.0039 – PFOS Concentration (μg/L) <b>Notes:</b> μg/L = micrograms per liter - Aerial imagery source: Google Earth Pro, August 2020.	<b>Sensitivity Assessment for Fate and Transport Model (Sensitivity 4)</b> Lower Issaquah Valley Issaquah, Washington		<b>Figure</b> <b>7-1d</b>
	 consultants		
 0 850 Feet		PNG0989	August 2023



# **TABLES**



Table 2-1 Summary of Hydrostratigraphic Units in Boring Logs

Boring Location	Total Depth	Aquifer designation	Aquitard 1 Top (ft bgs)	Aquitard 1 Bottom (ft bgs)	Aquitard 2 Top (ft bgs)	Aquitard 2 Bottom (ft bgs)	Deep (A/B) Aquitard Top (ft bgs)	Deep (A/B) Aquitard Bottom (ft bgs)	Used in Layering
COI-MW01	80	Shallow Zone Aquifer	17	30	39	68	-	-	Yes
COI-MW02	100	A Zone Aquifer	9	53	55	69	-	-	Yes
COI-MW03	100	A Zone Aquifer	24	36	48	65	-	-	Yes
COI-MW04	90	A Zone Aquifer	22	34	45	47	-	-	Yes
COI-MW05	90.5	A Zone Aquifer	32	35	43	55	-	-	Yes
COI-MW06	100	A Zone Aquifer	11	18	65	80	-	-	Yes
COI-MW07	110	A Zone Aquifer	-	-	58	70	-	-	Yes
COI-MW08	300	B Zone Aquifer	26	28	54	65	134	167	Yes
COI-PW01	107	Shallow Zone Aquifer	7	28	72	79	-	-	Yes
COI-PW02	200	Shallow Zone Aquifer	-	-	97	109	141	153	Yes
COI-PW04	200	A Zone Aquifer	0	35	-	-	135	200	Yes
COI-PW05	412	B Zone Aquifer	0	35	-	-	135	200	Yes
COI-TW03	292	B/C Zone Aquifer	-	-	85	109	120	180	Yes
COI-TW06	380	B/C Zone Aquifer	-	-	87	240	-	-	Yes
DG-PW01	113	A Zone Aquifer	-	-	68	80	-	-	Yes
IES-MW01	30	Shallow Zone Aquifer	13	16	-	-	-	-	Yes
IES-MW02	25	Shallow Zone Aquifer	7	11	-	-	-	-	Yes
IES-MW03	25	Shallow Zone Aquifer	5	18	-	-	-	-	Yes
IES-MW04	30	Shallow Zone Aquifer	8	22	-	-	-	-	Yes
IES-MW05	30	Shallow Zone Aquifer	11	19	-	-	-	-	Yes
IES-MW06	90	A Zone Aquifer	32	32	70	79	-	-	Yes
IES-MW07	35	Shallow Zone Aquifer	-	-	-	-	-	-	-
IES-MW08	35	Shallow Zone Aquifer	8	10	-	-	-	-	Yes
IES-MW09	85	A Zone Aquifer	-	-	75	76	-	-	No for top of Aquitard 2
IES-MW10	85	A Zone Aquifer	31	31	55	56	-	-	No for bottom of Aquitard 2
IES-MW12	130	A Zone Aquifer	25	30	60	69	-	-	Yes
Lakeside	94	A Zone Aquifer	3	18	18	30	-	-	No for top of Aquitard 2
MF-MW01	45	Shallow Zone Aquifer	-	-	-	-	-	-	Yes
MF-MW02	40	Shallow Zone Aquifer	-	-	-	-	-	-	Yes
MF-MW03	50	Shallow Zone Aquifer	-	-	-	-	-	-	Yes
MF-MW04	75	A Zone Aquifer	-	-	-	-	-	-	Yes
NDS-MW01	35	Shallow Zone Aquifer	6	9	-	-	-	-	Yes
NDS-MW02	90	A Zone Aquifer	10	11	-	-	-	-	Yes
NDS-MW04	90	A Zone Aquifer	10	16	67	72	-	-	Yes
NWN-MW01	40	Shallow Zone Aquifer	-	-	-	-	-	-	Yes
NWN-MW02	30	Shallow Zone Aquifer	-	-	-	-	-	-	Yes
NWN-MW03	30	Shallow Zone Aquifer	-	-	-	-	-	-	Yes
NWN-MW04	30	Shallow Zone Aquifer	23	30	-	-	-	-	Yes
NWN-MW05	25	Shallow Zone Aquifer	25	25	-	-	-	-	Yes
NWN-MW06	25	Shallow Zone Aquifer	10	11	-	-	-	-	Yes
NWN-MW07	27	Shallow Zone Aquifer	-	-	-	-	-	-	Yes
NWN-MW08	94	A Zone Aquifer	-	-	50	68	-	-	Yes
NWN-MW09	94	Shallow Zone Aquifer	-	-	53	95	-	-	Yes
NWN-R02		Shallow Zone Aquifer	22	39	-	-	-	-	Yes
RBN-MW01	80	A Zone Aquifer	-	-	-	-	-	-	Yes
RBN-MW02	80	A Zone Aquifer	-	-	-	-	-	-	Yes
RT-MW04	40	Shallow Zone Aquifer	37	40	-	-	-	-	Yes
SP-MW07-1/2	295	A Zone Aquifer	0	33	58	109	227	295	No for bottom of Aquitard 2 and for bottom of A/B Aquitard
SP-MW07-3	205	A Zone Aquifer	-	-	59	70	160	205	No for Aquitard 1
SP-PW07	151	A Zone Aquifer	20	24	-	-	148	151	No for bottom of A/B Aquitard; Yes for Bottom of Aquitard 1
SP-PW08	190	A Zone Aquifer	32	34	79	96	-	-	No for bottom of Aquitard 1 and 2
SP-PW09	303	B/C Zone Aquifer	-	-	60	68	160	185	Yes
SP-VT1	187	Shallow Zone Aquifer	0	8	93	119	163	187	Yes
SP-VT2-3	174	A Zone Aquifer	28	33	39	71	120	174	Yes
SP-VT3	169	A Zone Aquifer	-	-	62	66	152	169	Yes
SP-VT5-2	260	B/C Zone Aquifer	0	18	81	89	218	260	No for bottom of Aquitard 2
SP-VT7	217	Shallow Zone Aquifer	-	-	-	-	135	217	Yes
SP-VT8	223	Shallow Zone Aquifer	8	17	55	60	-	-	Yes

Notes:

ft bgs = feet below ground surface



**Table 2-2 Production Well Summary**

<b>Well Name</b>	<b>X</b>	<b>Y</b>	<b>Aquifer</b>	<b>Top of Screen (feet bgs)</b>	<b>Bottom of Screen (feet bgs)</b>	<b>Steady-state Pumping Rate (gpm)</b>
COI-PW01	1344158	197898	Shallow Zone Aquifer	90	106	240
COI-PW02	1344184	197865	Shallow Zone Aquifer	82	97	430
COI-PW04	1341271	200772	A Zone Aquifer	77	102	190
COI-PW05	1341310	200669	B Zone Aquifer	323	405	210
Darigold	1342972	197877	A Zone Aquifer	81	96	400
Lakeside	1344222	200519	A Zone Aquifer	102	108	600
SP-PW07	1342984	200506	A Zone Aquifer	82.6	146.9	0
SP-PW08	1343076	200077	A Zone Aquifer	105	179	0
SP-PW09	1343953	199191	B/C Zone Aquifer	194	219	910

**Notes**

bgs = below ground surface

gpm = gallons per minute



**Table 2-3 - Summary of Calibrated Hydraulic Properties**

<b>MODFLOW Layers</b>	<b>Hydrostratigraphic Unit</b>	<b>Horizontal Hydraulic Conductivity (ft/day)</b>	<b>CARA Model</b>	<b>1993 Wellhead Protection Plan 1999 Groundwater Exploration and Pumping Tests 2000 Groundwater Modeling Pumping COI-6 Report*</b>
1	Shallow Aquifer (including Aquitard 1)	25	5	80 - 150 50 - 300
2		1.5	0.1	
3		80-300	50	
4	Shallow Aquitard (Aquitard 2)	5	1	
5	A Zone Aquifer	75-120	100	
6	Deep Aquitard	5	0.5	0.02 - 0.08 to 5 25
7	B Zone Aquifer and B/C Zone Aquifer	10 to 150 (B Aquifer) 320-450 (B/C Aquifer)	200-400	100 - 200 (B Aquifer) 40 - 300 (B Aquifer)
8	B Zone Aquifer and B/C Zone Aquifer	10 to 150 (B Aquifer) 320-450 (B/C Aquifer)	200-400	200 - 300 (channel)
9	Lower Deep Aquitard	0.1	0.1	Not available

ft/day = feet per day

\*multiple ranges are provided based on values reported in the different documents



Table 3-1 - Observation Locations and Average Groundwater Elevations

Well	X	Y	Screened Aquifer	Top of Screen (feet bgs)	Bottom of Screen (feet bgs)	Midpoint Elevation (feet NAVD88)	Average Groundwater Elevation (feet NAVD88)	Simulated Steady-State Groundwater Elevation (feet NAVD88)	Residual (feet)
B-12	1341680	196381	Shallow Zone Aquifer	20	30	69.0	74.3	73.3	1.0
B-2	1339406	199916	Shallow Zone Aquifer	20	30	56.0	70.5	69.9	0.6
B-4	1340063	198862	Shallow Zone Aquifer	20	30	49.4	66.5	67.1	-0.6
B-7	1340581	198050	Shallow Zone Aquifer	23	33	62.5	62.4	66.9	-4.4
COI-MW01	1338949	201384	Shallow Zone Aquifer	28	38	25.4	55.6	56.9	-1.4
DF-MW01	1341733	197859	Shallow Zone Aquifer	5	15	67.7	67.5	66.8	0.8
DF-MW02	1341342	197988	Shallow Zone Aquifer	15	25	54.2	66.7	66.5	0.2
DF-MW03	1341663	198264	Shallow Zone Aquifer	20	30	49.4	66.0	66.0	0.0
IES-MW01	1341197	197783	Shallow Zone Aquifer	16	26	55.3	68.1	66.9	1.3
IES-MW02	1340885	197926	Shallow Zone Aquifer	15	25	53.7	67.2	66.7	0.5
IES-MW03	1340736	198407	Shallow Zone Aquifer	15	25	52.7	66.1	66.1	0.0
IES-MW04	1341051	198402	Shallow Zone Aquifer	15	30	49.9	66.2	66.1	0.1
IES-MW05	1341434	198390	Shallow Zone Aquifer	20	30	47.8	66.0	65.9	0.1
IES-MW07	1341387	199096	Shallow Zone Aquifer	20	30	45.3	64.6	63.9	0.6
IES-MW08	1341809	198349	Shallow Zone Aquifer	20	30	47.1	65.6	65.8	-0.2
MF-MW01	1343913	195913	Shallow Zone Aquifer	16	26	81.6	68.2	71.0	-2.8
MF-MW02	1343727	196215	Shallow Zone Aquifer	25	45	64.5	68.5	70.5	-2.0
MF-MW03	1343967	196294	Shallow Zone Aquifer	35	50	61.7	68.2	70.4	-2.3
NDS-MW01	1341326	197104	Shallow Zone Aquifer	22	32	58.5	68.9	68.6	0.3
NDS-MW03	1341935	197357	Shallow Zone Aquifer	25	35	52.1	69.1	67.8	1.3
NGB-MW01	1341022	200694	Shallow Zone Aquifer	20	30	38.0	56.0	58.1	-2.1
NLS-MW01	1340501	199667	Shallow Zone Aquifer	19.5	29.5	42.1	63.6	64.0	-0.4
NWN-MW01	1341269	196417	Shallow Zone Aquifer	15	30	68.2	71.4	74.3	-2.9
NWN-MW02	1341462	196584	Shallow Zone Aquifer	15	30	67.3	69.7	71.1	-1.4
NWN-MW03	1341264	196600	Shallow Zone Aquifer	15	30	68.9	70.1	72.2	-2.1
NWN-MW04	1341096	196495	Shallow Zone Aquifer	13	23	72.4	79.2	79.3	0.0
NWN-MW05	1341075	196597	Shallow Zone Aquifer	7	17	78.3	77.1	78.6	-1.6
NWN-MW06	1341125	196598	Shallow Zone Aquifer	15	25	71.0	76.0	76.6	-0.6
NWN-MW07	1341204	196570	Shallow Zone Aquifer	16.5	26.5	69.4	71.2	74.0	-2.9
NWN-MW09	1341257	196600	Shallow Zone Aquifer	45	50	43.8	69.6	70.8	-1.2
NWN-MW10	1341148	196565	Shallow Zone Aquifer	10	25	73.2	74.7	76.2	-1.5
NWN-MW11	1342184	196195	Shallow Zone Aquifer	15	25	70.6	72.7	70.6	2.1
NWN-MW12	1341146	196492	Shallow Zone Aquifer	8	23	75.1	78.7	77.4	1.3
NWN-MW13	1341046	196465	Shallow Zone Aquifer	3	18	79.4	82.2	81.6	0.7
NWN-MW14	1341141	196443	Shallow Zone Aquifer	7	22	76.2	78.7	78.3	0.4
NWN-MW15	1341234	196460	Shallow Zone Aquifer	15	30	67.9	71.3	74.1	-2.9
NWN-MW16	1341235	196537	Shallow Zone Aquifer	15	30	68.1	71.0	73.4	-2.4
NWN-PZ01	1341235	196537	Shallow Zone Aquifer	20	30	65.8	70.2	73.0	-2.8
NWN-PZ02	1341243	196576	Shallow Zone Aquifer	20	30	65.4	71.3	72.2	-0.9
RT-MW01	1343590	195910	Shallow Zone Aquifer	25	45	63.7	67.8	70.9	-3.1
RT-MW03	1343676	195900	Shallow Zone Aquifer	25	45	64.1	67.7	70.9	-3.3
RT-MW04	1343630	195466	Shallow Zone Aquifer	28	38	67.8	71.3	71.6	-0.2
SP-VT1-1	1343702	199872	Shallow Zone Aquifer	28	38	40.2	65.9	64.3	1.6
SP-VT2-1	1341545	201239	Shallow Zone Aquifer	19	24	37.9	57.6	59.4	-1.8
SP-VT2-2	1341579	201204	Shallow Zone Aquifer	34	39	25.4	59.9	59.3	0.6
SP-VT7-1	1344491	198956	Shallow Zone Aquifer	23	33	54.8	64.6	65.4	-0.8
SP-VT7-2	1344491	198956	Shallow Zone Aquifer	43	53	34.8	64.5	65.4	-0.9
SP-VT8-1	1344235	199055	Shallow Zone Aquifer	45	55	29.7	65.0	65.1	-0.1
COI-MW02	1340781	201348	A Zone Aquifer	70	90	-17.2	60.0	57.6	2.4
COI-MW03	1341030	200668	A Zone Aquifer	78	98	-25.1	58.5	58.4	0.1
COI-MW04	1341895	199847	A Zone Aquifer	70	90	-6.9	63.5	63.2	0.4
COI-MW05	1341394	199048	A Zone Aquifer	70	90	-8.1	65.1	64.6	0.5
COI-MW06	1341319	197107	A Zone Aquifer	80	100	-3.7	69.1	68.3	0.8
COI-MW07	1342211	196184	A Zone Aquifer	100	110	-14.7	72.5	70.4	2.1
COI-TMW1	1342570	197378	A Zone Aquifer	84	94	-7.1	NA	NA	NA
IES-MW06	1341204	197797	A Zone Aquifer	80	90	-9.1	67.1	66.9	0.3
IES-MW09	1341819	198351	A Zone Aquifer	75	85	-7.8	66.4	65.8	0.6
IES-MW10	1340747	198407	A Zone Aquifer	75	85	-7.3	65.6	66.0	-0.4
IES-MW11	1341191	197794	A Zone Aquifer	120	130	-49.3	66.2	66.9	-0.7
IES-MW12	1341460	199134	A Zone Aquifer	120	130	-58.2	61.7	64.4	-2.7
MF-MW04	1343721	196214	A Zone Aquifer	65	75	29.9	67.8	70.5	-2.6
NDS-MW02	1341398	197439	A Zone Aquifer	71	81	5.8	68.8	67.5	1.3
NDS-MW04	1341933	197337	A Zone Aquifer	72	82	4.7	68.8	67.8	1.0
NLS-MW02	1340495	199668	A Zone Aquifer	70	80	-8.1	63.4	63.8	-0.4
NWN-MW08	1341456	196583	A Zone Aquifer	70	80	15.0	68.8	69.6	-0.8
RBN-MW01	1342586	199284	A Zone Aquifer	70	80	-0.8	65.6	64.5	1.1
RBN-MW02	1343631	197109	A Zone Aquifer	70	80	24.0	66.9	69.0	-2.1
SP-MW07-1	1343024	200205	A Zone Aquifer	35	58	25.8	NA	NA	NA
SP-MW07-2	1343024	200205	A Zone Aquifer	135	220	-105.2	NA	NA	NA
SP-MW07-3	1343022	200507	A Zone Aquifer	85	150	-47.4	NA	NA	NA
SP-VT1-2	1343702	199872	A Zone Aquifer	70	80	-1.8	65.5	64.1	1.3
SP-VT1-3	1343702	199872	A Zone Aquifer	150	160	-81.8	63.1	64.1	-1.0
SP-VT2-3	1341592	201153	A Zone Aquifer	74	79	-14.4	57.9	59.4	-1.5
SP-VT5-1	1342872	201253	A Zone Aquifer	75	85	-13.9	61.4	62.4	-1.0
SP-VT7-3	1344491	198956	A Zone Aquifer	51	71	21.8	64.4	65.4	-0.9
SP-VT7-4	1344491	198956	A Zone Aquifer	108	118	-30.2	64.3	65.4	-1.0
SP-VT8-2	1344235	199055	A Zone Aquifer	83	93	-8.3	64.2	65.0	-0.7
SP-VT8-3	1344235	199055	A Zone Aquifer	158	168	-83.3	64.1	64.5	-0.5
COI-MW08	1341386	199103	B/C Zone Aquifer	238	248	-173.2	65.5	64.5	1.0
COI-TW03	1342444	197417	B/C Zone Aquifer	284	289	-204.7	67.2	67.5	-0.4
COI-TW06	1342579	197291	B/C Zone Aquifer	258	362	-228.0	NA	NA	NA
SP-VT5-2	1342874	201247	B/C Zone Aquifer	180	190	-118.9	62.0	61.8	0.2
SP-VT8-4	1344235	199055	B/C Zone Aquifer	192	214	-123.3	64.1	64.5	-0.4
<b>Mean Residual</b>									<b>-0.5</b>

**Notes**

bgs = below ground surface  
 NA = Not available



**Table 4-1 Simulated Steady-State Water Balance**

Units	cfs	AFY	cf
<b>INFLOW</b>			
Southern Inflow	1.6	1,156	138,000
Western Margin Inflow	2.2	1,626	194,000
Eastern Margin Inflow	1.3	972	116,000
Areal Recharge	7.0	5,086	607,000
River			
North Fork Issaquah Creek	0.8	595	71,000
East Fork Issaquah Creek	0.2	159	19,000
Issaquah Creek	0.5	360	43,000
Tibbetts Creek	1.5	1,098	131,000
<b>Total Inflow</b>	<b>15.3</b>	<b>11,052</b>	<b>1,319,000</b>
<b>OUTFLOW</b>			
Discharge to Lake Sammamish	5.5	4,005	478,000
Production Wells	6.6	4,751	567,000
River			
North Fork Issaquah Creek	0.5	360	43,000
East Fork Issaquah Creek	0.0	0	0
Issaquah Creek	2.7	1,936	231,000
Tibbetts Creek	0.0	0	0
<b>Total Outflow</b>	<b>15.3</b>	<b>11,052</b>	<b>1,319,000</b>

Notes:

AFY = acre-ft-year

cf = cubic feet per day

cfs = cubic feet per second



**Table 5-1  
Fate and Transport Modeling Parameters**

Description	Calibrated Value
<b>Aquifer Parameters</b>	
Effective Porosity	0.15
Horizontal Dispersivity (feet)	20
Transverse Horizontal Dispersivity (feet)	2
Transverse Vertical Dispersivity (feet)	0.1
Fraction of Organic Carbon (foc) (%)	0.1%
Bulk Density ( $\rho_b$ ) (kg/L)	1.9
<b>LogK<sub>oc</sub>*</b>	
PFOS	2.2
PFHxS	2.5
PFBS	1.5
<b>Retardation Coefficient (R)</b>	
PFOS	2.0
PFHxS	3.0
PFBS	1.2

Abbreviations:

PFAS per- and poly- fluoroalkyl substances

PFBS perfluorobutanesulfonic acid

PFHxS perfluorohexanesulfonic acid

PFOS perfluorooctanesulfonic acid

\*from Interstate Technology Regulatory Council (ITRC), Table 4-1

(<https://pfas-1.itrcweb.org/>)



Table 6-1 - Simulated PFAS Concentrations

Concentration in µg/L		PFOS		PFHxS		PFBS	
Well	Aquifer	Measured	Simulated	Measured	Simulated	Measured	Simulated
<b>175 Newport Way Site</b>							
NWN-MW01	Shallow Zone Aquifer	0.047	0.490	0.016	0.118	0.007	0.020
NWN-MW02	Shallow Zone Aquifer	0.322	0.264	0.200	0.063	0.027	0.011
NWN-MW03	Shallow Zone Aquifer	1.344	4.008	0.521	0.962	0.119	0.160
NWN-MW04	Shallow Zone Aquifer	1.931	5.000	0.387	1.200	0.088	0.200
NWN-MW05	Shallow Zone Aquifer	4.100	5.000	1.567	1.200	0.174	0.200
NWN-MW06	Shallow Zone Aquifer	3.694	5.000	0.842	1.200	0.135	0.200
NWN-MW07	Shallow Zone Aquifer	1.403	5.000	0.523	1.200	0.198	0.200
NWN-MW09	Shallow Zone Aquifer	0.190	3.158	0.085	0.758	0.020	0.126
NWN-MW10	Shallow Zone Aquifer	0.726	5.000	0.162	1.200	0.028	0.200
NWN-MW11	Shallow Zone Aquifer	0.002	0.000	0.002	0.000	0.001	0.000
NWN-MW12	Shallow Zone Aquifer	0.744	5.000	0.313	1.200	0.064	0.200
NWN-MW13	Shallow Zone Aquifer	0.500	5.000	0.357	1.200	0.044	0.200
NWN-MW14	Shallow Zone Aquifer	0.945	5.000	0.400	1.200	0.060	0.200
NWN-MW15	Shallow Zone Aquifer	1.093	5.000	0.300	1.200	0.072	0.200
NWN-MW16	Shallow Zone Aquifer	0.663	5.000	0.276	1.200	0.048	0.200
NWN-MW08	A Zone Aquifer	0.004	0.434	0.002	0.103	0.001	0.017
<b>Issaquah Valley Elementary School &amp; Dodd Fields Park Site</b>							
DF-MW01	Shallow Zone Aquifer	0.048	0.019	0.018	0.004	0.004	0.001
DF-MW02	Shallow Zone Aquifer	0.454	0.398	0.176	0.106	0.018	0.016
DF-MW03	Shallow Zone Aquifer	0.130	0.217	0.033	0.053	0.008	0.009
IES-MW01	Shallow Zone Aquifer	0.205	0.194	0.062	0.048	0.019	0.008
IES-MW02	Shallow Zone Aquifer	0.248	0.089	0.173	0.057	0.046	0.015
IES-MW03	Shallow Zone Aquifer	0.069	0.011	0.062	0.007	0.015	0.002
IES-MW04	Shallow Zone Aquifer	0.490	0.111	0.233	0.037	0.054	0.007
IES-MW05	Shallow Zone Aquifer	0.483	0.307	0.193	0.080	0.031	0.012
IES-MW08	Shallow Zone Aquifer	0.035	0.124	0.014	0.029	0.004	0.005
IES-MW06	A Zone Aquifer	0.004	1.405	0.008	0.339	0.008	0.056
IES-MW09	A Zone Aquifer	0.017	0.212	0.004	0.039	0.002	0.010
IES-MW10	A Zone Aquifer	1.217	0.167	0.548	0.045	0.118	0.006
IES-MW11	A Zone Aquifer	0.029	1.524	0.058	0.360	0.042	0.061
IES-MW12	A Zone Aquifer	0.300	0.914	0.150	0.187	0.046	0.039
<b>Lower Issaquah Valley Regional Wells</b>							
B-12	Shallow Zone Aquifer	0.041	0.003	0.040	0.001	0.011	0.000
B-2	Shallow Zone Aquifer	0.004	0.000	0.003	0.000	0.002	0.000
B-4	Shallow Zone Aquifer	0.012	0.000	0.014	0.000	0.005	0.000
B-7	Shallow Zone Aquifer	0.270	0.000	0.310	0.000	0.027	0.000
COI-MW01	Shallow Zone Aquifer	0.001	0.000	0.001	0.000	0.001	0.000
IES-MW07	Shallow Zone Aquifer	0.411	0.211	0.144	0.052	0.045	0.009
NDS-MW01	Shallow Zone Aquifer	0.924	0.680	0.374	0.163	0.060	0.027
NDS-MW03	Shallow Zone Aquifer	0.017	0.019	0.010	0.004	0.005	0.001
NGB-MW01	Shallow Zone Aquifer	0.102	0.063	0.150	0.012	0.084	0.003
NLS-MW01	Shallow Zone Aquifer	0.117	0.001	0.105	0.000	0.029	0.000
RBN-MW02	Shallow Zone Aquifer	0.006	0.005	0.004	0.002	0.004	0.001
COI-MW02	A Zone Aquifer	0.002	0.031	0.003	0.002	0.005	0.003
COI-MW03	A Zone Aquifer	0.178	0.238	0.121	0.036	0.048	0.012
COI-MW04	A Zone Aquifer	0.002	0.012	0.002	0.002	0.001	0.001
COI-MW05	A Zone Aquifer	0.391	0.760	0.163	0.168	0.053	0.031
COI-MW06	A Zone Aquifer	1.964	1.869	0.668	0.448	0.137	0.075
COI-MW07	A Zone Aquifer	0.004	0.000	0.004	0.000	0.002	0.000
NDS-MW02	A Zone Aquifer	0.275	1.497	0.130	0.352	0.037	0.061
NDS-MW04	A Zone Aquifer	0.005	0.032	0.002	0.006	0.001	0.001
NLS-MW02	A Zone Aquifer	0.120	0.014	0.088	0.004	0.018	0.000
RBN-MW01	A Zone Aquifer	0.006	0.002	0.005	0.001	0.005	0.000
COI-MW08	B/C Zone Aquifer	0.370	0.159	0.160	0.019	0.043	0.009
COI-TW03	B/C Zone Aquifer	0.002	0.000	0.002	0.000	0.002	0.000
<b>Memorial Field Site</b>							
MF-MW01	Shallow Zone Aquifer	0.006	0.100	0.005	0.030	0.003	0.010
MF-MW02	Shallow Zone Aquifer	0.090	0.003	0.037	0.001	0.012	0.000
MF-MW03	Shallow Zone Aquifer	0.004	0.038	0.002	0.011	0.002	0.004
MF-MW04	A Zone Aquifer	0.003	0.000	0.002	0.000	0.003	0.000
<b>Rainier Trail Site</b>							
RT-MW01	Shallow Zone Aquifer	0.040	0.020	0.023	0.012	0.011	0.004
RT-MW03	Shallow Zone Aquifer	0.045	0.003	0.029	0.001	0.008	0.000
RT-MW04	Shallow Zone Aquifer	0.008	0.050	0.003	0.030	0.003	0.010
<b>Production Wells</b>							
COI-PW01	Shallow Zone Aquifer	0.002	0.002	0.001	0.001	0.001	0.000
COI-PW02	Shallow Zone Aquifer	0.002	0.000	0.001	0.000	0.001	0.000
COI-PW04	A Zone Aquifer	0.315	0.075	0.102	0.011	0.030	0.004
DG-PW01	A Zone Aquifer	0.007	0.001	0.009	0.001	0.003	0.000
COI-PW05	B/C Zone Aquifer	0.037	0.011	0.020	0.001	0.006	0.001
SP-PW07	B/C Zone Aquifer	0.025	0.000	0.027	0.000	0.007	0.000
SP-PW08	B/C Zone Aquifer	0.033	0.000	0.032	0.000	0.008	0.000
SP-PW09	B/C Zone Aquifer	0.006	0.000	0.006	0.000	0.003	0.000

Green highlight = Difference between measured and simulated over a factor 5  
 Measured concentrations are based on average of monitoring data



**Table 7-1 Summary of Sensitivity Runs and Calibration  
Sensitivity Results**

<b>Steady-State Model</b>			
		<b>Head</b>	
<b>Parameter</b>	<b>Factor</b>	<b>RMSE (feet)</b>	<b>Normalized Sensitivity Coefficient*</b>
Baseline	-	1.53	--
Horizontal Hydraulic Conductivity	X1.5	2.26	96%
	X0.5	5.60	-534%
Vertical Anisotropy Ratio	X1.5	2.06	71%
	X0.5	1.62	-12%
Riverbed Conductance	X1.5	2.47	123%
	X0.5	1.76	-31%
Areal Recharge	X1.2	3.51	649%
	X0.8	2.70	-384%
Mountain Front Recharge	X1.2	2.92	457%
	X0.8	2.07	-178%

RMSE = root mean square error

\*see Section 7.1.2 for calculation of normalized sensitivity coefficient